Mass spectrometry imaging establishes two distinct metabolic phenotypes of aldosterone-producing cell clusters in primary aldosteronism

Na Sun[1], Lucie S. Meyer[2], Annette Feuchtinger[1], Thomas Kunzke[1], Thomas Knösel[3], Martin Reincke [2], Axel Walch[1#], Tracy Ann Williams[2,4#]

[1]Research Unit Analytical Pathology, German Research Center for Environmental Health, Helmholtz Zentrum München, Germany

[2]Medizinische Klinik und Poliklinik IV, Klinikum der Universität München, LMU München, Germany

[3]Institute of Pathology, Ludwig-Maximilians-Universität München, Germany

[4]Division of Internal Medicine and Hypertension, Department of Medical Sciences, University of Turin, Turin, Italy

Corresponding authors:

Tracy Ann Williams PhD, Medizinische Klinik und Poliklinik IV, Klinikum der Universität München**,** LMU München, Ziemssenstr. 1**,** D-80336 München**,** Germany.

Tel: +49 89 4400 52941**;** Fax: +49 89 4400 54428; Email: Tracy.Williams@med.uni-muenchen.de

Axel Walch MD, Helmholtz Zentrum München, German Research Center for Environmental Health, Research Unit Analytical Pathology, Ingolstaedter Landstrasse 1, 85764 Neuherberg, Germany

Tel: +49 89 3187-2739; Fax +49 89 3187-3349; Email: axel.walch@helmholtz-muenchen.de

Total words*:** 6500; ***5 figures; 1 table

***Running title*:** Mass spectrometry imaging in primary aldosteronism

Abstract

Aldosterone-producing adenomas (APAs) are one of the main causes of primary aldosteronism and the most prevalent surgically correctable form of hypertension. Aldosterone-producing cell clusters (APCCs) comprise tight nests of zona glomerulosa cells, strongly positive for CYP11B2 (aldosterone synthase) in immunohistochemistry. APCCs have been suggested as possible precursors of APAs because they frequently carry driver mutations for constitutive aldosterone production and a few adrenal lesions with histopathologic features of both APCCs and APAs have been identified. Our objective was to investigate the metabolic phenotypes of APCCs (n=27) compared with APAs (n=6) using *in situ* matrix-assisted laser desorption/ionization mass spectrometry imaging of formalin-fixed paraffin embedded adrenals from patients with unilateral primary aldosteronism. Specific distribution patterns of metabolites were associated with APCCs and classified 2 separate APCC subgroups (subgroups 1 and 2) indistinguishable by CYP11B2 immunohistochemistry. Metabolic profiles of APCCs in subgroup 1 were tightly clustered and distinct from subgroup 2 and APAs. Multiple APCCs from the same adrenal displayed metabolic profiles of the same subgroup. Metabolites of APCC subgroup 2 were highly similar to the APA group and indicated enhanced metabolic pathways favoring cell proliferation compared with APCC subgroup 1. In conclusion, we demonstrate specific subgroups of APCCs with strikingly divergent distribution patterns of metabolites. One subgroup displays a metabolic phenotype convergent with APAs and may represent the progression of APCCs to APAs.

Key words: mass spectrometry imaging; hyperaldosteronism; adrenal cortex; adenoma; metabolic profiling; endocrine hypertension

Introduction

Primary aldosteronism is a common but underdiagnosed cause of secondary hypertension characterized by the overproduction of aldosterone relative to suppressed plasma renin levels.[1, 2] Unilateral aldosterone-producing adenomas (APAs) and bilateral adrenal hyperplasia (also called idiopathic hyperaldosteronism) are the main subtypes of primary aldosteronism which together account for more than 80% of all diagnosed cases of the disease.[3] Specific monoclonal antibodies to the highly homologous adrenal steroidogenic enzymes CYP11B2 (aldosterone synthase) and CYP11B1 (11β-hydroxylase) have proven valuable for immunohistochemistry studies and have established the broad spectrum of histologic abnormality associated with primary aldosteronism.[4, 5] In some cases, adrenals from patients with unilateral primary aldosteronism do not show evidence of a well circumscribed APA but display micronodular or diffuse hyperplasia.[4-6] Small nests of CYP11B2-positive cells located beneath the adrenal capsule, referred to as aldosterone-producing cell clusters (APCCs), have been described in normal adrenals and in adrenals from patients with primary aldosteronism.[7-9]

Somatic mutations in genes encoding the ion channels KCNJ5 (or GIRK4, G protein coupled inwardly rectifying potassium channel) and CACNA1D (Cav1.3 calcium channel) and the ATP1A1 (Na^+/K^+-ATPase 1) and ATP2B3 (Ca^{2+}-ATPase 3) ion transporters have been identified in APAs which activate Ca^{2+} signaling in adrenocortical cells and are associated with increased aldosterone production in primary aldosteronism.[10-15] APCCs frequently carry mutations in CACNA1D, a lower incidence is observed in ATP1A1 and ATP2B3 whereas KCNJ5 mutations (highly prevalent in APAs) are largely absent.[6,9] This latter observation is

potentially related to the cell toxicity of mutated KCNJ5 and the high expression level of KCNJ5 in APCCs.[16]

The origin of APAs is unknown. The identification of APCC mutations in genes also mutated in APAs suggests that APCCs may represent precursors of APAs.[9] This proposal is seemingly supported by the description of a few adrenal lesions with histologic features characteristic of both APCCs and APAs, interpreted as APCCs transitioning to APAs (referred to as possible APCC-to-APA transitional lesions).[17]

Matrix-assisted laser desorption/ionization mass spectrometry imaging (MALDI-MSI) acquires molecular images based on the spatially resolved, label-free semi-quantitative detection of thousands of different molecules in biological specimens.[18-20] We have developed a protocol for high throughput *in situ* metabolic profiling from formalin-fixed paraffin-embedded (FFPE) samples using a high mass resolution matrix-assisted laser desorption/ionization Fourier-transform ion cyclotron resonance mass spectrometry imaging (MALDI-FT-ICR-MSI) platform for the detection of over 1700 metabolites within the mass range of m/z 50-1000.[21, 22] This technique has been recently used in several metabolic profiling studies of endocrine tissues and successfully applied to visualize the distribution of hormones and metabolites in the normal and diseased adrenal.[23-26]

Here, we used *in situ* metabolic imaging analysis by MALDI-FT-ICR-MSI of FFPE adrenals resected from patients with unilateral primary aldosteronism to investigate the potential existence of diverse metabolic phenotypes of APCCs.

Methods

The data that support the findings of this study are available from the corresponding authors upon reasonable request.

Patient samples

The study was performed on 16 adrenals removed by unilateral adrenalectomy from patients diagnosed with unilateral primary aldosteronism according to the diagnostic flowchart recommended by the Endocrine Society Guideline with an adrenal venous sampling protocol described previously.[27,28] Samples were selected from surgical cases from the Medizinische Klinik IV, Klinikum der Ludwig-Maximilians-Universität München, Munich, Germany over a 2 year period (n=63). The 16 adrenal samples comprised adrenals with the unusual histopathologic phenotype of unilateral PA with the absence of an APA and the presence of APCCs from a consecutive series of 63 adrenals surgically removed in the 2-year period (n=10) and the first six operated adrenals of the series with the prevalent histopathologic phenotype of an APA (used as controls). An APCC was defined as a CYP11B2-positive aggregate of cells beneath the adrenal capsule. A flow chart showing the sample set of adrenals and analyses performed is shown in **Figure 1**. One adrenal (sample 3-4) showed 3 APCCs in the cortical tissue adjacent to the APA which were also analyzed. In total, 27 APCCs were used for metabolic profiling analyses and compared with CYP11B2 positive regions of 6 APAs. All patients gave informed consent and the protocol was approved by the local ethics committee.

MALDI-MSI experiments

FFPE adrenal samples were cut into 3 µm sections on a microtome (HM 355S, Microm, ThermoScientific) and mounted onto indium-tin-oxide coated glass slides. The FFPE sections

were incubated at 60 °C for one hour, deparaffinized in xylene (2x8 min), and dried on a hotplate at 37 °C. The matrix solution consisted of 10 mg/ml 9-aminoacridine hydrochloride monohydrate (9-AA) (Sigma-Aldrich, Germany) in water/methanol 30:70 (v/v). SunCollect™ automatic sprayer (Sunchrom, Friedrichsdorf, Germany) was used for matrix application. The flow rates were 10, 20, 30 and 40 µl/min, respectively, for the first four layers. The other 4 layers were performed at 40 µl/min. The MALDI-MSI measurement was performed on a Bruker Solarix 7T FT-ICR-MS (Bruker Daltonik, Bremen, Germany) in negative ion mode using 50 laser shots per spot at a frequency of 1000 Hz. The MALDI-MSI data were acquired over a mass range of m/z 50-1000 with 50 µm lateral resolution. After MALDI-MSI measurements, acquired data underwent spectra processing in FlexImaging v. 4.0 (Bruker Daltonics, Bremen, Germany) and SCiLS Lab v. 2019 (Bruker Daltonics, Bremen, Germany). MALDI-MSI data were normalized to the root mean square of all data points.

Immunohistochemistry and image analysis

Sequential adrenal sections for MALDI-MSI experiments were used for immunostaining. CYP11B2 immunohistochemistry was performed under standardized conditions on a Discovery XT automated stainer (Ventana Discovery XT Systems, Ventana Medical Systems, Inc., Tucson, USA) employing monoclonal antibodies against human CYP11B2 (diluted 1:100, a gift from Prof. Celso Gomez-Sanchez, University of Mississippi, USA,), and detected by the Discovery DAB Map Kit (Roche Diagnostics/Ventana Medical Systems), including incubation with anti-mouse and anti-rabbit ready-to-use universal secondary antibodies (catalog 760-4205, Roche Diagnostics/Ventana Medical Systems). APCC regions were annotated according to the CYP11B2 immunostaining. The average spectral data of annotated APCC regions were exported from FlexImaging v. 4.0 (Bruker Daltonics, Bremen, Germany) and used for further bioinformatics analysis.

Bioinformatics analysis and metabolite annotation

MATLAB® R2014b (v.7.10.0, Mathworks, Inc., Natick, MA) was used for pre-processing of MALDI spectra as described previously.[21, 29] Mass spectra underwent resampling, smoothing and baseline subtraction to decrease the data dimensionality and to remove noise-level peaks and artifacts. Peak picking was performed using an adapted version of the LIMPIC algorithm[30] with *m/z* 0.0005 minimum peak width. The signal-to-noise and intensity threshold was set to 2 and 0.01% respectively. Isotopes were automatically identified and excluded. Peaks in the mass range of *m/z* 50 to 1000 were resolved and annotated by accurate mass matching in Human Metabolome Database (HMDB, http://www.hmdb.ca/) and METASPACE (http://annotate.metaspace2020.eu/) (Ion mode: negative, Adduct type: [M-H], [M-H-H2O], [M+Na-2H], [M+Cl] and [M+K-2H], mass accuracy$\leqslant$4 ppm).[31,32] Pathway analysis was performed with the MetaboAnalyst 4.0 (http://www.metaboanalyst.ca)[33,34] and Kyoto Encyclopedia of Genes and Genomes (KEGG) database (http://www.genome.jp/kegg/).[35]

For pathway enrichment analysis of CYP11B2-positive regions, the MS spectrum of each individual region (Region 1, 2 or 3) was compared with the average spectrum of regions 1, 2 and 3 combined. Masses with a peak intensity higher than the average spectrum were defined as discriminative masses of the corresponding region. The discriminative masses of each region were then annotated in metabolite databases (HMDB and METASPACE). Pathway analyses were performed with MetaboAnalyst 4.0. Briefly, algorithms including hypergeometric test for over representation analysis and relative-betweeness centrality for pathway topology analysis were selected. Homo sapiens (KEGG) were specified as pathway library. The metabolome view was generated according to the p values from the pathway enrichment analysis and pathway impact values from the pathway topology analysis.[33,34]

Hierarchical clustering analysis and component analysis by sparse Partial Least Squares Discriminant Analysis (sPLSDA) were performed with MetaboAnalyst 4.0.[33] Briefly, peak lists with respective intensities were uploaded, without data filtering or data transformation and without scaling. Using MetaboAnalyst, a heatmap was created to visualize sample clustering based on the 182 annotated mass peaks. Each colored cell on the map corresponds to an intensity value, with samples in rows and features in columns. Euclidean distance and Ward's method were applied for clustering analysis. The sPLSDA algorithm was used for discriminant analysis with data shown on a 2D score plot with the x-axis representing component 1 and the y-axis representing component 2. Box plots were created with GraphPad PRISM v. 5.00 (GraphPad Software, Inc, La Jolla, USA). Statistical Significance Testing was performed using the One-Way-ANOVA (One-way analysis of variance) and Kruskal-Wallis test (alpha=0.05).

CYP11B2 and CYP11B1 double immunofluorescence

Double immunofluorescence CYP11B2 and CYP11B1 staining used monoclonal antibodies against CYP11B2 (clone 41-17B, diluted 1:200) and CYP11B1 (clone 80-7-5, diluted 1:50), both a kind gift from Celso E. Gomez-Sanchez, University of Mississippi, USA. Alexa Fluor 488 anti-mouse and Alexa Fluor 594 anti-rat secondary antibodies both diluted 1:200 were used to detect bound CYP11B2 and CYP11B1 primary antibodies, respectively (Invitrogen). Tissue sections were washed for 7 min in 10 mM Copper Sulfate buffer (pH 5) to reduce autofluorescence before mounting with Hard Set mounting medium with DAPI (Vectashield).

Genotyping of FFPE adrenal samples

After CYP11B2 immunohistochemistry and metabolic profiling analyses, 7 additional sequential sections of FFPE adrenals were cut for CYP11B2 immunohistochemistry and DNA

extraction. The first and last of the 7 additional sections (3 µm, sections 1 and 7) were used for CYP11B2 immunohistochemistry. The intervening sections (10 µm, sections 2-6) were used for DNA extraction of regions corresponding to CYP11B2-positive zones which were scraped using a 22G Microlance™ 3 under a stereo microscope. DNA extraction was performed using a Maxwell® 16 device according to the manufacturer's protocol. DNA fragments of target sequences were amplified by 35 PCR cycles (annealing temperature 56-60°C) using around 25 ng template DNA. PCR products were reamplified by an additional 35 cycles before analysis for specific fragment amplification on a 1% agarose gel, purification (Qiagen QIAquick PCR Purification Kit) and Sanger sequencing. Validation of detected mutations was performed by an independent PCR amplification and Sanger sequencing. Genomic DNA was analyzed for mutations in *KCNJ5*, *ATP1A1* exons 4 and 8, *ATP2B3* exon 8 and *CACNA1D* exons 6, 14, 16, 23, 27 and 32 using primers detailed previously.[36]

Results

Patient characteristics and adrenal samples

Adrenals were classified into 3 groups stratified by metabolic phenotype: those with APCCs in subgroup 1 (labelled 1-1 to 1-6), APCCs in subgroup 2 (2-1 to 2-4) and group 3 comprising APAs (3-1 to 3-6). The clinical description of the 16 adrenalectomized patients according to subgroup of metabolite clustering (APCC subgroup 1 or 2 or APA) is shown in **Table 1**. Clinical parameters for individual patients and available genotype data are shown in **Table S1** in the online-only Data Supplement. In this small group of patients, overall group differences were observed for age and ARR_DRC (*P*=0.026 and *P*=0.028, respectively). Pairwise comparisons demonstrated the younger age of APCC subgroup 1 compared with subgroup 2 (*P*=0.037) and the lower aldosterone-to-renin ratio of APCC subgroup 1 than the APA group (*P*=0.023).

Comprehensive in situ metabolic profiling analysis using high resolution MALDI FT-ICR MS imaging

APCCs (n=27 from 10 different pieces of adrenal tissue) and regions of 6 different APAs were analyzed using *in situ* metabolic MS imaging. The MSI spectra data of more than one million pixels were extracted and subjected to bioinformatics analysis. Within the mass range of *m/z* 50 to 1000, 182 mass peaks were annotated using the HMDB database and METASPACE (**Table S2**). The annotated metabolites covered 46 KEGG metabolic pathways. The top 5 most dominant metabolic pathways were amino acid biosynthesis, pentose phosphate pathway, 2-oxocarboxylic acid metabolism, fructose and mannose metabolism, amino sugar and nucleotide sugar metabolism.

Co-registration of immunohistochemistry and MALDI FT-ICR MS imaging

An example of the CYP11B2 immunohistochemistry-guided MS imaging approach is shown for adrenal 1-1 in **Figure 2**. CYP11B2 immunohistochemistry and spatial distribution of metabolites identified 2 specific patterns of metabolites related to CYP11B2-positive lesions which are shown for adrenal 1-1 (**Figure 2**). Pattern 1 displayed a continuous distribution throughout the *zona glomerulosa* but with absent or low abundance in CYP11B2-positive lesions and was characterized by the localization of *N*-acetylglucosamine sulfate (**Figure 2**, shown in red). Pattern 2, with guanosine diphosphate (GDP) as a characteristic metabolite, was highly abundant in APCC regions and had a distribution pattern closely related to CYP11B2 immunostaining but was otherwise largely absent throughout the *zona glomerulosa* layer (**Figure 2**, shown in green). The mass peaks which co-localized with the distinct distribution patterns 1 and 2 were automatically elucidated using SCiLS Lab v. 2019 using Pearson's correlation analysis. *N*-acetylglucosamine sulfate, belonging to the glycosaminoglycan degradation metabolite pathway, was the only metabolite co-localized

with pattern 1 whereas 16 mass peaks co-localized with pattern 2, with biological functions related to purine metabolism and amino acid biosynthesis. The list of the 16 mass peaks co-localized with GDP distribution pattern 2 are shown in **Table S3** together with correlation scores for co-localization of each mass peak with GDP.

Figure 2 shows magnified CYP11B2-positive zones (regions 1 to 3) of adrenal 1-1 (corresponding to Regions Of Interest [ROI] ROI01, ROI02 and ROI03 in **Figure 3**). Regions 1 and 3 represent high abundance of GDP and an absence of *N*-acetylglucosamine sulfate. Region 2 shows uniform expression of GDP and *N*-acetylglucosamine sulfate without specific localization to the *zona glomerulosa*. Pathway enrichment analysis identified which metabolite pathways were over-represented in CYP11B2-positive regions 1 to 3 (**Figure 3**). Each discriminative pathway associated with regions 1 to 3 is shown in **Table S4** with pathway impact and the significance of overall metabolic changes within each pathway.

Metabolic phenotyping of aldosterone-producing cell clusters

Metabolic data of 27 APCCs and the 6 APA regions were exported and used for hierarchical clustering and component analyses (**Figure 4**[A] and [B], respectively). The hierarchical cluster analysis identified groups of adrenals based on similarity of metabolite patterns. The associated heat map demonstrated a striking separation of APCCs into two distinct subgroups (APCC subgroups 1 and 2) with one subgroup (subgroup 2) displaying similar metabolite profiles to APAs (**Figure 4**[A]). Component analysis using sPLSDA was used to emphasize variations in the metabolite dataset for pattern identification and visualization. APCC subgroup 1, APCC subgroup 2 and APAs were clearly separated with APCCs in subgroup 1 tightly clustered and distinct from APCC subgroup 2 and the APA group. As in the

hierarchical cluster analysis, APCC subgroup 2 showed high similarity to the APA group (**Figure 4**[B]).

There were no discernable differences at histopathology in APCCs belonging to subgroups 1 and 2 (**Figure 4[C]**) or with double immunofluorescence staining for CYP11B2 and CYP11B1 (11β-hydroxylase) (**Figure 4[D]**). In sections analyzed, the APCCs appeared to cover a range of different sizes with a large APCC both in subgroup 1 (adrenal 1-2) and in subgroup 2 (adrenal 2-3).

APCCs originating from the same adrenal displayed similar metabolic profiles. Despite differences in metabolite pathway enrichment (based on discriminative metabolites only) of the 2 APCCs corresponding to regions 1 and 2 of adrenal 1-1 (**Figure 2, Figure 3**), hierarchical clustering and component analysis (based on 182 annotated mass peaks) demonstrated their highly similar metabolic profiles classifying both to APCC subgroup 1. Similarly, all 3 APCCs analyzed from adrenal samples 1-1, 1-6 and 3-4 and the 5 APCCs from 1-2 and 4 APCCs from 1-4 were assigned to APCC subgroup 1; the 2 APCCs from adrenal 2-1 and all 3 APCCs from adrenal 2-3 were assigned to APCC subgroup 2 (**Figure 4**).

The genotypes of the APAs were No Mutation Detected (NMD, 3-1 and 3-5), KCNJ5-Gly151Arg (3-2), KCNJ5-Thr158Ala (3-3), KCNJ5-Leu168Arg (3-4), ATP1A1-Leu104Arg (3-6). Because of limited tissue availability for APCC samples after metabolic MS imaging analysis, only a subset of APCCs were genotyped. Available genotypes in APCC subgroup 1: ATP1A1-Gly99Arg (corresponding to ROI03 in adrenal 1-1; a double CACNA1D-Met1344Thr, ATP1A1-Ala114Val mutation (ROI01, **Figure S1**) and CACNA1D-Ile1342Met (ROI05) in adrenal 1-2; NMD (ROI01) in adrenal 1-3; CACNA1D-Tyr1349His (ROI01) in adrenal 1-4; NMD (ROI01) in adrenal 3-4 (an APCC in the cortical tissue adjacent to the APA in adrenal 3-4); and in APCC

subgroup 2: NMD (ROI01) in adrenal 2-1; ATP2B3-Val424Ala (ROI01) in adrenal 2-2. The genotyped APCCs are highlighted in **Figure 4, panel C** and indicated in **Table S1**. Mutations in KCNJ5 were not detected in any APCCs.

Metabolic pathway analysis

Enriched metabolic pathways in APCC or APA subgroups contributing to group discrimination include glycolysis, pentose phosphate pathway, tryptophan metabolism, steroid hormone biosynthesis, purine metabolism, citric acid cycle, amino sugar and nucleotide sugar metabolism (**Figure 5**). Specifically, hexose phosphate from glycolysis metabolism, ribose phosphate and erythrose phosphate from the pentose phosphate pathway were increased in APCC subgroup 2 and in APAs compared with APCC subgroup 1. In addition, APCC subgroup 2 displayed enhanced metabolism of tryptophan and purine metabolism via the kynurenine pathway, nucleotide derivatives (ADP, GMP, GDP) and phosphoribosyl glycinamide. The significant enhancement of estrone 3-sulfate and estradiol-17 beta 3-sulfate from steroid hormone biosynthesis, succinate from citric acid cycle and N-acetylglucosamine sulfate from amino sugar and nucleotide sugar metabolism were also observed in APCC subgroup 2.

Discussion

APCCs are characterized by strong and homogeneous CYP11B2 immunostaining and frequently carry variants in genes mutated in APAs which stimulate CYP11B2 expression and aldosterone overproduction.[9] Nishimoto et al [17] proposed that some APCCs may represent precursors for APAs based on observations of a few cases of CYP11B2-positive micronodular lesions beneath the adrenal capsule comprising both subcapsular APCC-like and inner APA-like components termed pAATLs (possible APCC-to-APA transitional lesions).

283 Metabolic phenotyping combining CYP11B2 immunohistochemistry with *in situ* MALDI-MSI
284 has been applied recently to the study of the human adrenal. In a metabolic tissue imaging
285 study of normal human adrenals, Sun et al.,[23] detected a wide range of metabolites,
286 including steroid hormone sulfated metabolites, and established a complex molecular
287 pattern of adrenal zonation.[23] MS imaging analysis of APCCs is technically challenging due to
288 their small size but the use of fresh frozen surgical adrenal specimens enabled visualization
289 of selected steroids with chemical derivatization using Girard's T (GirT) reagent to increase
290 ionization efficiency.[37] Using this approach, Sugiura et al. directly detected aldosterone on
291 adrenal samples and demonstrated the co-accumulation of aldosterone and the hybrid
292 steroid 18-oxocortisol, in APCCs and APAs.[37]

293 Herein we used immunohistochemistry-guided high spatial resolution MSI for the metabolic
294 visualization of 27 APCCs compared with regions of 6 APAs from archival FFPE adrenal
295 samples.[21,22] The validity of the MSI protocol we used for FFPE tissues was demonstrated by
296 a multicenter interlaboratory round robin study which showed a high level of between-
297 center reproducibility of FFPE tissue metabolite data.[38] Although removal of hydrophobic
298 lipids during the organic solvent preparation process of FFPE samples was observed,
299 comparison of fresh frozen and FFPE tissue samples revealed a high overlap of metabolic
300 content in the low mass range (Mw 50-400 Da).[21,22] Nevertheless, previous studies have
301 demonstrated that certain steroids can be detected in FFPE tissue.[25,39] Aldosterone was not
302 detected in our study because it requires specific chemical derivatization of fresh frozen
303 tissue samples.[37]

304 In contrast to the study of Sugiura et al.,[37] our analysis covered a wide range of central
305 metabolic and steroid hormone biosynthesis pathways and determined heterogeneous

patterns of metabolites associated with APCCs. Two distinct subgroups of APCCs with markedly divergent metabolic profiles were established. One subgroup (APCC subgroup 1) comprised the majority of the APCCs analyzed (20 of 27 lesions) with tightly clustered patterns of metabolites clearly diverse from the APA group. Conversely, the second subgroup, which included the remaining 7 APCCs, displayed metabolic profiles similar to the APA group (APCC subgroup 2).

APCC subgroup 2 show evidence of a metabolic switch towards pathways supporting cell proliferation. Hexose monophosphate shunt activity (the pentose phosphate pathway) was increased in APCC subgroup 2 and APAs compared with APCC subgroup 1. This pathway bypasses glycolysis for glucose metabolism and occurs predominantly in tissues synthesizing steroids or fatty acids (such as the adrenal gland and the liver) and supports cell proliferation.[40] Both oxidative and non-oxidative phases of the hexose monophosphate shunt were increased in APCC subgroup 2 as shown by increased ribose phosphate and erythose phosphate, respectively. APCC subgroup 2 also displays enhanced metabolism of tryptophan via the kynurenine pathway to increase NAD^+ (oxidized nicotinamide adenine dinucleotide) production compared with APCC subgroup 1 which may influence the activity of senescent cells to promote tumor progression.[41]

We also observed a distribution pattern of *N*-acetylglucosamine sulfate remarkably related to CYP11B2-positive lesions. *N*-acetylglucosamine sulfate is a native extracellular glycane fragment and substrate of glycosaminoglycan metabolism. Immunodetection of the glycoproteins laminin and fibronectin in the adult rat adrenal cortex indicates high abundancy in the main extracellular matrix (ECM) of the *zona glomerulosa*. ECM proteins favor basal proliferation and modulate the effect of hormones.[42] Previous proteomic

329 analyses of APAs reveal an altered ECM composition affecting ECM-cell surface interactions
330 and actin cytoskeleton rearrangements.[43] The low abundance of *N*-acetylglucosamine sulfate
331 in APCC subgroup 1 and the significant enhancement of *N*-acetylglucosamine sulfate in APCC
332 subgroup 2 suggests an altered ECM composition in APCCs which may be relevant to
333 proliferation and APCC to APA transition.

334 In a previous *in situ* MALDI-MSI metabolomics study of a tissue microarray representing 132
335 genotyped APAs, Murakami et al.,[25] demonstrated an absence of sample clustering according
336 to genotype in the total data set. When hierarchical cluster analysis was restricted to
337 genotype pairs, the metabolic profiles of APAs with KCNJ5 mutations could be distinguished
338 from those with CACNA1D mutations. Differences in metabolic signatures between APAs of
339 other genotypes were not detected. Metabolites of purine metabolism and steroidogenesis
340 contributed to this distinction; increased purine synthesis in APAs with KCNJ5 mutations
341 potentially resulted from enhanced cell cycling and proliferation. Herein, metabolites of
342 purine metabolism and steroid hormone biosynthesis were also significant components of
343 the molecular signature which distinguished APCC subgroups 1 and 2.

344 In the present study, insufficient sample material for the analysis of both metabolites and
345 genotype only allowed genotype determination for *KCNJ5*, *CACNA1D*, *ATP1A1* and *ATP2B3* in
346 a subset of APCCs. Notwithstanding this limitation, we demonstrated apparent
347 heterogeneity of genotype in APCC subgroup 1 (NMD, CACNA1D and ATP1A1 mutations),
348 the absence of KCNJ5 mutations in all APCCs and an APCC with an ATP2B3 mutation in
349 subgroup 2. Because only a pairwise comparison of APAs with KCNJ5 and CACNA1D
350 mutations resulted in sample clustering in the MALDI-MSI metabolomics study of Murakami

et al.,[25] it is unlikely that differences in genotype determined the discrimination of APCCs in subgroups 1 and 2.

Both subgroups of APCCs comprise lesions of a range of different sizes and there was no evident differentiation of the 2 diverse metabolic subgroups based on histopathology. In all 7 adrenals with multiple APCCs, those originating from the same adrenal display similar metabolic profiles and classify to the same subgroup. Patient-related intra-adrenal or circulating factors specific to subgroup 2 may contribute to and at least partially explain this finding. We recently demonstrated that agonistic AT1R-Ab (angiotensin II receptor type 1 autoantibody) levels were higher in patients with primary aldosteronism with evidence of adrenal hyperplasia at computed tomography scanning than those without hyperplasia.[44,45] In the present context, chronic stimulation of the zona glomerulosa cells of APCCs by agonistic AT1R-Abs in a subset of patients with primary aldosteronism may lead to cell proliferation and nodule formation.

In conclusion, we present the first high throughput *in situ* metabolic MS imaging analysis of FFPE adrenal tissue samples from patients with primary aldosteronism using a high mass resolution MALDI-FT-ICR-MSI platform. We establish heterogeneous metabolic profiles of APCCs which determine 2 specific subgroups. The diverse APCC subgroups are in part characterized by the differential activation of metabolic pathways leading to cell proliferation and tumorigenesis which may favor the progression of a subset of APCCs towards the molecular phenotype of APAs.

Perspectives

We will apply the MALDI-FT-ICR-MSI platform we have developed for the analysis of archival FFPE adrenal tissues to provide further insight into the role of APCCs in primary aldosteronism as well as addressing the complex histopathologic phenotypes of this disease. Since the correlation between APCCs and steroid production is still poorly understood, it will be necessary to perform *in situ* chemical derivatization with MALDI-MSI using fresh frozen tissue samples (both normal adrenals and surgical adrenal specimens from patients with primary aldosteronism) for the detection of steroids and any biased co-localization to specific APCC subgroups.

Acknowledgements

We thank Claudia-Marieke Pflüger, Ulrike Buchholz, Cristina Huebner Freitas, Elenore Samson, and Andreas Voss from the Research Unit Analytical Pathology for providing technical assistance.

Sources of Funding

This work was supported by the European Research Council (ERC) under the European Union's Horizon 2020 research and innovation programme (grant agreement No [694913] to M Reincke), the Deutsche Krebshilfe (no. 70112617 to A Walch) and by the Deutsche Forschungsgemeinschaft (DFG, German Research Foundation) Projektnummer: 314061271-TRR 205 to M Reincke, A Walch and TA Williams; and by DFG grant RE 752/20-1 to M Reincke. This work was also supported by the Else Kröner-Fresenius Stiftung in support of the German Conns Registry-Else-Kröner Hyperaldosteronism Registry (2013_A182 and 2015_A171 to M Reincke).

Conflicts of Interest/Disclosure

None

References

1. Stowasser M, Gordon RD. Primary aldosteronism: Changing definitions and new concepts of physiology and pathophysiology both inside and outside the kidney. *Physiol Rev*. 2016;96:1327-1384.
2. Mulatero P, Monticone S, Burrello J, Veglio F, Williams TA, Funder J. Guidelines for primary aldosteronism: Uptake by primary care physicians in Europe. *J Hypertens*. 2016;34:2253-2257.
3. Young WF, Jr. Diagnosis and treatment of primary aldosteronism: Practical clinical perspectives. *J Intern Med*. 2019;285:126-148.
4. Gomez-Sanchez CE, Qi X, Gomez-Sanchez EP, Sasano H, Bohlen MO, Wisgerhof M. Disordered zonal and cellular CYP11B2 enzyme expression in familial hyperaldosteronism type 3. *Mol Cell Endocrinol*. 2017;439:74-80.
5. Meyer LS, Wang X, Susnik E, et al. Immunohistopathology and steroid profiles associated with biochemical outcomes after adrenalectomy for unilateral primary aldosteronism. *Hypertension* 2018;72:650-657.
6. Yamazaki Y, Nakamura Y, Omata K, Ise K, Tezuka Y, Ono Y, Morimoto R, Nozawa Y, Gomez-Sanchez CE, Tomlins SA, Rainey WE, Ito S, Satoh F, Sasano H. Histopathological classification of cross-sectional image-negative hyperaldosteronism. *J Clin Endocrinol Metab*. 2017;102:1182-1192.
7. Nishimoto K, Nakagawa K, Li D, Kosaka T, Oya M, Mikami S, Shibata H, Itoh H, Mitani F, Yamazaki T, Ogishima T, Suematsu M, Mukai K. Adrenocortical zonation in humans under normal and pathological conditions. *J Clin Endocrinol Metab*. 2010;95:2296-2305.

8. Boulkroun S, Samson-Couterie B, Dzib JF, Lefebvre H, Louiset E, Amar L, Plouin PF, Lalli E, Jeunemaitre X, Benecke A, Meatchi T, Zennaro MC. Adrenal cortex remodeling and functional zona glomerulosa hyperplasia in primary aldosteronism. *Hypertension* 2010;56:885-892.

9. Nishimoto K, Tomlins SA, Kuick R, Cani AK, Giordano TJ, Hovelson DH, Liu CJ, Sanjanwala AR, Edwards MA, Gomez-Sanchez CE, Nanba K, Rainey WE. Aldosterone-stimulating somatic gene mutations are common in normal adrenal glands. *Proc Natl Acad Sci U S A*. 2015;112:E4591-4599.

10. Choi M, Scholl UI, Yue P, et al. K+ channel mutations in adrenal aldosterone-producing adenomas and hereditary hypertension. *Science* 2011;331:768-772.

11. Oki K, Plonczynski MW, Luis Lam M, Gomez-Sanchez EP, Gomez-Sanchez CE. Potassium channel mutant KCNJ5 T158A expression in HAC-15 cells increases aldosterone synthesis. *Endocrinology* 2012;153:1774-1782.

12. Oki K, Plonczynski MW, Lam ML, Gomez-Sanchez EP, Gomez-Sanchez CE. The potassium channel, kir3.4 participates in angiotensin ii-stimulated aldosterone production by a human adrenocortical cell line. *Endocrinology* 2012;153:4328-4335.

13. Scholl UI, Goh G, Stolting G, et al. Somatic and germline CACNA1D calcium channel mutations in aldosterone-producing adenomas and primary aldosteronism. *Nat Genet.* 2013;45:1050-1054.

14. Azizan EA, Poulsen H, Tuluc P, et al. Somatic mutations in ATP1A1 and CACNA1D underlie a common subtype of adrenal hypertension. *Nat Genet*. 2013;45:1055-1060.

15. Beuschlein F, Boulkroun S, Osswald A, et al. Somatic mutations in ATP1A1 and ATP2B3 lead to aldosterone-producing adenomas and secondary hypertension. *Nat Genet*. 2013;45:440-444.

16. Yang Y, Gomez-Sanchez CE, Jaquin D, Aristizabal Prada ET, Meyer LS, Knösel T, Schneider H, Beuschlein F, Reincke M, Williams TA. Primary Aldosteronism: KCNJ5 mutations and adrenocortical cell growth. *Hypertension.* 2019;74(4):809-816. doi: 10.1161/HYPERTENSIONAHA.119.13476.

17. Nishimoto K, Seki T, Kurihara I, Yokota K, Omura M, Nishikawa T, Shibata H, Kosaka T, Oya M, Suematsu M, Mukai K. Case report: Nodule development from subcapsular aldosterone-producing cell clusters causes hyperaldosteronism. *J Clin Endocrinol Metab*. 2016;101:6-9.

18. Norris JL, Caprioli RM. Analysis of tissue specimens by matrix-assisted laser desorption/ionization imaging mass spectrometry in biological and clinical research. *Chem Rev*. 2013;113:2309-2342.

19. Walch A, Rauser S, Deininger SO, Hofler H. MALDI imaging mass spectrometry for direct tissue analysis: A new frontier for molecular histology. *Histochem Cell Biol*. 2008;130:421-434.

20. Miura D, Fujimura Y, Wariishi H. In situ metabolomic mass spectrometry imaging: Recent advances and difficulties. *J Proteomics* 2012;75:5052-5060.

21. Ly A, Buck A, Balluff B, et al. High-mass-resolution MALDI mass spectrometry imaging of metabolites from formalin-fixed paraffin-embedded tissue. *Nat Protoc*. 2016;11:1428-1443.

22. Buck A, Ly A, Balluff B, et al. High-resolution MALDI-FT-ICR MS imaging for the analysis of metabolites from formalin-fixed, paraffin-embedded clinical tissue samples. *J Pathol*. 2015;237:123-132.

23. Sun N, Wu Y, Nanba K, Sbiera S, Kircher S, Kunzke T, Aichler M, Berezowska S, Reibetanz J, Rainey WE, Fassnacht M, Walch A, Kroiss M. High-resolution tissue mass

spectrometry imaging reveals a refined functional anatomy of the human adult adrenal gland. *Endocrinology* 2018;159:1511-1524.

24. Sun N, Kunzke T, Sbiera S, et al. Prognostic relevance of steroid sulfation in adrenocortical carcinoma revealed by molecular phenotyping using high-resolution mass spectrometry imaging. *Clin Chem.* 2019;65(10):1276-1286. doi: 10.1373/clinchem.2019.306043.

25. Murakami M, Rhayem Y, Kunzke T, Sun N, Feuchtinger A, Ludwig P, Strom TM, Gomez-Sanchez C, Knosel T, Kirchner T, Williams TA, Reincke M, Walch AK, Beuschlein F. In situ metabolomics of aldosterone-producing adenomas. *JCI Insight* 2019;4(17). pii: 130356.

26. Papathomas TG, Sun N, Chortis V, Taylor AE, Arlt W, Richter S, Eisenhofer G, Ruiz-Babot G, Guasti L, Walch AK. Novel methods in adrenal research: A metabolomics approach. *Histochem Cell Biol*. 2019;151:201-216.

27. Funder JW, Carey RM, Mantero F, Murad MH, Reincke M, Shibata H, Stowasser M, Young WF, Jr. The management of primary aldosteronism: Case detection, diagnosis, and treatment: An Endocrine Society Clinical Practice Guideline. *J Clin Endocrinol Metab*. 2016;101:1889-1916.

28. Williams TA, Reincke M. Management of Endocrine Disease: Diagnosis and management of primary aldosteronism: The Endocrine Society Guideline 2016 revisited. *Eur J Endocrinol.* 2018;179:R19-R29.

29. Sun N, Ly A, Meding S, Witting M, Hauck SM, Ueffing M, Schmitt-Kopplin P, Aichler M, Walch A. High-resolution metabolite imaging of light and dark treated retina using MALDI-FTICR mass spectrometry. *Proteomics* 2014;14:913-923.

30. Mantini D, Petrucci F, Pieragostino D, Del Boccio P, Di Nicola M, Di Ilio C, Federici G, Sacchetta P, Comani S, Urbani A. Limpic: A computational method for the separation of protein MALDI-TOF-MS signals from noise. *BMC Bioinformatics* 2007;8:101.

31. Wishart DS, Feunang YD, Marcu A, et al.. HMDB 4.0 — The Human Metabolome Database for 2018. *Nucleic Acids Res.* 2018;46(D1):D608-17.

32. Palmer A, Phapale P, Chernyavsky I, Lavigne R, Fay D, Tarasov A, Kovalev V, Fuchser J, Nikolenko S, Pineau C, Becker M, Alexandrov T. FDR-controlled metabolite annotation for high-resolution imaging mass spectrometry. *Nat Methods* 2017;14:57-60.

33. Chong J, Soufan O, Li C, Caraus I, Li S, Bourque G, Wishart DS, Xia J. Metaboanalyst 4.0: Towards more transparent and integrative metabolomics analysis. *Nucleic Acids Res*. 2018; 46(W1):W486-W494.

34. Xia J, Wishart DS. Metpa: A web-based metabolomics tool for pathway analysis and visualization. *Bioinformatics*. 2010;26:2342-2344.

35. Kanehisa M, Goto S. Kegg: Kyoto encyclopedia of genes and genomes. *Nucleic Acids Res*. 2000;28(1):27-30.

36. Yang Y, Burrello J, Burrello A, Eisenhofer G, Peitzsch M, Tetti M, Knosel T, Beuschlein F, Lenders JWM, Mulatero P, Reincke M, Williams TA. Classification of microadenomas in patients with primary aldosteronism by steroid profiling. *J Steroid Biochem Mol Biol*. 2019;189:274-282.

37. Sugiura Y, Takeo E, Shimma S, Yokota M, Higashi T, Seki T, Mizuno Y, Oya M, Kosaka T, Omura M, Nishikawa T, Suematsu M, Nishimoto K. Aldosterone and 18-oxocortisol coaccumulation in aldosterone-producing lesions. *Hypertension.* 2018;72:1345-1354.

38. Buck A, Heijs B, Beine B, Schepers J, Cassese A, Heeren RMA, McDonnell LA, Henkel C, Walch A, Balluff B. Round robin study of formalin-fixed paraffin-embedded tissues in mass spectrometry imaging. *Anal Bioanal Chem.* 2018;410(23):5969-5980. doi: 10.1007/s00216-018-1216-2.

39 Sun N, Kunzke T, Sbiera S, Kircher S, et al. Prognostic Relevance of Steroid Sulfation in Adrenocortical Carcinoma Revealed by Molecular Phenotyping Using High-Resolution Mass Spectrometry Imaging. *Clin Chem.* 2019; 65(10):1276-1286.

40. Schwartz L, Supuran CT, Alfarouk KO. The Warburg effect and the hallmarks of cancer. *Anticancer Agents Med Chem.* 2017;17:164-170.

41. Nacarelli T, Lau L, Fukumoto T, et al. NAD^+ metabolism governs the proinflammatory senescence-associated secretome. *Nat Cell Biol.* 2019;21:397-407.

42. Otis M, Campbell S, Payet MD, Gallo-Payet N. Expression of extracellular matrix proteins and integrins in rat adrenal gland: Importance for ACTH-associated functions. *J Endocrinol*. 2007;193:331-347.

43. Swierczynska MM, Betz MJ, Colombi M, Dazert E, Jeno P, Moes S, Pfaff C, Glatz K, Reincke M, Beuschlein F, Donath MY, Hall MN. Proteomic landscape of aldosterone-producing adenoma. *Hypertension.* 2019;73:469-480.

44. Williams TA, Jaquin D, Burrello J, Philippe A, Yang Y, Rank P, Nirschl N, Sturm L, Hubener C, Dragun D, Bidlingmaier M, Beuschlein F, Reincke M. Diverse responses of autoantibodies to the angiotensin II type 1 receptor in primary aldosteronism. *Hypertension.* 2019;74(4):784-792. doi: 10.1161/HYPERTENSIONAHA.119.13156.

45. Armanini D, Sabbadin C, Bordin L. Enigma of the origin of primary aldosteronism. *Hypertension.* 2019;74(4):745-746. doi: 10.1161/HYPERTENSIONAHA.119.13302.

46. Burrello J, Burrello A, Stowasser M, Nishikawa T, Quinkler M, Prejbisz A, Lenders JWM, Satoh F, Mulatero P, Reincke M, Williams TA. The Primary Aldosteronism Surgical Outcome Score for the Prediction of Clinical Outcomes After Adrenalectomy for Unilateral Primary Aldosteronism. *Ann Surg.*: doi: 10.1097/SLA.0000000000003200. [Epub ahead of print]

Novelty and Significance

What is New?

- We performed *in situ* metabolic mass spectrometry imaging (MALDI-FT-ICR-MSI) of selected cell populations of FFPE adrenals from patients with primary aldosteronism
- Specific distribution patterns of metabolites were associated with aldosterone-producing cell clusters (APCCs) and identified 2 specific subgroups of APCCs (subgroups 1 and 2)

What is relevant?

- The metabolic profiles of APCCs in subgroup 1 were tightly clustered and clearly distinct from those of subgroup 2 and APAs
- The metabolic profiles of APCCs in subgroup 2 were highly similar to those of aldosterone-producing adenomas (APAs)
- Metabolic pathways which support cell proliferation were enhanced in APCC subgroup 2 compared with subgroup 1

Summary

We applied high mass resolution MALDI-MSI to FFPE adrenals from patients with unilateral PA and provide evidence from metabolic phenotyping and pathway analyses that a subset of APCCs may transition to APAs

Figure Legends

Figure 1 Study work flow for the analysis of surgical adrenal specimens from patients with unilateral primary aldosteronism

Flow chart illustrating the number of adrenals or aldosterone-producing cell clusters (APCCs) used for each analytical step of the study.

Figure 2 CYP11B2 immunohistochemistry-guided *in situ* mass spectrometry imaging of an adrenal showing multiple CYP11B2-positive regions

The figure shows co-registration of *N*-acetylglucosamine sulfate (red) and guanosine diphosphate (GDP, green) with immunohistochemistry of CYP11B2 (aldosterone synthase). Mass spectrometry images and zoomed regions 1, 2 and 3 (ROI01, ROI02 and ROI03) of adrenal 1-1 are shown. Red arrows (**top panel**) indicate CYP11B2-positive regions including aldosterone-producing cell clusters; white arrows (**bottom panel**) indicate corresponding regions with co-registration of *N*-acetylglucosamine sulfate and GDP. The mass (*m/z* ratio) of metabolites co-localized with GDP metabolite distribution (pattern 2, see text for details) is shown in online supplemental **Table S3**.

Figure 3 Pathway enrichment analysis of CYP11B2-positive region with distinct metabolic profiles

Pathway enrichment analysis was performed on regions 1, 2 and 3 using MetaboAnalyst 4.0 (http://www.metaboanalyst.ca). Metabolic pathways are represented as circles according to their scores from enrichment (**vertical axis**) and topology analyses (**pathway impact, horizontal axis**). The color of circles indicates the statistical significance of the overall metabolic changes within the pathway and circle diameter represents the relative impact of

differential metabolites within the pathway as indicated. The different pattern of discriminative pathways between regions 1 to 3 are summarized in the table and discriminative pathways associated with each region with pathway impact and significance is shown in **Table S4** in the online-only supplemental file.

Figure 4 Hierarchical clustering and component analysis.

Heatmap-based clustering analysis of the 182 mass peaks with a HMDB annotation demonstrated different metabolic profiles in APCC subgroup 1, APCC subgroup 2 and APAs. Peak lists with respective intensities were uploaded to MetaboAnalyst. Each colored cell corresponds to an intensity value, with samples in rows and features in columns. Euclidean distance and Ward's method were applied for cluster analysis (**Panel A**). Component analysis using sPLSDA identified 3 patterns of metabolites comprising 2 subgroups of clearly separated APCCs (subgroup 1 and subgroup 2) and the APA group (**Panel B**). CYP11B2 (aldosterone synthase) immunohistochemistry of adrenal samples included in the metabolic analyses showing APCCs in subgroup 1, APCCs in subgroup 2 and APAs. ROI (region of interest) identification numbers are shown for each APCC analyzed. The ROI identification numbers of genotyped APCCs are indicated in red and are defined in **Table S1** of the online-only supplement (**Panel C**). The metabolic signatures of 3 APCCs in the adrenal cortex adjacent to APA 3-4 were analyzed in addition to that of the tumor itself. Double immunofluorescence staining of CYP11B1 (11β hydroxylase) (**red**) and CYP11B2 (**green**) of representative APCCs from subgroups 1 and 2 as shown (adrenal 1-4, APCC ROI01; adrenal 2-2, APCC ROI01, respectively) (**Panel D**). The merged image also includes DAPI staining in blue. Scale bar = 200 μm**.**

Figure 5 Metabolic pathways distinguish APCC subgroups 1 and 2 and APA.

Box plots of representative metabolites associated with metabolic pathways distinguishing the diverse subgroups of APCCs are shown. One-way ANOVA and Kruskal-Wallis test (alpha=0.05) were used for statistical analyses (*$p<0.05$, **$p<0.01$, ***$p<0.001$)

Sample ID	APCC subgroup 1 N= 6	APCC subgroup 2 N=4	APA N=6	Overall P value
Age (years)	47 ± 6.7	61 ± 7.6	48 ± 9.1	0.026*
Sex (m/f)	4/2	1/4	1/5	0.115
BMI (kg/m^2)	27.7 ± 4.9	28.0 ± 4.4	25.1 ± 5.2	0.566
Duration HTN (months)	71 [39-105]	126 [48-168]	89 [30-156]	0.464
Aldo (pmol/L) Aldo [ng/dL]	333 [300-524] *12.0[10.8-18.9]*	291 [160-430] *10.5 [5.8-15.5]*	364 [334-954] *12.1 [12.0-34.4*]	0.441
DRC (mU/L)	9.5 [3.7-16.4]	2.0 [2.0-4.8]	2.0 [2.0-5.1]	0.059
ARR_DRC	35 [30-128]	91 [74-166]	182 [140-284]	0.028**
Serum K^+ (mmol/L)	3.1 ± 0.4	3.3 ± 0.5	3.1 ± 0.4	0.617
SBP (mmHg)	145 ± 7.3	155 ± 9.1	146 ± 13.0	0.318
DBP (mmHg)	91 ± 11.0	94 ± 13.8	90 ± 13.6	0.896
AntiHTN meds (DDD)	1.50 [0.75-4.08]	2.0 [0.3-3.75]	3.0 [0.7-4.4]	0.892

Table 1. Clinical characteristics of patients with unilateral PA according to metabolic profiles of different groups of adrenals.

Metabolic profiling separated adrenals into 3 distinct groups based on patterns of metabolites corresponding to APCC subgroups 1 and 2 and APAs. Clinical data of patients in each subgroup are presented as average values ± SD, absolute numbers or as medians with lower and upper quartiles in parentheses. Numbers of patients in each group are indicated

(N). P values designate the presence of group differences by the ANOVA and Bonferroni post-hoc tests (age, BMI, systolic and diastolic BP), Kruskal–Wallis test (PAC, DRC, ARR_DRC and potassium), or Chi square test (sex). *Pairwise difference (*P*=0.037) APCC subgroup 1 *vs*. APCC subgroup 2; ** pairwise difference (*P*=0.023) ARR_DRC APCC subgroup 1 *vs* APA. The clinical variables for each individual patient and available genotype data are shown in **Table S1**.

Aldo, plasma aldosterone concentration; APA, aldosterone-producing adenoma; APCC, aldosterone-producing cell cluster; ARR, aldosterone-to-renin ratio; ARR_DRC, aldosterone-to-renin ratio calculated using direct renin concentrations; BMI, body mass index; BP, blood pressure; DDD, defined daily dose; DRC, direct renin concentration; f, female; HTN, hypertension; ID, identification; m, male; N, number; serum K^+, lowest serum potassium ion concentration. Defined daily dose is the assumed average maintenance dose per day for a drug used from its main indication in adults according to ATC/DDD Index 2018 https://www.whocc.no/atc_ddd_index/) and can be calculated using an online tool (https://github.com/ABurrello/PASO-Predictor/raw/master/00 - PASO Predictor.xlsm).[46]

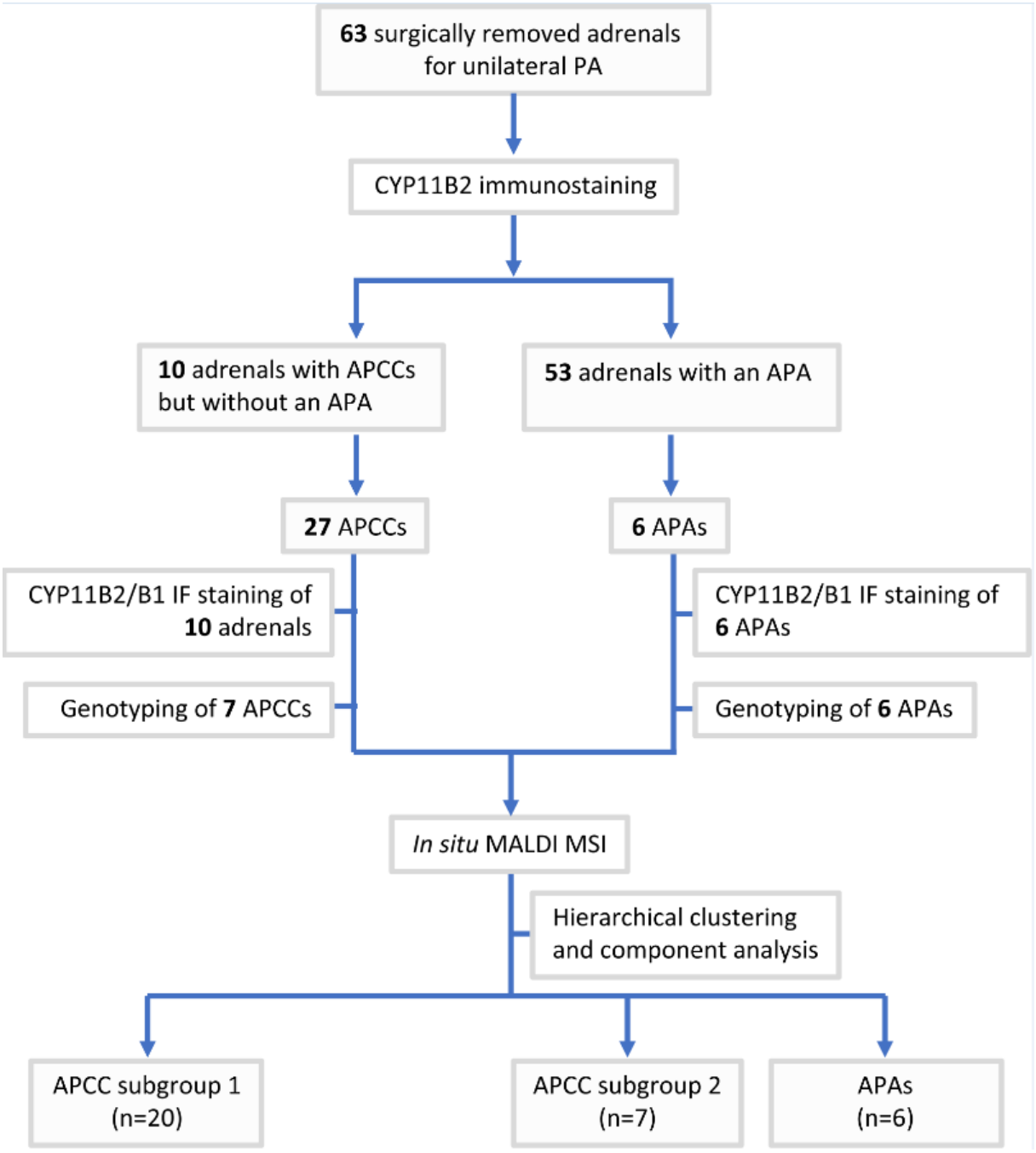
63 surgically removed adrenals for unilateral PA
CYP11B2 immunostaining
10 adrenals with APCCs but without an APA
53 adrenals with an APA
27 APCCs
6 APAs
CYP11B2/B1 IF staining of **10** adrenals
CYP11B2/B1 IF staining of **6** APAs
Genotyping of **7** APCCs
Genotyping of **6** APAs
In situ MALDI MSI
Hierarchical clustering and component analysis
APCC subgroup 1 (n=20)
APCC subgroup 2 (n=7)
APAs (n=6)

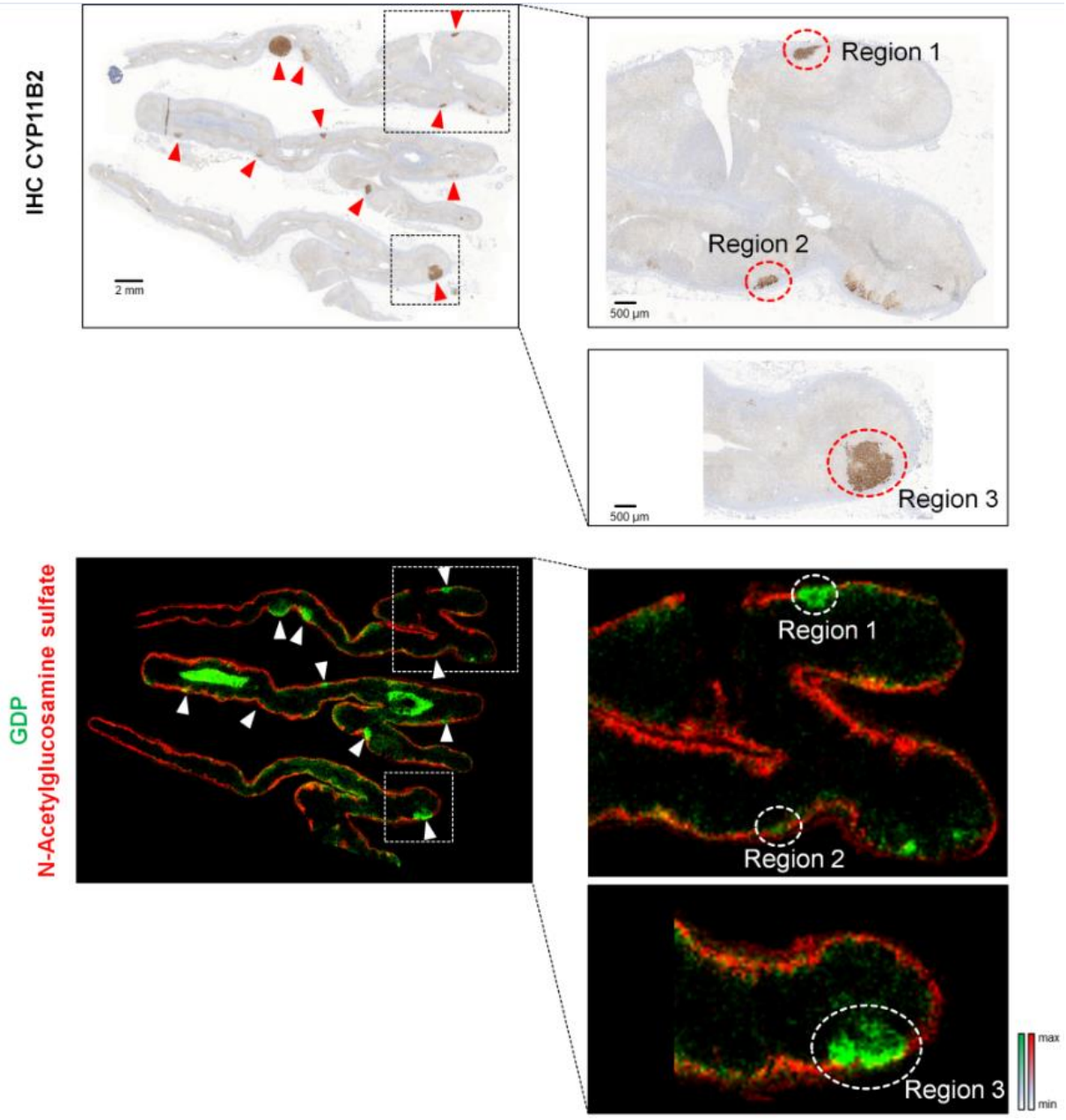
IHC CYP11B2
2 mm
Region 1
Region 2
500 µm
Region 3
500 µm
GDP
N-Acetylglucosamine sulfate
Region 1
Region 2
Region 3
max
min

Region 1

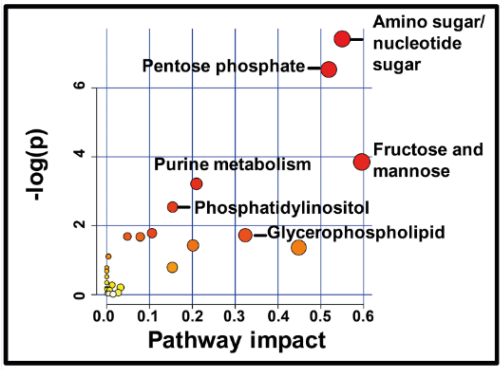

Region 2

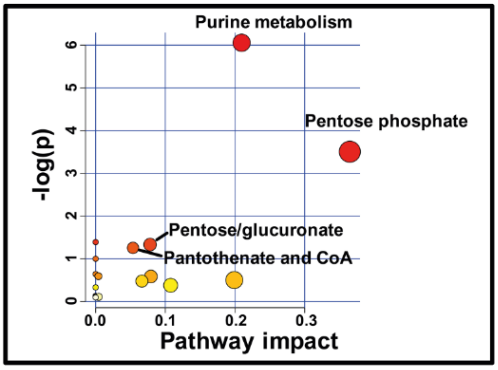

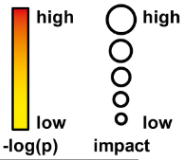

Region 3

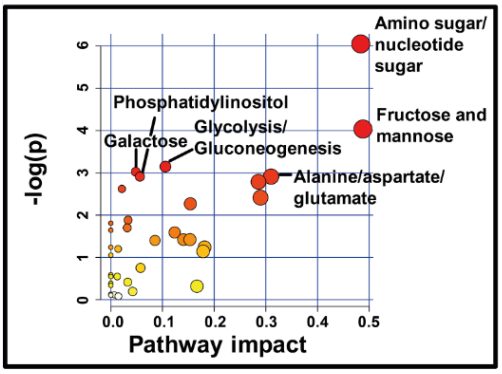

Discriminative pathways	Region 1	Region 2	Region 3
Pentose phosphate pathway	Yes	Yes	No
Purine metabolism	Yes	Yes	No
Amino sugar and nucleotide sugar metabolism	Yes	No	Yes
Fructose and mannose metabolism	Yes	No	Yes
Phosphatidylinositol signaling	Yes	No	Yes
Glycerophospholipid metabolism	Yes	No	No
Pentose and glucuronate interconversions	No	Yes	No
Pantothenate and CoA biosynthesis	No	Yes	No
Glycolysis / Gluconeogenesis	No	No	Yes
Galactose metabolism	No	No	Yes
Alanine, aspartate and glutamate metabolism	No	No	Yes

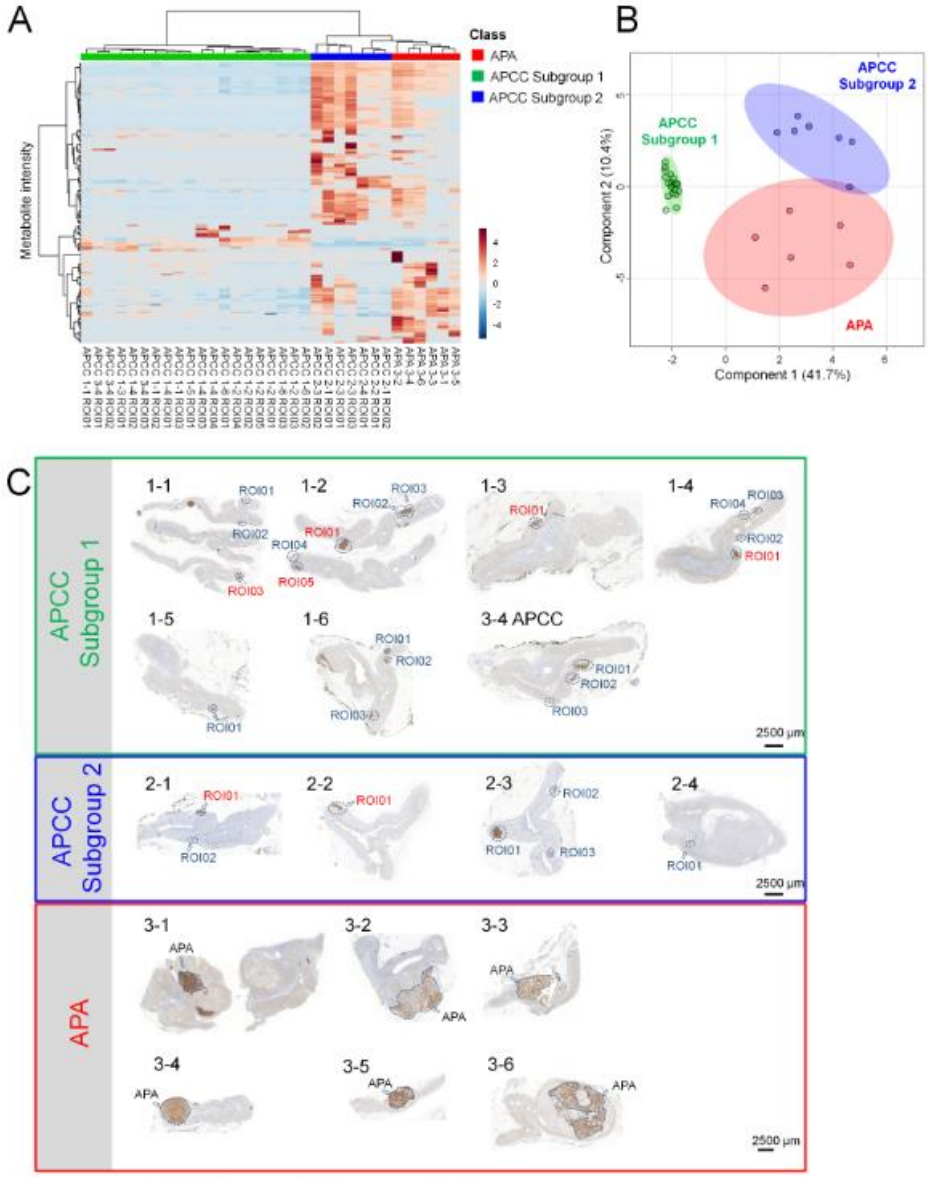
A
Class
APA
APCC Subgroup 1
APCC Subgroup 2
Metabolite intensity
B
APCC Subgroup 2
APCC Subgroup 1
APA
Component 2 (10.4%)
Component 1 (41.7%)
C
APCC Subgroup 1
APCC Subgroup 2
APA
1-1
1-2
1-3
1-4
1-5
1-6
3-4 APCC
2-1
2-2
2-3
2-4
3-1
3-2
3-3
3-4
3-5
3-6
2500 μm
D
CYP11B1
CYP11B2
merged
APCC Subgroup 1
APCC Subgroup 2

Glycolysis

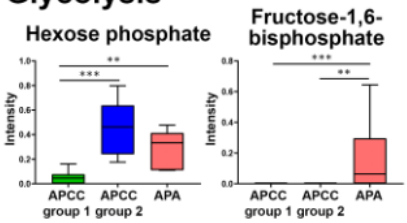

Purine metabolism

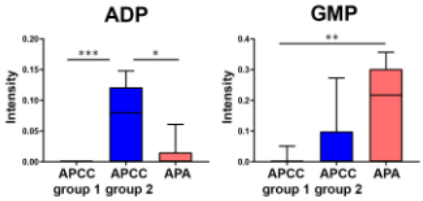

Pentose phosphate pathway

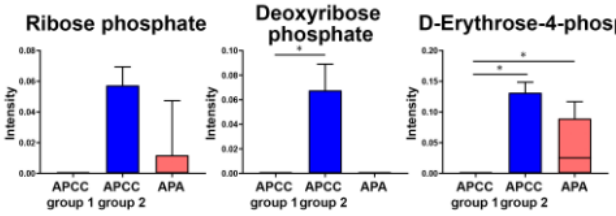

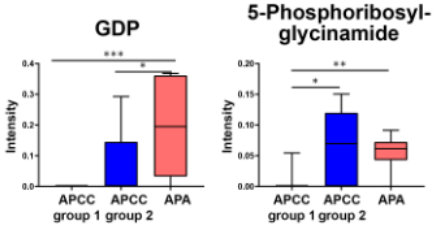

Tryptophan metabolism

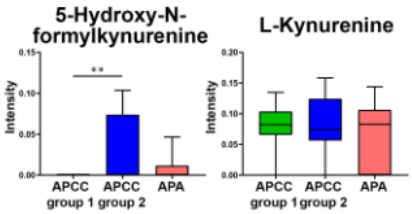

Citric acid cycle

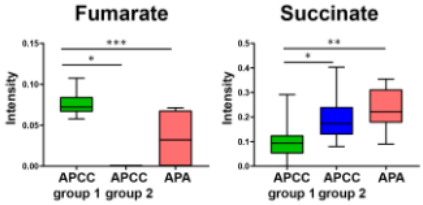

Steroid hormone biosynthesis

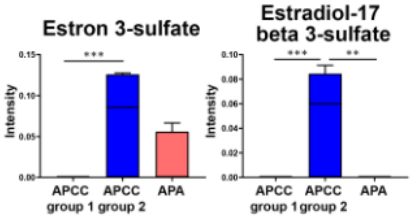

Amino sugar and nucleotide sugar metabolism

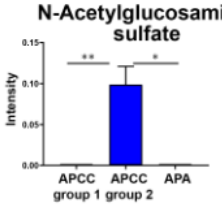

ONLINE SUPPLEMENTAL FILE

Mass spectrometry imaging establishes two distinct metabolic phenotypes of aldosterone-producing cell clusters in primary aldosteronism

Na Sun[1], Lucie S. Meyer[2], Annette Feuchtinger[1], Thomas Kunzke[1], Thomas Knösel[3], Martin Reincke [2], Axel Walch[1#], Tracy Ann Williams[2,4#]

[1]Research Unit Analytical Pathology, German Research Center for Environmental Health, Helmholtz Zentrum München, Germany

[2]Medizinische Klinik und Poliklinik IV, Klinikum der Universität München, LMU München, Germany

[3]Institute of Pathology, Ludwig-Maximilians-Universität München, Germany

[4]Division of Internal Medicine and Hypertension, Department of Medical Sciences, University of Turin, Turin, Italy

Corresponding authors:

Tracy Ann Williams PhD, Medizinische Klinik und Poliklinik IV, Klinikum der Universität München**,** LMU München, Ziemssenstr. 1**,** D-80336 München**,** Germany.
Tel: +49 89 4400 52941**;** Fax: +49 89 4400 54428 ; Email: Tracy.Williams@med.uni-muenchen.de

Axel Walch MD, PhD, Helmholtz Zentrum München, German Research Center for Environmental Health, Research Unit Analytical Pathology, Ingolstaedter Landstrasse 1, 85764 Neuherberg, Germany
Tel: +49 89 3187-2739 ; Fax +49 89 3187-3349 ; Email: axel.walch@helmholtz-muenchen.de

Variable	APCC subgroup 1						APCC subgroup 2				APAs					
Sample ID	1-1	1-2	1-3	1-4	1-5	1-6	2-1	2-2	2-3	2-4	3-1	3-2	3-3	3-4	3-5	3-6
Age (years)	42	59	49	44	42	43	52	68	67	58	46	60	51	32	48	48
Sex (m/f)	M	M	M	M	F	F	F	M	M	M	M	F	F	F	F	F
BMI (kg/m^2)	25.0	34.4	33.3	26.0	23.0	24.6	25.0	34.6	26.1	26.3	30.9	30.1	20.9	21.9	18.8	27.9
Duration HTN (months)	132	79	62	6	50	96	24	132	180	120	36	283	111	66	11	113
Aldo (pmol/L)	518	305	308	541	358	286	449	144	207	374	929	380	302	347	344	1029
Aldo [ng/dL]	*18.7*	*11.0*	*11.1*	*19.5*	*12.9*	*10.3*	*16.2*	*5.2*	*7.5*	*13.5*	*33.5*	*13.7*	*10.9*	*12.5*	*12.4*	*37.1*
DRC (mU/L)	4.2	17.8	9.0	15.9	9.9	2.0	5.7	2.0	2.0	2.0	4.5	2.0	6.7	2.0	2.0	2.0
ARR_DRC	123	17	34	34	36	143	79	72	103	187	207	190	45	173	172	515
Serum K^+ (mmol/L)	2.9	2.7	3.2	3.9	3.3	2.9	3.4	2.8	3.9	3.2	2.6	3.2	2.7	3.7	3.2	2.9
SBP (mmHg)	135	152	143	149	152	138	166	150	157	145	138	143	166	139	156	131
DBP (mmHg)	80	92	75	96	102	100	108	77	102	89	79	76	108	106	85	88
AntiHTN meds (DDD)	0.00	4.00	10.0	4.33	1.00	2.00	0.00	1.00	4.00	3.00	3.00	7.25	3.00	0.75	0.50	3.50
Genotype	ATP1A1-G99R (03)	CACNA1D-I1342M (05) CACNA1D-M1344T (01) ATP1A1-A114V (01)	NMD (01)	CACNA1D-Y1349H (01)	ND	ND	NMD (01)	ATP2B3-Val424Ala (01)	ND	ND	NMD	KCNJ5-G151R	KCNJ5-T158A	KCNJ5-L168R	NMD	ATP1A1-L104R

Table S1. Clinical characteristics of individual patients with unilateral PA according to metabolic profiles and genotypes of different groups of adrenals.

Metabolic profiling separated adrenals into 3 distinct groups based on patterns of metabolites corresponding to APCC subgroups 1 and 2 and APAs. Clinical data of individual patients in each subgroup are shown. Adrenals from patients belonging to APCC groups 1 and 2 did not have an evident APA and genotypes correspond to APCCs. The numbers in parenthesis after APCC genotypes indicate the identification (ROI, Region Of Interest, number) of the APCC within each adrenal according to **Figure 4** of the main manuscript. Aldo, plasma aldosterone concentration; APA, aldosterone-producing adenoma; APCC, aldosterone-producing cell cluster; ARR, aldosterone-to-renin ratio; BMI, body mass index; BP, blood pressure; DDD, defined daily dose; DRC, direct renin concentration; f, female; HTN, hypertension; ID, identification; m, male; N, number; serum K^+, lowest serum potassium ion concentration. Defined daily dose is the assumed average maintenance dose per day for a drug used from its main indication in adults according to ATC/DDD Index 2018 https://www.whocc.no/atc_ddd_index/). KCNJ5 mutations were not detected in any APC

HMDB ID	Chemical formula	Adduct type	Adduct mass	Δppm
HMDB0033875	C4H6S	M+Na-2H	106.993687	3
HMDB0033922	C4H6S	M+Na-2H	106.993687	3
HMDB0032651	C6H6O3	M-H20-H	107.013304	3
HMDB0187592	C6H6O3	M-H20-H	107.013304	3
HMDB0031256	C6H6O3	M-H20-H	107.013304	3
HMDB0029750	C6H6O3	M-H20-H	107.013304	3
HMDB0030776	C6H6O3	M-H20-H	107.013304	3
HMDB0013674	C6H6O3	M-H20-H	107.013304	3
HMDB0013675	C6H6O3	M-H20-H	107.013304	3
HMDB0034355	C6H6O3	M-H20-H	107.013304	3
HMDB0124831	C6H6O3	M-H20-H	107.013304	3
HMDB0059735	C6H6O3	M-H20-H	107.013304	3
HMDB0187591	C6H6O3	M-H20-H	107.013304	3
HMDB0039790	C5H10S2	M-H20-H	115.004002	0
HMDB0038974	C5H10S2	M-H20-H	115.004002	0
HMDB0039789	C5H10S2	M-H20-H	115.004002	0
HMDB0000134	C4H4O4	M-H	115.003683	3
HMDB0000176	C4H4O4	M-H	115.003683	3
HMDB0187641	C4H4O4	M-H	115.003683	3
HMDB0000254	C4H6O4	M+Cl	152.996011	0
HMDB0031204	C4H6O4	M+Cl	152.996011	0
HMDB0130020	C4H6O4	M+Cl	152.996011	0
HMDB0157670	C4H6O4	M+Cl	152.996011	0
HMDB0000202	C4H6O4	M+Cl	152.996011	0
HMDB0187640	C4H6O4	M+Cl	152.996011	0
HMDB0039324	C4H6O4	M+Cl	152.996011	0
HMDB0000349	C4H6O4	M+Cl	152.996011	0
HMDB0000940	C4H6O4	M+Cl	152.996011	0
HMDB0168839	C5H8O3	M+K-2H	152.99595	0
HMDB0003771	C5H8O3	M+K-2H	152.99595	0
HMDB0177210	C5H8O3	M+K-2H	152.99595	0
HMDB0177209	C5H8O3	M+K-2H	152.99595	0
HMDB0168838	C5H8O3	M+K-2H	152.99595	0
HMDB0169666	C5H8O3	M+K-2H	152.99595	0
HMDB0128916	C5H8O3	M+K-2H	152.99595	0
HMDB0128943	C5H8O3	M+K-2H	152.99595	0
HMDB0129096	C5H8O3	M+K-2H	152.99595	0
HMDB0129098	C5H8O3	M+K-2H	152.99595	0
HMDB0128917	C5H8O3	M+K-2H	152.99595	0
HMDB0132477	C5H8O3	M+K-2H	152.99595	0
HMDB0034466	C5H8O3	M+K-2H	152.99595	0
HMDB0000310	C5H8O3	M+K-2H	152.99595	0
HMDB0012233	C5H8O3	M+K-2H	152.99595	0
HMDB0029172	C5H8O3	M+K-2H	152.99595	0
HMDB0001865	C5H8O3	M+K-2H	152.99595	0
HMDB0031643	C5H8O3	M+K-2H	152.99595	0
HMDB0000019	C5H8O3	M+K-2H	152.99595	0
HMDB0129097	C5H8O3	M+K-2H	152.99595	0
HMDB0000720	C5H8O3	M+K-2H	152.99595	0
HMDB0030967	C8H4O2	M+Na-2H	152.995795	1
HMDB0040002	C7H6O2S	M-H	153.001574	3
HMDB0163422	C4H10OS2	M+Na-2H	158.991973	3
HMDB0035661	Cl2Co	M+Cl	163.840308	2
HMDB0037176	C7H13NS	M+Na-2H	164.051536	3
HMDB0038435	C7H13NS	M+Na-2H	164.051536	3
HMDB0038432	C7H13NS	M+Na-2H	164.051536	3
HMDB0155275	C5H14NO4S	M-H20-H	165.045416	4
HMDB0012897	C11H8N2	M-H	167.061472	0
HMDB0040973	C11H10N2O	M-H20-H	167.060923	3
HMDB0034904	Cl2Zn	M+Cl	168.836254	1
HMDB0001292	C5H10O4	M+K-2H	171.006515	0
HMDB0012485	C5H10O4	M+K-2H	171.006515	0
HMDB0158455	C5H10O4	M+K-2H	171.006515	0
HMDB0029576	C5H10O4	M+K-2H	171.006515	0
HMDB0158454	C5H10O4	M+K-2H	171.006515	0
HMDB0158453	C5H10O4	M+K-2H	171.006515	0
HMDB0000421	C5H10O4	M+K-2H	171.006515	0
HMDB0003224	C5H10O4	M+K-2H	171.006515	0
HMDB0012141	C5H10O4	M+K-2H	171.006515	0
HMDB0127615	C5H10O4	M+K-2H	171.006515	0
HMDB0167973	C5H10O4	M+K-2H	171.006515	0
HMDB0062620	C4H8O5	M+Cl	171.006575	0
HMDB0000943	C4H8O5	M+Cl	171.006575	0
HMDB0000613	C4H8O5	M+Cl	171.006575	0
HMDB0002520	C3H9O6P	M-H	171.006399	1
HMDB0000126	C3H9O6P	M-H	171.006399	1
HMDB0032612	C8H6O3	M+Na-2H	171.00636	1
HMDB0032598	C8H6O3	M+Na-2H	171.00636	1
HMDB0031515	C8H6O3	M+Na-2H	171.00636	1
HMDB0001587	C8H6O3	M+Na-2H	171.00636	1
HMDB0040528	C8H6O3	M+Na-2H	171.00636	1
HMDB0001061	H3IO3	M-H	174.889762	1
HMDB0125218	C6H6O4	M+Cl	176.996011	0

HMDB0134002	C6H6O4	M+Cl	176.996011	0
HMDB0062661	C6H6O4	M+Cl	176.996011	0
HMDB0062704	C6H6O4	M+Cl	176.996011	0
HMDB0059762	C6H6O4	M+Cl	176.996011	0
HMDB0032923	C6H6O4	M+Cl	176.996011	0
HMDB0002349	C6H6O4	M+Cl	176.996011	0
HMDB ID	**Chemical formula**	**Adduct type**	**Adduct mass**	**Δppm**
HMDB0032988	C6H6O4	M+Cl	176.996011	0
HMDB0002432	C6H6O4	M+Cl	176.996011	0
HMDB0029188	C6H6O4	M+Cl	176.996011	0
HMDB0006331	C6H6O4	M+Cl	176.996011	0
HMDB0059880	C7H8O3	M+K-2H	176.99595	0
HMDB0169073	C7H8O3	M+K-2H	176.99595	0
HMDB0125538	C7H8O3	M+K-2H	176.99595	0
HMDB0031735	C7H8O3	M+K-2H	176.99595	0
HMDB0137137	C7H8O3	M+K-2H	176.99595	0
HMDB0172014	C7H8O3	M+K-2H	176.99595	0
HMDB0059862	C7H8O3	M+K-2H	176.99595	0
HMDB0151713	C7H8O3	M+K-2H	176.99595	0
HMDB0179995	C7H8O3	M+K-2H	176.99595	0
HMDB0169074	C7H8O3	M+K-2H	176.99595	0
HMDB0133970	C7H8O3	M+K-2H	176.99595	0
HMDB0125014	C7H8O3	M+K-2H	176.99595	0
HMDB0034246	C7H8O3	M+K-2H	176.99595	0
HMDB0137138	C7H8O3	M+K-2H	176.99595	0
HMDB0132905	C7H8O3	M+K-2H	176.99595	0
HMDB0181055	C7H8O3	M+K-2H	176.99595	0
HMDB0166792	C7H16O4S	M-H20-H	177.05854	0
HMDB0167824	C7H16O4S	M-H20-H	177.05854	0
HMDB0061008	C10H13ClN2	M-H20-H	177.058336	1
HMDB0144665	C6H15NO4S	M-H20-H	178.053789	1
HMDB0029442	C6H13NO3S	M-H	178.054338	2
HMDB0172921	C6H13NO3S	M-H	178.054338	2
HMDB0031340	C6H13NO3S	M-H	178.054338	2
HMDB0172920	C6H13NO3S	M-H	178.054338	2
HMDB0015435	C8H8O3S	M-H	183.012139	2
HMDB0186747	C7H8O5S	M-H20-H	184.990855	3
HMDB0186746	C7H8O5S	M-H20-H	184.990855	3
HMDB0166121	C7H8O5S	M-H20-H	184.990855	3
HMDB0166075	C7H8O5S	M-H20-H	184.990855	3
HMDB0166074	C7H8O5S	M-H20-H	184.990855	3
HMDB0060013	C7H8O5S	M-H20-H	184.990854	3
HMDB0014747	C8H10N2S	M+Na-2H	187.031135	3

HMDB0003072	C7H12O6	M-H	191.056112	2
HMDB0177065	C7H12O6	M-H	191.056112	2
HMDB0002123	C8H10N4O3	M-H20-H	191.0569	2
HMDB0036431	C8H10N4O3	M-H20-H	191.0569	2
HMDB0029048	C6H12N2O5	M-H	191.067345	2
HMDB0060348	C6H6O5	M+Cl	192.990925	0
HMDB0137818	C6H6O5	M+Cl	192.990925	0
HMDB0037759	C6H6O5	M+Cl	192.990925	0
HMDB0031210	C6H6O5	M+Cl	192.990925	0
HMDB ID	**Chemical formula**	**Adduct type**	**Adduct mass**	**Δppm**
HMDB0183470	C6H6O5	M+Cl	192.990925	0
HMDB0172619	C7H8O4	M+K-2H	192.990865	1
HMDB0172142	C7H8O4	M+K-2H	192.990865	1
HMDB0140891	C7H8O4	M+K-2H	192.990865	1
HMDB0140890	C7H8O4	M+K-2H	192.990865	1
HMDB0125077	C7H8O4	M+K-2H	192.990865	1
HMDB0125064	C7H8O4	M+K-2H	192.990865	1
HMDB0059731	C7H8O4	M+K-2H	192.990865	1
HMDB0029610	C7H8O4	M+K-2H	192.990865	1
HMDB0158408	C8H14O3	M+Cl	193.063696	2
HMDB0040447	C8H14O3	M+Cl	193.063696	2
HMDB0060685	C8H14O3	M+Cl	193.063696	2
HMDB0031307	C8H14O3	M+Cl	193.063696	2
HMDB0060683	C8H14O3	M+Cl	193.063696	2
HMDB0059939	C8H14O3	M+Cl	193.063696	2
HMDB0059938	C8H14O3	M+Cl	193.063696	2
HMDB0158406	C8H14O3	M+Cl	193.063696	2
HMDB0013211	C8H14O3	M+Cl	193.063696	2
HMDB0158407	C8H14O3	M+Cl	193.063696	2
HMDB0158405	C8H14O3	M+Cl	193.063696	2
HMDB0062788	C8H14O3	M+Cl	193.063696	2
HMDB0030303	C8H14O3	M+Cl	193.063696	2
HMDB0010721	C8H14O3	M+Cl	193.063696	2
HMDB0000909	C8H14O3	M+Cl	193.063696	2
HMDB0000451	C8H14O3	M+Cl	193.063696	2
HMDB0031177	C8H14O3	M+Cl	193.063696	2
HMDB0036230	C8H14O3	M+Cl	193.063696	2
HMDB0038305	C8H14O3	M+Cl	193.063696	2
HMDB0041616	C8H14O3	M+Cl	193.063696	2
HMDB0036395	C8H14O3	M+Cl	193.063696	2
HMDB0167047	C9H16O2	M+K-2H	193.063636	2
HMDB0163455	C9H16O2	M+K-2H	193.063636	2
HMDB0163458	C9H16O2	M+K-2H	193.063636	2

HMDB0163454	C9H16O2	M+K-2H	193.063636	2
HMDB0179804	C9H16O2	M+K-2H	193.063636	2
HMDB0163457	C9H16O2	M+K-2H	193.063636	2
HMDB0179782	C9H16O2	M+K-2H	193.063636	2
HMDB0179783	C9H16O2	M+K-2H	193.063636	2
HMDB0179785	C9H16O2	M+K-2H	193.063636	2
HMDB0179784	C9H16O2	M+K-2H	193.063636	2
HMDB0179786	C9H16O2	M+K-2H	193.063636	2
HMDB0179787	C9H16O2	M+K-2H	193.063636	2
HMDB0179788	C9H16O2	M+K-2H	193.063636	2
HMDB0179806	C9H16O2	M+K-2H	193.063636	2
HMDB0179805	C9H16O2	M+K-2H	193.063636	2
HMDB ID	**Chemical formula**	**Adduct type**	**Adduct mass**	**Δppm**
HMDB0179803	C9H16O2	M+K-2H	193.063636	2
HMDB0179807	C9H16O2	M+K-2H	193.063636	2
HMDB0180000	C9H16O2	M+K-2H	193.063636	2
HMDB0180426	C9H16O2	M+K-2H	193.063636	2
HMDB0180428	C9H16O2	M+K-2H	193.063636	2
HMDB0180425	C9H16O2	M+K-2H	193.063636	2
HMDB0180427	C9H16O2	M+K-2H	193.063636	2
HMDB0179753	C9H16O2	M+K-2H	193.063636	2
HMDB0179751	C9H16O2	M+K-2H	193.063636	2
HMDB0179754	C9H16O2	M+K-2H	193.063636	2
HMDB0163456	C9H16O2	M+K-2H	193.063636	2
HMDB0163459	C9H16O2	M+K-2H	193.063636	2
HMDB0166518	C9H16O2	M+K-2H	193.063636	2
HMDB0166519	C9H16O2	M+K-2H	193.063636	2
HMDB0167040	C9H16O2	M+K-2H	193.063636	2
HMDB0167041	C9H16O2	M+K-2H	193.063636	2
HMDB0167039	C9H16O2	M+K-2H	193.063636	2
HMDB0167042	C9H16O2	M+K-2H	193.063636	2
HMDB0167043	C9H16O2	M+K-2H	193.063636	2
HMDB0167045	C9H16O2	M+K-2H	193.063636	2
HMDB0167044	C9H16O2	M+K-2H	193.063636	2
HMDB0167048	C9H16O2	M+K-2H	193.063636	2
HMDB0167049	C9H16O2	M+K-2H	193.063636	2
HMDB0167050	C9H16O2	M+K-2H	193.063636	2
HMDB0167057	C9H16O2	M+K-2H	193.063636	2
HMDB0179750	C9H16O2	M+K-2H	193.063636	2
HMDB0179752	C9H16O2	M+K-2H	193.063636	2
HMDB0180429	C9H16O2	M+K-2H	193.063636	2
HMDB0031271	C9H16O2	M+K-2H	193.063636	2
HMDB0038272	C9H16O2	M+K-2H	193.063636	2

HMDB0036208	C9H16O2	M+K-2H	193.063636	2
HMDB0032491	C9H16O2	M+K-2H	193.063636	2
HMDB0032265	C9H16O2	M+K-2H	193.063636	2
HMDB0032307	C9H16O2	M+K-2H	193.063636	2
HMDB0059728	C9H16O2	M+K-2H	193.063636	2
HMDB0059817	C9H16O2	M+K-2H	193.063636	2
HMDB0059894	C9H16O2	M+K-2H	193.063636	2
HMDB0059840	C9H16O2	M+K-2H	193.063636	2
HMDB0060286	C9H16O2	M+K-2H	193.063636	2
HMDB0038275	C9H16O2	M+K-2H	193.063636	2
HMDB0039794	C9H16O2	M+K-2H	193.063636	2
HMDB0037629	C9H16O2	M+K-2H	193.063636	2
HMDB0004362	C9H16O2	M+K-2H	193.063636	2
HMDB0035307	C9H16O2	M+K-2H	193.063636	2
HMDB0037618	C9H16O2	M+K-2H	193.063636	2
HMDB ID	**Chemical formula**	**Adduct type**	**Adduct mass**	**Δppm**
HMDB0037023	C9H16O2	M+K-2H	193.063636	2
HMDB0031531	C9H16O2	M+K-2H	193.063636	2
HMDB0036222	C9H16O2	M+K-2H	193.063636	2
HMDB0039736	C9H16O2	M+K-2H	193.063636	2
HMDB0031263	C9H16O2	M+K-2H	193.063636	2
HMDB0034716	C9H16O2	M+K-2H	193.063636	2
HMDB0033167	C9H16O2	M+K-2H	193.063636	2
HMDB0040210	C9H16O2	M+K-2H	193.063636	2
HMDB0037496	C9H16O2	M+K-2H	193.063636	2
HMDB0031514	C9H16O2	M+K-2H	193.063636	2
HMDB0170941	C9H16O2	M+K-2H	193.063636	2
HMDB0032413	C9H16O2	M+K-2H	193.063636	2
HMDB0029688	C12H12O	M+Na-2H	193.063481	3
HMDB0031621	C12H12O	M+Na-2H	193.063481	3
HMDB0059744	C11H16O4	M-H2O-H	193.086469	2
HMDB0153808	C11H16O4	M-H2O-H	193.086469	2
HMDB0169511	C11H16O4	M-H2O-H	193.086469	2
HMDB0029743	C13H9NO	M-H	194.061138	2
HMDB0159825	C6H8O5	M+Cl	195.006575	2
HMDB0159826	C6H8O5	M+Cl	195.006575	2
HMDB0159827	C6H8O5	M+Cl	195.006575	2
HMDB0158424	C6H8O5	M+Cl	195.006575	2
HMDB0158423	C6H8O5	M+Cl	195.006575	2
HMDB0000225	C6H8O5	M+Cl	195.006575	2
HMDB0000398	C6H8O5	M+Cl	195.006575	2
HMDB0180629	C6H8O5	M+Cl	195.006575	2
HMDB0039447	C6H8O5	M+Cl	195.006575	2

HMDB0180630	C6H8O5	M+Cl	195.006575	2
HMDB0180628	C6H8O5	M+Cl	195.006575	2
HMDB0174740	C7H12S2	M+Cl	195.007445	2
HMDB0174741	C7H12S2	M+Cl	195.007445	2
HMDB0163408	C7H10O4	M+K-2H	195.006515	2
HMDB0163409	C7H10O4	M+K-2H	195.006515	2
HMDB0163406	C7H10O4	M+K-2H	195.006515	2
HMDB0163405	C7H10O4	M+K-2H	195.006515	2
HMDB0163407	C7H10O4	M+K-2H	195.006515	2
HMDB0059815	C7H10O4	M+K-2H	195.006515	2
HMDB0036380	C7H10O4	M+K-2H	195.006515	2
HMDB0012241	C7H10O4	M+K-2H	195.006515	2
HMDB0000635	C7H10O4	M+K-2H	195.006515	2
HMDB0030577	C10H6O3	M+Na-2H	195.00636	3
HMDB0166097	C10H6O3	M+Na-2H	195.00636	3
HMDB0030773	C10H6O3	M+Na-2H	195.00636	3
HMDB0032749	C6H12OS2	M+K-2H	200.981562	3
HMDB0039965	C6H12OS2	M+K-2H	200.981562	3
HMDB ID	**Chemical formula**	**Adduct type**	**Adduct mass**	**Δppm**
HMDB0032748	C6H12OS2	M+K-2H	200.981562	3
HMDB0032741	C6H12OS2	M+K-2H	200.981562	3
HMDB0167849	C6H12OS2	M+K-2H	200.981563	3
HMDB0167848	C6H12OS2	M+K-2H	200.981563	3
HMDB0167850	C6H12OS2	M+K-2H	200.981563	3
HMDB0186749	C7H6O5S	M-H	200.986318	1
HMDB0168694	C7H6O5S	M-H	200.986318	1
HMDB0181057	C7H8O6S	M-H20-H	200.985769	4
HMDB0180027	C7H8O6S	M-H20-H	200.985769	4
HMDB0180026	C7H8O6S	M-H20-H	200.985769	4
HMDB0169083	C7H8O6S	M-H20-H	200.985769	4
HMDB0169079	C7H8O6S	M-H20-H	200.985769	4
HMDB0169078	C7H8O6S	M-H20-H	200.985769	4
HMDB0155164	C8H11NO3	M+Cl	204.043295	3
HMDB0035178	C8H11NO3	M+Cl	204.043295	3
HMDB0004817	C8H11NO3	M+Cl	204.043295	3
HMDB0000239	C8H11NO3	M+Cl	204.043295	3
HMDB0037685	C8H11NO3	M+Cl	204.043295	3
HMDB0001537	C8H11NO3	M+Cl	204.043295	3
HMDB0000216	C8H11NO3	M+Cl	204.043295	3
HMDB0002182	C9H13NO2	M+K-2H	204.043235	4
HMDB0062811	C9H13NO2	M+K-2H	204.043235	4
HMDB0039837	C9H13NO2	M+K-2H	204.043235	4
HMDB0062266	C9H13NO2	M+K-2H	204.043235	4
HMDB0014748	C9H13NO2	M+K-2H	204.043235	4
HMDB0015165	C9H13NO2	M+K-2H	204.043235	4
HMDB0032020	C9H13NO2	M+K-2H	204.043235	4
HMDB0041888	C9H13NO2	M+K-2H	204.043235	4
HMDB0060592	C9H13NO2	M+K-2H	204.043235	4
HMDB0038869	C9H13NO2	M+K-2H	204.043235	4
HMDB0012162	C9H13NO2	M+K-2H	204.043235	4
HMDB0004826	C9H13NO2	M+K-2H	204.043235	4
HMDB0000022	C9H13NO2	M+K-2H	204.043235	4
HMDB0060807	C9H13NO2	M+K-2H	204.043235	4
HMDB0167325	C9H13NO2	M+K-2H	204.043235	4
HMDB0062462	C10H10ClN3	M-H	206.049049	0
HMDB0062463	C10H10ClN3	M-H	206.049049	0
HMDB0030411	C7H13NO4S	M-H	206.049253	1
HMDB0031200	C7H13NO4S	M-H	206.049253	1
HMDB0031155	C2Cl3F3	M+Na-2H	206.876434	2
HMDB0030876	C2H6S2Se	M+Cl	208.877015	0
HMDB0094703	C7H15NO3Si	M+Na-2H	210.056786	1
HMDB0030216	C13H9NO2	M-H	210.056053	2
HMDB0161787	C13H9NO2	M-H	210.056053	2
HMDB0012286	C8H15NO2S	M+Na-2H	210.057015	2
HMDB ID	**Chemical formula**	**Adduct type**	**Adduct mass**	**Δppm**
HMDB0033208	C2H6Se2	M+Na-2H	210.85466	2
HMDB0014273	C6H8O6	M+Cl	211.00149	0
HMDB0000004	C6H8O6	M+Cl	211.00149	0
HMDB0006355	C6H8O6	M+Cl	211.00149	0
HMDB0031193	C6H8O6	M+Cl	211.00149	0
HMDB0160740	C7H10O5	M+K-2H	211.001429	0
HMDB0160741	C7H10O5	M+K-2H	211.001429	0
HMDB0062194	C7H10O5	M+K-2H	211.001429	0
HMDB0062377	C7H10O5	M+K-2H	211.001429	0
HMDB0160739	C7H10O5	M+K-2H	211.001429	0
HMDB0160738	C7H10O5	M+K-2H	211.001429	0
HMDB0130150	C7H10O5	M+K-2H	211.001429	0
HMDB0061388	C7H10O5	M+K-2H	211.001429	0
HMDB0003070	C7H10O5	M+K-2H	211.001429	0
HMDB0012149	C7H10O5	M+K-2H	211.001429	0
HMDB0039147	C10H6O4	M+Na-2H	211.001275	1
HMDB0039045	C10H6O4	M+Na-2H	211.001275	1
HMDB0128619	C10H6O4	M+Na-2H	211.001275	1
HMDB0128616	C10H6O4	M+Na-2H	211.001275	1
HMDB0128617	C10H6O4	M+Na-2H	211.001275	1
HMDB0032944	C10H6O4	M+Na-2H	211.001275	1

HMDB0128618	C10H6O4	M+Na-2H	211.001275	1
HMDB0001489	C5H11O8P	M-H20-H	211.000764	3
HMDB0000868	C5H11O8P	M-H20-H	211.000764	3
HMDB0000618	C5H11O8P	M-H20-H	211.000764	3
HMDB0012195	C5H11O8P	M-H20-H	211.000764	3
HMDB0011734	C5H11O8P	M-H20-H	211.000764	3
HMDB0006534	C5H11O8P	M-H20-H	211.000764	3
HMDB0001548	C5H11O8P	M-H20-H	211.000764	3
HMDB0030483	C12H8N2O2	M-H	211.051302	1
HMDB0028768	C6H12N2O3S	M+Na-2H	213.031529	2
HMDB0028684	C6H12N2O3S	M+Na-2H	213.031529	2
HMDB0034633	C10H13ClO4	M-H20-H	213.031847	4
HMDB0034291	C15H8N2O	M-H20-H	213.045273	3
HMDB0015274	C5H15N2O3PS	M-H	213.046824	4
HMDB0180004	C8H10O6S	M-H20-H	215.001419	0
HMDB0180005	C8H10O6S	M-H20-H	215.001419	0
HMDB0128030	C8H10O6S	M-H20-H	215.001419	0
HMDB0124978	C8H8O5S	M-H	215.001969	2
HMDB0167832	C8H8O5S	M-H	215.001969	2
HMDB0167834	C8H8O5S	M-H	215.001969	2
HMDB0033566	C9H14OS3	M-H20-H	215.002287	4
HMDB0061037	C15H10N2O	M-H20-H	215.060923	3
HMDB0172476	C15H10N2O	M-H20-H	215.060923	3
HMDB0060711	C14H11N3O	M-H20-H	218.071822	3
HMDB ID	**Chemical formula**	**Adduct type**	**Adduct mass**	**Δppm**
HMDB0060334	C2H4Br2	M+K-2H	222.816581	3
HMDB0036545	Cl2Sn	M+Cl	224.809304	1
HMDB0179734	C10H12O5S	M-H20-H	225.022155	2
HMDB0133737	C10H12O5S	M-H20-H	225.022155	2
HMDB0133741	C10H12O5S	M-H20-H	225.022155	2
HMDB0133740	C10H12O5S	M-H20-H	225.022155	2
HMDB0133745	C10H12O5S	M-H20-H	225.022155	2
HMDB0133766	C10H12O5S	M-H20-H	225.022155	2
HMDB0133768	C10H12O5S	M-H20-H	225.022155	2
HMDB0133770	C10H12O5S	M-H20-H	225.022155	2
HMDB0133772	C10H12O5S	M-H20-H	225.022155	2
HMDB0133774	C10H12O5S	M-H20-H	225.022155	2
HMDB0135245	C10H12O5S	M-H20-H	225.022155	2
HMDB0135653	C10H12O5S	M-H20-H	225.022155	2
HMDB0151265	C10H12O5S	M-H20-H	225.022155	2
HMDB0151266	C10H12O5S	M-H20-H	225.022155	2
HMDB0170986	C10H12O5S	M-H20-H	225.022155	2
HMDB0133738	C10H12O5S	M-H20-H	225.022155	2
HMDB0133734	C10H12O5S	M-H20-H	225.022155	2
HMDB0133637	C10H12O5S	M-H20-H	225.022155	2
HMDB0133640	C10H12O5S	M-H20-H	225.022155	2
HMDB0133642	C10H12O5S	M-H20-H	225.022155	2
HMDB0133644	C10H12O5S	M-H20-H	225.022155	2
HMDB0133646	C10H12O5S	M-H20-H	225.022155	2
HMDB0133649	C10H12O5S	M-H20-H	225.022155	2
HMDB0133648	C10H12O5S	M-H20-H	225.022155	2
HMDB0133651	C10H12O5S	M-H20-H	225.022155	2
HMDB0133652	C10H12O5S	M-H20-H	225.022155	2
HMDB0133658	C10H12O5S	M-H20-H	225.022155	2
HMDB0133656	C10H12O5S	M-H20-H	225.022155	2
HMDB0133735	C10H12O5S	M-H20-H	225.022155	2
HMDB0059983	C10H12O5S	M-H20-H	225.022154	2
HMDB0133731	C10H12O4S	M-H	227.038354	1
HMDB0180488	C10H12O4S	M-H	227.038354	1
HMDB0133620	C10H12O4S	M-H	227.038354	1
HMDB0181702	C10H14O5S	M-H20-H	227.037805	3
HMDB0180486	C10H14O5S	M-H20-H	227.037805	3
HMDB0181704	C10H14O5S	M-H20-H	227.037805	3
HMDB0180484	C10H14O5S	M-H20-H	227.037805	3
HMDB0180483	C10H14O5S	M-H20-H	227.037805	3
HMDB0180480	C10H14O5S	M-H20-H	227.037805	3
HMDB0163135	C10H14O5S	M-H20-H	227.037805	3
HMDB0163124	C10H14O5S	M-H20-H	227.037805	3
HMDB0135750	C10H14O5S	M-H20-H	227.037805	3
HMDB0181706	C10H14O5S	M-H20-H	227.037805	3
HMDB ID	**Chemical formula**	**Adduct type**	**Adduct mass**	**Δppm**
HMDB0168834	C9H12O8	M-H20-H	229.034827	3
HMDB0039670	C10H14O2S2	M-H	229.036245	3
HMDB0163157	C10H14O4S	M-H	229.054004	2
HMDB0133674	C10H14O4S	M-H	229.054004	2
HMDB0062720	C10H14O4S	M-H	229.054004	2
HMDB0180477	C10H14O4S	M-H	229.054004	2
HMDB0000684	C10H12N2O3	M+Na-2H	229.059458	2
HMDB0012948	C10H12N2O3	M+Na-2H	229.059458	2
HMDB0060757	C10H12N2O3	M+Na-2H	229.059458	2
HMDB0037809	C10H16O2S2	M-H	231.051895	2
HMDB0037808	C10H16O2S2	M-H	231.051895	2
HMDB0180728	C9H12O7	M-H	231.051027	2
HMDB0187651	C4H6O7S	M+Cl	232.952826	3
HMDB0157678	C4H6O7S	M+Cl	232.952826	3
HMDB0157547	C4H6O7S	M+Cl	232.952826	3

HMDB0157546	C4H6O7S	M+Cl	232.952826	3
HMDB0040585	C4H6O7S	M+Cl	232.952825	3
HMDB0177220	C5H8O6S	M+K-2H	232.952765	3
HMDB0177217	C5H8O6S	M+K-2H	232.952765	3
HMDB0169681	C5H8O6S	M+K-2H	232.952765	3
HMDB0168844	C5H8O6S	M+K-2H	232.952765	3
HMDB0128930	C5H8O6S	M+K-2H	232.952765	3
HMDB0129117	C5H8O6S	M+K-2H	232.952765	3
HMDB0132491	C5H8O6S	M+K-2H	232.952765	3
HMDB0129120	C5H8O6S	M+K-2H	232.952765	3
HMDB0166675	C8H6Cl2O4	M-H	234.957038	0
HMDB0031292	C4F8	M+Cl	234.956628	2
HMDB0029014	C8H14N2O3S	M+Na-2H	239.047179	3
HMDB0028783	C8H14N2O3S	M+Na-2H	239.047179	3
HMDB0015175	C13H10N2O4	M-H20-H	239.045667	3
HMDB0060827	C11H13N3S	M+Na-2H	240.057684	3
HMDB0061056	C11H13N3S	M+Na-2H	240.057684	3
HMDB0059932	C7H10O7	M+Cl	241.012055	1
HMDB0003518	C7H10O7	M+Cl	241.012055	1
HMDB0006471	C7H10O7	M+Cl	241.012055	1
HMDB0000379	C7H10O7	M+Cl	241.012055	1
HMDB0041031	C8H12O6	M+K-2H	241.011994	1
HMDB0001125	C6H11O8P	M-H	241.011878	2
HMDB0030789	C11H8O5	M+Na-2H	241.011839	2
HMDB0129373	C11H8O5	M+Na-2H	241.011839	2
HMDB0036346	C11H8O5	M+Na-2H	241.011839	2
HMDB0039820	C11H8O5	M+Na-2H	241.011839	2
HMDB0149153	C11H8O5	M+Na-2H	241.011839	2
HMDB0035086	C11H8O5	M+Na-2H	241.011839	2
HMDB0014312	C8H14O2S2	M+Cl	241.012923	3

HMDB ID	Chemical formula	Adduct type	Adduct mass	Δppm
HMDB0001451	C8H14O2S2	M+Cl	241.012923	3
HMDB0180436	C9H16O4S	M+Na-2H	241.051596	4
HMDB0167060	C9H16O4S	M+Na-2H	241.051596	4
HMDB0163629	C11H16O5S	M-H20-H	241.053455	4
HMDB0176278	C11H16O5S	M-H20-H	241.053455	4
HMDB0176274	C11H16O5S	M-H20-H	241.053455	4
HMDB0176276	C11H16O5S	M-H20-H	241.053455	4
HMDB0176271	C11H16O5S	M-H20-H	241.053455	4
HMDB0164143	C11H16O5S	M-H20-H	241.053455	4
HMDB0163643	C11H16O5S	M-H20-H	241.053455	4
HMDB0151283	C11H16O5S	M-H20-H	241.053455	4
HMDB0163638	C11H16O5S	M-H20-H	241.053455	4
HMDB0163641	C11H16O5S	M-H20-H	241.053455	4
HMDB0163637	C11H16O5S	M-H20-H	241.053455	4
HMDB0163635	C11H16O5S	M-H20-H	241.053455	4
HMDB0163630	C11H16O5S	M-H20-H	241.053455	4
HMDB0163626	C11H16O5S	M-H20-H	241.053455	4
HMDB0163640	C11H16O5S	M-H20-H	241.053455	4
HMDB0037163	C11H24O4	M+Na-2H	241.142125	3
HMDB0133691	C11H12O5S	M-H	255.033269	1
HMDB0133695	C11H12O5S	M-H	255.033269	1
HMDB0132989	C11H12O5S	M-H	255.033269	1
HMDB0133693	C11H12O5S	M-H	255.033269	1
HMDB0133689	C11H12O5S	M-H	255.033269	1
HMDB0151271	C11H14O6S	M-H20-H	255.032719	3
HMDB0152822	C11H14O6S	M-H20-H	255.032719	3
HMDB0151268	C11H14O6S	M-H20-H	255.032719	3
HMDB0163648	C11H14O6S	M-H20-H	255.032719	3
HMDB0163656	C11H14O6S	M-H20-H	255.032719	3
HMDB0163659	C11H14O6S	M-H20-H	255.032719	3
HMDB0164137	C11H14O6S	M-H20-H	255.032719	3
HMDB0164139	C11H14O6S	M-H20-H	255.032719	3
HMDB0164141	C11H14O6S	M-H20-H	255.032719	3
HMDB0166271	C11H14O6S	M-H20-H	255.032719	3
HMDB0182841	C11H14O6S	M-H20-H	255.032719	3
HMDB0151263	C11H14O6S	M-H20-H	255.032719	3
HMDB0151259	C11H14O6S	M-H20-H	255.032719	3
HMDB0151256	C11H14O6S	M-H20-H	255.032719	3
HMDB0126242	C11H14O6S	M-H20-H	255.032719	3
HMDB0126373	C11H14O6S	M-H20-H	255.032719	3
HMDB0132288	C11H14O6S	M-H20-H	255.032719	3
HMDB0133253	C11H14O6S	M-H20-H	255.032719	3
HMDB0133255	C11H14O6S	M-H20-H	255.032719	3
HMDB0133259	C11H14O6S	M-H20-H	255.032719	3
HMDB0132295	C11H14O6S	M-H20-H	255.032719	3

HMDB ID	Chemical formula	Adduct type	Adduct mass	Δppm
HMDB0135676	C11H14O6S	M-H20-H	255.032719	3
HMDB0135699	C11H14O6S	M-H20-H	255.032719	3
HMDB0135698	C11H14O6S	M-H20-H	255.032719	3
HMDB0059981	C11H14O6S	M-H20-H	255.032719	3
HMDB0094714	Cl2MgO8	M+Cl	256.851466	3
HMDB0173554	C6H6O7S	M+K-2H	258.93203	2
HMDB0060467	C6H13O9P	M-H	259.022443	0
HMDB0062705	C6H13O9P	M-H	259.022443	0
HMDB0001313	C6H13O9P	M-H	259.022443	0

HMDB0001401	C6H13O9P	M-H	259.022443	0
HMDB0001078	C6H13O9P	M-H	259.022443	0
HMDB0001076	C6H13O9P	M-H	259.022443	0
HMDB0000994	C6H13O9P	M-H	259.022443	0
HMDB0000213	C6H13O9P	M-H	259.022443	0
HMDB0000124	C6H13O9P	M-H	259.022443	0
HMDB0006330	C6H13O9P	M-H	259.022443	0
HMDB0001586	C6H13O9P	M-H	259.022443	0
HMDB0002985	C6H13O9P	M-H	259.022443	0
HMDB0003498	C6H13O9P	M-H	259.022443	0
HMDB0006873	C6H13O9P	M-H	259.022443	0
HMDB0006814	C6H13O9P	M-H	259.022443	0
HMDB0006800	C6H13O9P	M-H	259.022443	0
HMDB0006797	C6H13O9P	M-H	259.022443	0
HMDB0006328	C6H13O9P	M-H	259.022443	0
HMDB0003971	C6H13O9P	M-H	259.022443	0
HMDB0000645	C6H13O9P	M-H	259.022443	0
HMDB0125202	C8H14O7	M+K-2H	259.022559	0
HMDB0131286	C8H14O7	M+K-2H	259.022559	0
HMDB0010325	C8H14O7	M+K-2H	259.022559	0
HMDB0128679	C11H10O6	M+Na-2H	259.022404	0
HMDB0137297	C11H10O6	M+Na-2H	259.022404	0
HMDB0039494	C11H10O6	M+Na-2H	259.022404	0
HMDB0137298	C11H10O6	M+Na-2H	259.022404	0
HMDB0128680	C11H10O6	M+Na-2H	259.022404	0
HMDB0041108	C20H38	M-H20-H	259.278961	2
HMDB0041107	C20H38	M-H20-H	259.278961	2
HMDB0041106	C20H38	M-H20-H	259.278961	2
HMDB0031489	C3Cl6O	M-H	260.800755	3
HMDB0163347	C5H6O6S2	M+Cl	260.929982	2
HMDB0163349	C5H6O6S2	M+Cl	260.929982	2
HMDB0151310	C11H14O3S	M+K-2H	263.014971	0
HMDB0180488	C10H12O4S	M+Cl	263.015032	0
HMDB0133731	C10H12O4S	M+Cl	263.015032	0
HMDB0133620	C10H12O4S	M+Cl	263.015032	0
HMDB0015521	C11H12N4O2S	M-H	263.06082	3
HMDB ID	**Chemical formula**	**Adduct type**	**Adduct mass**	**Δppm**
HMDB0169466	C6H13NO5S2	M+Na-2H	263.998181	1
HMDB0041887	C9H12FN3O3	M+Cl	264.055671	3
HMDB0142089	C10H12O6	M+K-2H	265.011994	0
HMDB0141334	C10H12O6	M+K-2H	265.011994	0
HMDB0125596	C10H12O6	M+K-2H	265.011994	0
HMDB0125592	C10H12O6	M+K-2H	265.011994	0
HMDB0125049	C10H12O6	M+K-2H	265.011994	0
HMDB0125034	C10H12O6	M+K-2H	265.011994	0
HMDB0166820	C10H12O6	M+K-2H	265.011994	0
HMDB0182126	C10H12O6	M+K-2H	265.011994	0
HMDB0166822	C10H12O6	M+K-2H	265.011994	0
HMDB0166821	C10H12O6	M+K-2H	265.011994	0
HMDB0182127	C10H12O6	M+K-2H	265.011994	0
HMDB0156354	C10H12O6	M+K-2H	265.011994	0
HMDB0179552	C10H12O6	M+K-2H	265.011994	0
HMDB0168258	C13H8O5	M+Na-2H	265.011839	1
HMDB0142401	C13H8O5	M+Na-2H	265.011839	1
HMDB0142398	C13H8O5	M+Na-2H	265.011839	1
HMDB0142400	C13H8O5	M+Na-2H	265.011839	1
HMDB0142399	C13H8O5	M+Na-2H	265.011839	1
HMDB0029218	C13H8O5	M+Na-2H	265.011839	1
HMDB0029463	C13H8O5	M+Na-2H	265.011839	1
HMDB0039670	C10H14O2S2	M+Cl	265.012923	3
HMDB0163157	C10H14O4S	M+Cl	265.030682	1
HMDB0133674	C10H14O4S	M+Cl	265.030682	1
HMDB0062720	C10H14O4S	M+Cl	265.030682	1
HMDB0180477	C10H14O4S	M+Cl	265.030682	1
HMDB0037517	C18H34O	M-H	265.25369	3
HMDB0030965	C18H34O	M-H	265.25369	3
HMDB0031070	C13H12O2S	M+Cl	267.025202	2
HMDB0038634	C11H12N2O2S2	M-H	267.026743	4
HMDB0181561	C10H20N2O2S	M+Cl	267.093951	4
HMDB0181560	C10H20N2O2S	M+Cl	267.093951	4
HMDB0181559	C10H20N2O2S	M+Cl	267.093951	4
HMDB0042010	C18H13N3O	M-H20-H	268.087472	4
HMDB0013851	C14H14N2O3S	M-H20-H	271.054123	1
HMDB0028781	C8H16N2O3S2	M+Na-2H	273.0349	1
HMDB0028970	C8H16N2O3S2	M+Na-2H	273.0349	1
HMDB0169522	C11H16O7S	M-H20-H	273.043284	1
HMDB0163672	C11H16O7S	M-H20-H	273.043284	1
HMDB0163669	C11H16O7S	M-H20-H	273.043284	1
HMDB0014704	C15H12N2O	M+K-2H	273.043569	2
HMDB0033122	C15H12N2O	M+K-2H	273.043569	2
HMDB0152822	C11H14O6S	M-H	273.043833	3
HMDB0163648	C11H14O6S	M-H	273.043833	3
HMDB ID	**Chemical formula**	**Adduct type**	**Adduct mass**	**Δppm**
HMDB0163656	C11H14O6S	M-H	273.043833	3
HMDB0163659	C11H14O6S	M-H	273.043833	3
HMDB0182841	C11H14O6S	M-H	273.043833	3

HMDB015127 1	C11H14O6S	M-H	273.043833	3
HMDB016413 7	C11H14O6S	M-H	273.043833	3
HMDB016413 9	C11H14O6S	M-H	273.043833	3
HMDB016414 1	C11H14O6S	M-H	273.043833	3
HMDB016627 1	C11H14O6S	M-H	273.043833	3
HMDB015126 8	C11H14O6S	M-H	273.043833	3
HMDB015126 3	C11H14O6S	M-H	273.043833	3
HMDB012624 2	C11H14O6S	M-H	273.043833	3
HMDB012637 3	C11H14O6S	M-H	273.043833	3
HMDB013228 8	C11H14O6S	M-H	273.043833	3
HMDB013229 5	C11H14O6S	M-H	273.043833	3
HMDB013325 3	C11H14O6S	M-H	273.043833	3
HMDB013325 5	C11H14O6S	M-H	273.043833	3
HMDB013325 9	C11H14O6S	M-H	273.043833	3
HMDB013567 6	C11H14O6S	M-H	273.043833	3
HMDB013569 9	C11H14O6S	M-H	273.043833	3
HMDB013569 8	C11H14O6S	M-H	273.043833	3
HMDB015125 6	C11H14O6S	M-H	273.043833	3
HMDB015125 9	C11H14O6S	M-H	273.043833	3
HMDB005998 1	C11H14O6S	M-H	273.043833	3
HMDB016180 5	C13H11NO5S	M-H20-H	274.017404	4
HMDB016184 8	C13H11NO5S	M-H20-H	274.017404	4
HMDB003945 9	C6H10S5	M+Cl	276.908006	4
HMDB002962 7	C7H4Cl4O	M+Cl	278.871028	3
HMDB013536 3	C15H16O3	M+Cl	279.079346	2
HMDB016750 9	C15H16O3	M+Cl	279.079346	2
HMDB016751 1	C15H16O3	M+Cl	279.079346	2
HMDB016751 3	C15H16O3	M+Cl	279.079346	2
HMDB016751 2	C15H16O3	M+Cl	279.079346	2
HMDB003472 3	C15H16O3	M+Cl	279.079346	2
HMDB003063 6	C15H16O3	M+Cl	279.079346	2
HMDB003264 1	C15H16O3	M+Cl	279.079346	2
HMDB003854 8	C15H16O3	M+Cl	279.079346	2
HMDB003192 5	C15H16O3	M+Cl	279.079346	2
HMDB003073 1	C15H16O3	M+Cl	279.079346	2
HMDB016750 8	C15H16O3	M+Cl	279.079346	2
HMDB013561 8	C16H18O2	M+K-2H	279.079286	3
HMDB006084 2	C13H16N2O3S	M-H	279.080887	3
HMDB004185 8	C16H18ClN	M+Na-2H	280.087443	4
HMDB006040 5	C9H12FN3O4	M+K-2H	282.02979	1
HMDB004204 3	C14H12ClNO2	M+Na-2H	282.030322	3
HMDB001450 3	C10H10N4O2S	M+K-2H	287.001052	2
HMDB ID	**Chemical formula**	**Adduct type**	**Adduct mass**	**Δppm**

HMDB015914 7	C8H12O7S	M+Cl	286.999776	3
HMDB015915 0	C8H12O7S	M+Cl	286.999776	3
HMDB016712 3	C9H14O6S	M+K-2H	286.999715	3
HMDB016494 3	C9H14O6S	M+K-2H	286.999715	3
HMDB016494 7	C9H14O6S	M+K-2H	286.999715	3
HMDB016495 0	C9H14O6S	M+K-2H	286.999715	3
HMDB016495 1	C9H14O6S	M+K-2H	286.999715	3
HMDB016711 7	C9H14O6S	M+K-2H	286.999715	3
HMDB016712 0	C9H14O6S	M+K-2H	286.999715	3
HMDB016494 6	C9H14O6S	M+K-2H	286.999715	3
HMDB016493 9	C9H14O6S	M+K-2H	286.999715	3
HMDB016494 2	C9H14O6S	M+K-2H	286.999715	3
HMDB016493 5	C9H14O6S	M+K-2H	286.999715	3
HMDB016493 6	C9H14O6S	M+K-2H	286.999715	3
HMDB016713 2	C9H14O6S	M+K-2H	286.999715	3
HMDB013857 6	C14H10O6S	M-H20-H	287.001419	3
HMDB001401 6	C13H16ClNO2	M+Cl	288.056358	4
HMDB006055 0	C13H16ClNO2	M+Cl	288.056358	4
HMDB001401 7	C13H16ClNO2	M+Cl	288.056358	4
HMDB012493 8	C8H12O9	M+K-2H	288.996738	3
HMDB012493 9	C8H12O9	M+K-2H	288.996738	3
HMDB015974 6	C8H11O9	M+K-2H	288.996738	3
HMDB015136 5	C11H14O5S2	M-H	289.02099	0
HMDB015136 2	C11H14O5S2	M-H	289.02099	0
HMDB015135 7	C11H14O5S2	M-H	289.02099	0
HMDB015135 6	C11H14O5S2	M-H	289.02099	0
HMDB015135 2	C11H14O5S2	M-H	289.02099	0
HMDB015135 3	C11H14O5S2	M-H	289.02099	0
HMDB015135 0	C11H14O5S2	M-H	289.02099	0
HMDB015134 3	C11H14O5S2	M-H	289.02099	0
HMDB015134 0	C11H14O5S2	M-H	289.02099	0
HMDB015133 7	C11H14O5S2	M-H	289.02099	0
HMDB001528 5	C12H18N2O2S	M+Cl	289.078301	1
HMDB001223 5	C13H18ClNO2	M+Cl	290.072009	2
HMDB003221 6	C14H22ClNO	M+K-2H	292.087598	3
HMDB015546 7	C6H10O9S	M+Cl	292.973955	0
HMDB016403 5	C6H10O9S	M+Cl	292.973955	0
HMDB015546 5	C6H10O9S	M+Cl	292.973955	0
HMDB015546 4	C6H10O9S	M+Cl	292.973955	0
HMDB015546 6	C6H10O9S	M+Cl	292.973955	0
HMDB015493 8	C6H10O9S	M+Cl	292.973955	0
HMDB015493 6	C6H10O9S	M+Cl	292.973955	0
HMDB015493 5	C6H10O9S	M+Cl	292.973955	0

HMDB0154937	C6H10O9S	M+Cl	292.973955	0
HMDB0164034	C6H10O9S	M+Cl	292.973955	0
HMDB ID	**Chemical formula**	**Adduct type**	**Adduct mass**	**Δppm**
HMDB0184577	C6H10O9S	M+Cl	292.973955	0
HMDB0184578	C6H10O9S	M+Cl	292.973955	0
HMDB0184580	C6H10O9S	M+Cl	292.973955	0
HMDB0184579	C6H10O9S	M+Cl	292.973955	0
HMDB0186471	C7H12O8S	M+K-2H	292.973895	0
HMDB0160164	C7H12O8S	M+K-2H	292.973895	0
HMDB0160160	C7H12O8S	M+K-2H	292.973895	0
HMDB0160156	C7H12O8S	M+K-2H	292.973895	0
HMDB0186472	C7H12O8S	M+K-2H	292.973895	0
HMDB0128634	C10H8O7S	M+Na-2H	292.97374	1
HMDB0128638	C10H8O7S	M+Na-2H	292.97374	1
HMDB0128636	C10H8O7S	M+Na-2H	292.97374	1
HMDB0136770	C10H8O7S	M+Na-2H	292.97374	1
HMDB0136779	C10H8O7S	M+Na-2H	292.97374	1
HMDB0174747	C7H14O4S3	M+Cl	292.974824	3
HMDB0174743	C7H14O4S3	M+Cl	292.974824	3
HMDB0174745	C7H14O4S3	M+Cl	292.974824	3
HMDB0172029	C10H14O8	M+Cl	297.038269	1
HMDB0167149	C10H14O8	M+Cl	297.038269	1
HMDB0182846	C10H14O8	M+Cl	297.038269	1
HMDB0032924	C11H16O7	M+K-2H	297.038209	1
HMDB0146363	C14H12O6	M+Na-2H	297.038054	2
HMDB0033649	C14H12O6	M+Na-2H	297.038054	2
HMDB0031762	C11H10N4O4	M+Cl	297.039607	4
HMDB0039082	C12H23NOS2	M+K-2H	298.070712	1
HMDB0167368	C10H17NO7	M+Cl	298.069904	2
HMDB0062785	C11H19NO6	M+K-2H	298.069843	2
HMDB0061717	C11H19NO6	M+K-2H	298.069843	2
HMDB0034777	C11H19NO6	M+K-2H	298.069843	2
HMDB0013133	C11H19NO6	M+K-2H	298.069843	2
HMDB0033865	C11H19NO6	M+K-2H	298.069843	2
HMDB0001016	C9H18NO8P	M-H	298.069727	3
HMDB0062700	C9H18NO8P	M-H	298.069727	3
HMDB0014549	C16H19BrN2	M-H20-H	299.054771	1
HMDB0001941	C16H19BrN2	M-H20-H	299.054771	1
HMDB0159324	C10H16O8	M+Cl	299.053919	2
HMDB0167143	C10H16O8	M+Cl	299.053919	2
HMDB0167145	C10H16O8	M+Cl	299.053919	2
HMDB0130127	C10H16O8	M+Cl	299.053919	2
HMDB0159320	C10H16O8	M+Cl	299.053919	2

HMDB0172030	C10H16O8	M+Cl	299.053919	2
HMDB0159322	C10H16O8	M+Cl	299.053919	2
HMDB0172032	C10H16O8	M+Cl	299.053919	2
HMDB0126095	C10H16O8	M+Cl	299.053919	2
HMDB0034681	C10H16O8	M+Cl	299.053919	2
HMDB ID	**Chemical formula**	**Adduct type**	**Adduct mass**	**Δppm**
HMDB0171234	C11H18O7	M+K-2H	299.053859	2
HMDB0166266	C11H18O7	M+K-2H	299.053859	2
HMDB0136690	C11H18O7	M+K-2H	299.053859	2
HMDB0164616	C11H18O7	M+K-2H	299.053859	2
HMDB0180870	C11H18O7	M+K-2H	299.053859	2
HMDB0175217	C11H18O7	M+K-2H	299.053859	2
HMDB0171232	C11H18O7	M+K-2H	299.053859	2
HMDB0166226	C11H18O7	M+K-2H	299.053859	2
HMDB0136516	C14H14O6	M+Na-2H	299.053704	3
HMDB0138057	C14H14O6	M+Na-2H	299.053704	3
HMDB0136515	C14H14O6	M+Na-2H	299.053704	3
HMDB0132920	C14H14O6	M+Na-2H	299.053704	3
HMDB0132919	C14H14O6	M+Na-2H	299.053704	3
HMDB0128947	C14H14O6	M+Na-2H	299.053704	3
HMDB0164991	C14H14O6	M+Na-2H	299.053704	3
HMDB0153203	C16H14O7	M-H20-H	299.055563	4
HMDB0130326	C16H14O7	M-H20-H	299.055563	4
HMDB0130328	C16H14O7	M-H20-H	299.055563	4
HMDB0154098	C16H14O7	M-H20-H	299.055563	4
HMDB0131988	C16H14O7	M-H20-H	299.055563	4
HMDB0153278	C16H14O7	M-H20-H	299.055563	4
HMDB0130677	C16H14O7	M-H20-H	299.055563	4
HMDB0153277	C16H14O7	M-H20-H	299.055563	4
HMDB0130673	C16H14O7	M-H20-H	299.055563	4
HMDB0153204	C16H14O7	M-H20-H	299.055563	4
HMDB0153269	C16H14O7	M-H20-H	299.055563	4
HMDB0130174	C16H14O7	M-H20-H	299.055563	4
HMDB0130176	C16H14O7	M-H20-H	299.055563	4
HMDB0154095	C16H14O7	M-H20-H	299.055563	4
HMDB0126505	C16H14O7	M-H20-H	299.055563	4
HMDB0126509	C16H14O7	M-H20-H	299.055563	4
HMDB0126511	C16H14O7	M-H20-H	299.055563	4
HMDB0127502	C16H14O7	M-H20-H	299.055563	4
HMDB0127501	C16H14O7	M-H20-H	299.055563	4
HMDB0128199	C16H14O7	M-H20-H	299.055563	4
HMDB0128212	C16H14O7	M-H20-H	299.055563	4
HMDB0128760	C16H14O7	M-H20-H	299.055563	4

HMDB0128759	C16H14O7	M-H20-H	299.055563	4
HMDB0129342	C16H14O7	M-H20-H	299.055563	4
HMDB0129350	C16H14O7	M-H20-H	299.055563	4
HMDB0129356	C16H14O7	M-H20-H	299.055563	4
HMDB0130671	C16H14O7	M-H20-H	299.055563	4
HMDB0132135	C16H14O7	M-H20-H	299.055563	4
HMDB0132138	C16H14O7	M-H20-H	299.055563	4
HMDB0152196	C16H14O7	M-H20-H	299.055563	4
HMDB ID	**Chemical formula**	**Adduct type**	**Adduct mass**	**Δppm**
HMDB0140540	C16H14O7	M-H20-H	299.055563	4
HMDB0140537	C16H14O7	M-H20-H	299.055563	4
HMDB0141375	C16H14O7	M-H20-H	299.055563	4
HMDB0152190	C16H14O7	M-H20-H	299.055563	4
HMDB0152065	C16H14O7	M-H20-H	299.055563	4
HMDB0142313	C16H15O7	M-H20-H	299.055563	4
HMDB0146283	C16H14O7	M-H20-H	299.055563	4
HMDB0152017	C16H14O7	M-H20-H	299.055563	4
HMDB0146280	C16H14O7	M-H20-H	299.055563	4
HMDB0147861	C16H14O7	M-H20-H	299.055563	4
HMDB0148843	C16H14O7	M-H20-H	299.055563	4
HMDB0151420	C16H14O7	M-H20-H	299.055563	4
HMDB0148850	C16H14O7	M-H20-H	299.055563	4
HMDB0148856	C16H14O7	M-H20-H	299.055563	4
HMDB0153021	C16H14O7	M-H20-H	299.055563	4
HMDB0153027	C16H14O7	M-H20-H	299.055563	4
HMDB0132136	C16H14O7	M-H20-H	299.055563	4
HMDB0153198	C16H14O7	M-H20-H	299.055563	4
HMDB0132211	C16H14O7	M-H20-H	299.055563	4
HMDB0132216	C16H14O7	M-H20-H	299.055563	4
HMDB0153199	C16H14O7	M-H20-H	299.055563	4
HMDB0133572	C16H14O7	M-H20-H	299.055563	4
HMDB0142312	C16H15O7	M-H20-H	299.055563	4
HMDB0133838	C16H14O7	M-H20-H	299.055563	4
HMDB0135916	C16H14O7	M-H20-H	299.055563	4
HMDB0135920	C16H14O7	M-H20-H	299.055563	4
HMDB0135924	C16H14O7	M-H20-H	299.055563	4
HMDB0136021	C16H14O7	M-H20-H	299.055563	4
HMDB0136022	C16H14O7	M-H20-H	299.055563	4
HMDB0136023	C16H14O7	M-H20-H	299.055563	4
HMDB0153200	C16H14O7	M-H20-H	299.055563	4
HMDB0151418	C16H14O7	M-H20-H	299.055563	4
HMDB0126506	C16H14O7	M-H20-H	299.055563	4
HMDB0152016	C16H14O7	M-H20-H	299.055563	4

HMDB0124873	C16H14O7	M-H20-H	299.055563	4
HMDB0033892	C16H14O7	M-H20-H	299.055563	4
HMDB0037501	C16H14O7	M-H20-H	299.055563	4
HMDB0154308	C16H14O7	M-H20-H	299.055563	4
HMDB0002937	C16H14O7	M-H20-H	299.055563	4
HMDB0152312	C16H14O7	M-H20-H	299.055563	4
HMDB0125446	C16H14O7	M-H20-H	299.055563	4
HMDB0125011	C16H14O7	M-H20-H	299.055563	4
HMDB0125009	C16H14O7	M-H20-H	299.055563	4
HMDB0124876	C16H14O7	M-H20-H	299.055563	4
HMDB0153268	C16H14O7	M-H20-H	299.055563	4
HMDB ID	**Chemical formula**	**Adduct type**	**Adduct mass**	**Δppm**
HMDB0152183	C16H14O7	M-H20-H	299.055563	4
HMDB0039458	C6H10S7	M-H	304.875469	2
HMDB0015527	C19H17ClN2O	M-H20-H	305.084551	2
HMDB0015292	C13H19ClN2O2	M+Cl	305.082908	4
HMDB0126522	C14H20O4S	M+Na-2H	305.082896	4
HMDB0028786	C14H17N3O3S	M-H	306.091786	1
HMDB0029080	C14H17N3O3S	M-H	306.091786	1
HMDB0002022	C7H15N2O8P	M+Na-2H	307.031268	1
HMDB0061205	C17H19ClN2	M+Na-2H	307.098342	4
HMDB0015697	C14H22ClNO2	M+K-2H	308.082513	3
HMDB0000839	C20H14N4	M-H	309.11457	1
HMDB0032549	C17H28O3S	M-H	311.168639	1
HMDB0145822	C10H16O9	M+Cl	315.048834	1
HMDB0130135	C10H16O9	M+Cl	315.048834	1
HMDB0130132	C10H16O9	M+Cl	315.048834	1
HMDB0130133	C10H16O9	M+Cl	315.048834	1
HMDB0130129	C10H16O9	M+Cl	315.048834	1
HMDB0130019	C10H16O9	M+Cl	315.048834	1
HMDB0126113	C10H16O9	M+Cl	315.048834	1
HMDB0126115	C10H16O9	M+Cl	315.048834	1
HMDB0126116	C10H16O9	M+Cl	315.048834	1
HMDB0126114	C10H16O9	M+Cl	315.048834	1
HMDB0130136	C10H16O9	M+Cl	315.048834	1
HMDB0165475	C10H16O9	M+Cl	315.048834	1
HMDB0165472	C10H16O9	M+Cl	315.048834	1
HMDB0165471	C10H16O9	M+Cl	315.048834	1
HMDB0164665	C10H16O9	M+Cl	315.048834	1
HMDB0165476	C10H16O9	M+Cl	315.048834	1
HMDB0130130	C10H16O9	M+Cl	315.048834	1
HMDB0167016	C11H18O8	M+K-2H	315.048774	1
HMDB0167014	C11H18O8	M+K-2H	315.048774	1

HMDB0130798	C11H18O8	M+K-2H	315.048774	1
HMDB0126546	C11H18O8	M+K-2H	315.048774	1
HMDB0143217	C11H18O8	M+K-2H	315.048774	1
HMDB0167013	C11H18O8	M+K-2H	315.048774	1
HMDB0175219	C11H18O8	M+K-2H	315.048774	1
HMDB0130839	C11H18O8	M+K-2H	315.048774	1
HMDB0175227	C11H18O8	M+K-2H	315.048774	1
HMDB0002091	C11H18O8	M+K-2H	315.048774	1
HMDB0175224	C11H18O8	M+K-2H	315.048774	1
HMDB0175223	C11H18O8	M+K-2H	315.048774	1
HMDB0175220	C11H18O8	M+K-2H	315.048774	1
HMDB0172660	C14H14O7	M+Na-2H	315.048619	1
HMDB0172658	C14H14O7	M+Na-2H	315.048619	1
HMDB0172661	C14H14O7	M+Na-2H	315.048619	1
HMDB ID	**Chemical formula**	**Adduct type**	**Adduct mass**	**Δppm**
HMDB0172670	C14H14O7	M+Na-2H	315.048619	1
HMDB0172680	C14H14O7	M+Na-2H	315.048619	1
HMDB0172687	C14H14O7	M+Na-2H	315.048619	1
HMDB0172686	C14H14O7	M+Na-2H	315.048619	1
HMDB0172671	C14H14O7	M+Na-2H	315.048619	1
HMDB0172684	C14H14O7	M+Na-2H	315.048619	1
HMDB0172672	C14H14O7	M+Na-2H	315.048619	1
HMDB0172679	C14H14O7	M+Na-2H	315.048619	1
HMDB0172659	C14H14O7	M+Na-2H	315.048619	1
HMDB0172683	C14H14O7	M+Na-2H	315.048619	1
HMDB0011649	C9H19O11P	M-H2O-H	315.048108	3
HMDB0062044	C13H7Cl2FO2	M+Cl	318.950115	1
HMDB0060959	C16H18N4S	M+Na-2H	319.099883	1
HMDB0168137	C12H26O5S	M+K-2H	319.098701	3
HMDB0168134	C12H26O5S	M+K-2H	319.098701	3
HMDB0168135	C12H26O5S	M+K-2H	319.098701	3
HMDB0165442	C17H22O5S	M-H2O-H	319.100405	3
HMDB0165437	C17H22O5S	M-H2O-H	319.100405	3
HMDB0165435	C17H22O5S	M-H2O-H	319.100405	3
HMDB0015527	C19H17ClN2O	M-H	323.095665	2
HMDB0031031	C18H30O3S	M-H	325.18429	4
HMDB0059915	C18H30O3S	M-H	325.18429	4
HMDB0061835	C14H30O8	M-H	325.186792	4
HMDB0005037	C14H21N3O2S	M+Cl	330.10485	0
HMDB0035230	C17H10O6	M+Na-2H	331.022404	1
HMDB0033657	C17H10O6	M+Na-2H	331.022404	1
HMDB0172660	C14H14O7	M+K-2H	331.022559	2
HMDB0172659	C14H14O7	M+K-2H	331.022559	2

HMDB0172658	C14H14O7	M+K-2H	331.022559	2
HMDB0172661	C14H14O7	M+K-2H	331.022559	2
HMDB0172670	C14H14O7	M+K-2H	331.022559	2
HMDB0172671	C14H14O7	M+K-2H	331.022559	2
HMDB0172672	C14H14O7	M+K-2H	331.022559	2
HMDB0172680	C14H14O7	M+K-2H	331.022559	2
HMDB0172679	C14H14O7	M+K-2H	331.022559	2
HMDB0172683	C14H14O7	M+K-2H	331.022559	2
HMDB0172684	C14H14O7	M+K-2H	331.022559	2
HMDB0172686	C14H14O7	M+K-2H	331.022559	2
HMDB0172687	C14H14O7	M+K-2H	331.022559	2
HMDB0149525	C13H12O8	M+Cl	331.022619	2
HMDB0029318	C13H12O8	M+Cl	331.022619	2
HMDB0034620	C13H12O8	M+Cl	331.022619	2
HMDB0032957	C13H12O8	M+Cl	331.022619	2
HMDB0001425	C18H22O5S	M-H2O-H	331.100405	1
HMDB0158303	C12H24O6S	M+Cl	331.098762	4
HMDB ID	**Chemical formula**	**Adduct type**	**Adduct mass**	**Δppm**
HMDB0171039	C13H26O5S	M+K-2H	331.098701	4
HMDB0171033	C13H26O5S	M+K-2H	331.098701	4
HMDB0171035	C13H26O5S	M+K-2H	331.098701	4
HMDB0171037	C13H26O5S	M+K-2H	331.098701	4
HMDB0015113	C17H19F2N3O3	M-H2O-H	332.121058	2
HMDB0005012	C17H20N4S	M+Na-2H	333.115533	0
HMDB0155415	C18H24O5S	M-H2O-H	333.116055	2
HMDB0155493	C18H24O5S	M-H2O-H	333.116055	2
HMDB0004448	C18H24O5S	M-H2O-H	333.116055	2
HMDB0015061	C18H22ClNO	M+K-2H	340.087598	3
HMDB0240223	C18H22ClNO	M+K-2H	340.087598	3
HMDB0182043	C16H16N2O8	M-H2O-H	345.072275	2
HMDB0182045	C16H16N2O8	M-H2O-H	345.072275	2
HMDB0182046	C16H16N2O8	M-H2O-H	345.072275	2
HMDB0182044	C16H16N2O8	M-H2O-H	345.072275	2
HMDB0168470	C13H16N2O8	M+Na-2H	349.065331	0
HMDB0168469	C13H16N2O8	M+Na-2H	349.065331	0
HMDB0168467	C13H16N2O8	M+Na-2H	349.065331	0
HMDB0168468	C13H16N2O8	M+Na-2H	349.065331	0
HMDB0166300	C12H12O8S	M+Cl	350.994691	0
HMDB0166306	C12H12O8S	M+Cl	350.994691	0
HMDB0130069	C13H14O7S	M+K-2H	350.99463	0
HMDB0130068	C13H14O7S	M+K-2H	350.99463	0
HMDB0014766	C16H11ClN2O3	M+K-2H	350.994426	1
HMDB0158414	C14H22O9	M+Na-2H	355.101048	2

HMDB0158417	C14H22O9	M+Na-2H	355.101048	2
HMDB0158415	C14H22O9	M+Na-2H	355.101048	2
HMDB0158420	C14H22O9	M+Na-2H	355.101048	2
HMDB0158421	C14H22O9	M+Na-2H	355.101048	2
HMDB0159136	C14H22O9	M+Na-2H	355.101048	2
HMDB0158412	C14H22O9	M+Na-2H	355.101048	2
HMDB0158411	C14H22O9	M+Na-2H	355.101048	2
HMDB0159137	C14H22O9	M+Na-2H	355.101048	2
HMDB0015264	C19H20N2O3S	M-H	355.112187	1
HMDB0012996	C14H26N2O3S2	M+Na-2H	355.11315	2
HMDB0061011	C16H23N3O2S	M+Cl	356.1205	0
HMDB0014645	C21H23ClFNO2	M-H20-H	356.121745	3
HMDB0152100	C18H16O9	M-H20-H	357.061042	2
HMDB0132198	C18H16O9	M-H20-H	357.061042	2
HMDB0130279	C18H16O9	M-H20-H	357.061042	2
HMDB0138024	C18H16O9	M-H20-H	357.061042	2
HMDB0138521	C18H16O9	M-H20-H	357.061042	2
HMDB0146596	C18H16O9	M-H20-H	357.061042	2
HMDB0136140	C18H16O9	M-H20-H	357.061042	2
HMDB0152086	C18H16O9	M-H20-H	357.061042	2
HMDB ID	**Chemical formula**	**Adduct type**	**Adduct mass**	**Δppm**
HMDB0152085	C18H16O9	M-H20-H	357.061042	2
HMDB0146595	C18H16O9	M-H20-H	357.061042	2
HMDB0037691	C18H16O9	M-H20-H	357.061042	2
HMDB0136131	C18H16O9	M-H20-H	357.061042	2
HMDB0129273	C18H16O9	M-H20-H	357.061042	2
HMDB0129277	C18H16O9	M-H20-H	357.061042	2
HMDB0136135	C18H16O9	M-H20-H	357.061042	2
HMDB0130261	C18H16O9	M-H20-H	357.061042	2
HMDB0130275	C18H16O9	M-H20-H	357.061042	2
HMDB0132197	C18H16O9	M-H20-H	357.061042	2
HMDB0148094	C18H14O8	M-H	357.061591	3
HMDB0152218	C18H14O8	M-H	357.061591	3
HMDB0176930	C18H14O8	M-H	357.061591	3
HMDB0029272	C18H14O8	M-H	357.061591	3
HMDB0159490	C12H18O10	M+Cl	357.059399	3
HMDB0161127	C12H18O10	M+Cl	357.059399	3
HMDB0159830	C12H18O10	M+Cl	357.059399	3
HMDB0161128	C12H18O10	M+Cl	357.059399	3
HMDB0161132	C12H18O10	M+Cl	357.059399	3
HMDB0161130	C12H18O10	M+Cl	357.059399	3
HMDB0161129	C12H18O10	M+Cl	357.059399	3
HMDB0041096	C12H18O10	M+Cl	357.059399	3
HMDB0161133	C12H18O10	M+Cl	357.059399	3
HMDB0158755	C12H18O10	M+Cl	357.059399	3
HMDB0159491	C12H18O10	M+Cl	357.059399	3
HMDB0159488	C12H18O10	M+Cl	357.059399	3
HMDB0159487	C12H18O10	M+Cl	357.059399	3
HMDB0158759	C12H18O10	M+Cl	357.059399	3
HMDB0159485	C12H18O10	M+Cl	357.059399	3
HMDB0158877	C12H18O10	M+Cl	357.059399	3
HMDB0158758	C12H18O10	M+Cl	357.059399	3
HMDB0158756	C12H18O10	M+Cl	357.059399	3
HMDB0158752	C12H18O10	M+Cl	357.059399	3
HMDB0158751	C12H18O10	M+Cl	357.059399	3
HMDB0158753	C12H18O10	M+Cl	357.059399	3
HMDB0158750	C12H18O10	M+Cl	357.059399	3
HMDB0155928	C12H18O10	M+Cl	357.059399	3
HMDB0159484	C12H18O10	M+Cl	357.059399	3
HMDB0159483	C12H18O10	M+Cl	357.059399	3
HMDB0159482	C12H18O10	M+Cl	357.059399	3
HMDB0158876	C12H18O10	M+Cl	357.059399	3
HMDB0155927	C12H18O10	M+Cl	357.059399	3
HMDB0166865	C12H18O10	M+Cl	357.059399	3
HMDB0166785	C13H20O9	M+K-2H	357.059338	3
HMDB0166789	C13H20O9	M+K-2H	357.059338	3
HMDB ID	**Chemical formula**	**Adduct type**	**Adduct mass**	**Δppm**
HMDB0166788	C13H20O9	M+K-2H	357.059338	3
HMDB0166507	C13H20O9	M+K-2H	357.059338	3
HMDB0180342	C13H20O9	M+K-2H	357.059338	3
HMDB0164744	C13H20O9	M+K-2H	357.059338	3
HMDB0166516	C13H20O9	M+K-2H	357.059338	3
HMDB0180341	C13H20O9	M+K-2H	357.059338	3
HMDB0180347	C13H20O9	M+K-2H	357.059338	3
HMDB0180348	C13H20O9	M+K-2H	357.059338	3
HMDB0166782	C13H20O9	M+K-2H	357.059338	3
HMDB0166783	C13H20O9	M+K-2H	357.059338	3
HMDB0166780	C13H20O9	M+K-2H	357.059338	3
HMDB0164745	C13H20O9	M+K-2H	357.059338	3
HMDB0165788	C13H20O9	M+K-2H	357.059338	3
HMDB0166503	C13H20O9	M+K-2H	357.059338	3
HMDB0166506	C13H20O9	M+K-2H	357.059338	3
HMDB0164742	C13H20O9	M+K-2H	357.059338	3
HMDB0164741	C13H20O9	M+K-2H	357.059338	3
HMDB0163410	C13H20O9	M+K-2H	357.059338	3
HMDB0166504	C13H20O9	M+K-2H	357.059338	3

HMDB0166509	C13H20O9	M+K-2H	357.059338	3
HMDB0166512	C13H20O9	M+K-2H	357.059338	3
HMDB0166513	C13H20O9	M+K-2H	357.059338	3
HMDB0166515	C13H20O9	M+K-2H	357.059338	3
HMDB0166779	C13H20O9	M+K-2H	357.059338	3
HMDB0029288	C16H16O8	M+Na-2H	357.059183	4
HMDB0029287	C16H16O8	M+Na-2H	357.059183	4
HMDB0033999	C16H16O8	M+Na-2H	357.059183	4
HMDB0125054	C16H16O8	M+Na-2H	357.059183	4
HMDB0125053	C16H16O8	M+Na-2H	357.059183	4
HMDB0125051	C16H16O8	M+Na-2H	357.059183	4
HMDB0125066	C16H16O8	M+Na-2H	357.059183	4
HMDB0125065	C16H16O8	M+Na-2H	357.059183	4
HMDB0125069	C16H16O8	M+Na-2H	357.059183	4
HMDB0125068	C16H16O8	M+Na-2H	357.059183	4
HMDB0125078	C16H16O8	M+Na-2H	357.059183	4
HMDB0125080	C16H16O8	M+Na-2H	357.059183	4
HMDB0125050	C16H16O8	M+Na-2H	357.059183	4
HMDB0125039	C16H16O8	M+Na-2H	357.059183	4
HMDB0125038	C16H16O8	M+Na-2H	357.059183	4
HMDB0125036	C16H16O8	M+Na-2H	357.059183	4
HMDB0125035	C16H16O8	M+Na-2H	357.059183	4
HMDB0125083	C16H16O8	M+Na-2H	357.059183	4
HMDB0126514	C16H16O8	M+Na-2H	357.059183	4
HMDB0152030	C16H16O8	M+Na-2H	357.059183	4
HMDB0033997	C16H16O8	M+Na-2H	357.059183	4
HMDB ID	**Chemical formula**	**Adduct type**	**Adduct mass**	**Δppm**
HMDB0030654	C16H16O8	M+Na-2H	357.059183	4
HMDB0152517	C16H16O8	M+Na-2H	357.059183	4
HMDB0153273	C16H16O8	M+Na-2H	357.059183	4
HMDB0153282	C16H16O8	M+Na-2H	357.059183	4
HMDB0153279	C16H16O8	M+Na-2H	357.059183	4
HMDB0153285	C16H16O8	M+Na-2H	357.059183	4
HMDB0152024	C16H16O8	M+Na-2H	357.059183	4
HMDB0151203	C16H16O8	M+Na-2H	357.059183	4
HMDB0131935	C16H16O8	M+Na-2H	357.059183	4
HMDB0137873	C16H16O8	M+Na-2H	357.059183	4
HMDB0140541	C16H16O8	M+Na-2H	357.059183	4
HMDB0033563	C16H16O8	M+Na-2H	357.059183	4
HMDB0150794	C16H16O8	M+Na-2H	357.059183	4
HMDB0132142	C16H16O8	M+Na-2H	357.059183	4
HMDB0176339	C14H26O6S	M+Cl	357.114412	3
HMDB0159638	C14H26O6S	M+Cl	357.114412	3

HMDB0159812	C14H26O6S	M+Cl	357.114412	3
HMDB0159814	C14H26O6S	M+Cl	357.114412	3
HMDB0159820	C14H26O6S	M+Cl	357.114412	3
HMDB0159817	C14H26O6S	M+Cl	357.114412	3
HMDB0159823	C14H26O6S	M+Cl	357.114412	3
HMDB0176336	C14H26O6S	M+Cl	357.114412	3
HMDB0159635	C14H26O6S	M+Cl	357.114412	3
HMDB0159626	C14H26O6S	M+Cl	357.114412	3
HMDB0159629	C14H26O6S	M+Cl	357.114412	3
HMDB0159623	C14H26O6S	M+Cl	357.114412	3
HMDB0172046	C14H24O9	M+Na-2H	357.116698	3
HMDB0172048	C14H24O9	M+Na-2H	357.116698	3
HMDB0172050	C14H24O9	M+Na-2H	357.116698	3
HMDB0172052	C14H24O9	M+Na-2H	357.116698	3
HMDB0172054	C14H24O9	M+Na-2H	357.116698	3
HMDB0172045	C14H24O9	M+Na-2H	357.116698	3
HMDB0164650	C14H24O9	M+Na-2H	357.116698	3
HMDB0164649	C14H24O9	M+Na-2H	357.116698	3
HMDB0161160	C14H24O9	M+Na-2H	357.116698	3
HMDB0161159	C14H24O9	M+Na-2H	357.116698	3
HMDB0159451	C14H24O9	M+Na-2H	357.116698	3
HMDB0159452	C14H24O9	M+Na-2H	357.116698	3
HMDB0144635	C24H24ClNO	M-H2O-H	358.136252	2
HMDB0161177	C16H15NO10	M-H2O-H	362.051206	1
HMDB0161176	C16H15NO10	M-H2O-H	362.051206	1
HMDB0161175	C16H15NO10	M-H2O-H	362.051206	1
HMDB0161173	C16H15NO10	M-H2O-H	362.051206	1
HMDB0161174	C16H15NO10	M-H2O-H	362.051206	1
HMDB0161180	C16H15NO10	M-H2O-H	362.051206	1
HMDB ID	**Chemical formula**	**Adduct type**	**Adduct mass**	**Δppm**
HMDB0161179	C16H15NO10	M-H2O-H	362.051206	1
HMDB0161178	C16H15NO10	M-H2O-H	362.051206	1
HMDB0158557	C11H13N5O7	M+Cl	362.0509	2
HMDB0158556	C11H13N5O7	M+Cl	362.0509	2
HMDB0160081	C11H13N5O7	M+Cl	362.0509	2
HMDB0160080	C11H13N5O7	M+Cl	362.0509	2
HMDB0154952	C10H14N5O8P	M-H	362.050723	3
HMDB0011670	C10H14N5O8P	M-H	362.050723	3
HMDB0001397	C10H14N5O8P	M-H	362.050723	3
HMDB0059639	C10H14N5O8P	M-H	362.050723	3
HMDB0160491	C13H19NO11	M-H	364.088534	0
HMDB0000912	C14H17N5O8	M-H2O-H	364.089323	2
HMDB0160044	C14H17N5O8	M-H2O-H	364.089323	2

HMDB0130599	C17H18O7S	M-H	365.070048	1
HMDB0186918	C12H16N4O8	M+Na-2H	365.071479	3
HMDB0131561	C17H20O8S	M-H20-H	365.069499	3
HMDB0151326	C17H20O8S	M-H20-H	365.069499	3
HMDB0151319	C17H20O8S	M-H20-H	365.069499	3
HMDB0151322	C17H20O8S	M-H20-H	365.069499	3
HMDB0151317	C17H20O8S	M-H20-H	365.069499	3
HMDB0131601	C17H20O8S	M-H20-H	365.069499	3
HMDB0131596	C17H20O8S	M-H20-H	365.069499	3
HMDB0131593	C17H20O8S	M-H20-H	365.069499	3
HMDB0131590	C17H20O8S	M-H20-H	365.069499	3
HMDB0131572	C17H20O8S	M-H20-H	365.069499	3
HMDB0131567	C17H20O8S	M-H20-H	365.069499	3
HMDB0131558	C17H20O8S	M-H20-H	365.069499	3
HMDB0039526	C20H17F2N3O3	M-H20-H	366.105408	2
HMDB0164945	C15H22O9	M+Na-2H	367.101048	1
HMDB0164941	C15H22O9	M+Na-2H	367.101048	1
HMDB0164940	C15H22O9	M+Na-2H	367.101048	1
HMDB0164938	C15H22O9	M+Na-2H	367.101048	1
HMDB0164937	C15H22O9	M+Na-2H	367.101048	1
HMDB0164933	C15H22O9	M+Na-2H	367.101048	1
HMDB0164944	C15H22O9	M+Na-2H	367.101048	1
HMDB0164949	C15H22O9	M+Na-2H	367.101048	1
HMDB0164948	C15H22O9	M+Na-2H	367.101048	1
HMDB0167131	C15H22O9	M+Na-2H	367.101048	1
HMDB0167130	C15H22O9	M+Na-2H	367.101048	1
HMDB0167127	C15H22O9	M+Na-2H	367.101048	1
HMDB0167124	C15H22O9	M+Na-2H	367.101048	1
HMDB0167122	C15H22O9	M+Na-2H	367.101048	1
HMDB0167118	C15H22O9	M+Na-2H	367.101048	1
HMDB0167119	C15H22O9	M+Na-2H	367.101048	1
HMDB0167121	C15H22O9	M+Na-2H	367.101048	1
HMDB ID	**Chemical formula**	**Adduct type**	**Adduct mass**	**Δppm**
HMDB0167116	C15H22O9	M+Na-2H	367.101048	1
HMDB0167115	C15H22O9	M+Na-2H	367.101048	1
HMDB0164934	C15H22O9	M+Na-2H	367.101048	1
HMDB0036562	C15H22O9	M+Na-2H	367.101048	1
HMDB0035057	C15H22O9	M+Na-2H	367.101048	1
HMDB0040601	C15H22O9	M+Na-2H	367.101048	1
HMDB0032742	C15H22O9	M+Na-2H	367.101048	1
HMDB0040602	C15H22O9	M+Na-2H	367.101048	1
HMDB0041189	C15H22O9	M+Na-2H	367.101048	1
HMDB0179180	C15H24O9	M+Na-2H	369.116698	1

HMDB0163512	C15H24O9	M+Na-2H	369.116698	1
HMDB0163509	C15H24O9	M+Na-2H	369.116698	1
HMDB0163510	C15H24O9	M+Na-2H	369.116698	1
HMDB0163513	C15H24O9	M+Na-2H	369.116698	1
HMDB0163516	C15H24O9	M+Na-2H	369.116698	1
HMDB0163517	C15H24O9	M+Na-2H	369.116698	1
HMDB0163520	C15H24O9	M+Na-2H	369.116698	1
HMDB0163519	C15H24O9	M+Na-2H	369.116698	1
HMDB0163522	C15H24O9	M+Na-2H	369.116698	1
HMDB0015054	C17H25N3O2S	M+Cl	370.13615	2
HMDB0015087	C17H25N3O2S	M+Cl	370.13615	2
HMDB0015549	C18H26ClN3O	M+Cl	370.145842	2
HMDB0014867	C21H27NO4S	M-H20-H	370.147689	3
HMDB0142062	C17H12O8	M+Cl	379.022619	0
HMDB0142060	C17H12O8	M+Cl	379.022619	0
HMDB0152220	C17H12O8	M+Cl	379.022619	0
HMDB0030477	C17H12O8	M+Cl	379.022619	0
HMDB0142065	C17H12O8	M+Cl	379.022619	0
HMDB0037754	C17H12O8	M+Cl	379.022619	0
HMDB0176931	C18H14O7	M+K-2H	379.022559	0
HMDB0154058	C18H14O7	M+K-2H	379.022559	0
HMDB0154062	C18H14O7	M+K-2H	379.022559	0
HMDB0140694	C18H14O7	M+K-2H	379.022559	0
HMDB0140693	C18H14O7	M+K-2H	379.022559	0
HMDB0128882	C18H14O7	M+K-2H	379.022559	0
HMDB0128881	C18H14O7	M+K-2H	379.022559	0
HMDB0152210	C18H14O7	M+K-2H	379.022559	0
HMDB0154059	C18H14O7	M+K-2H	379.022559	0
HMDB0159599	C9H16N2O10S	M+Cl	379.021968	2
HMDB0159600	C9H16N2O10S	M+Cl	379.021968	2
HMDB0159601	C9H16N2O10S	M+Cl	379.021968	2
HMDB0001922	C22H17ClN2	M+Cl	379.077428	2
HMDB0170762	C12H20N4O6S2	M-H	379.075151	4
HMDB0142453	C22H20O4S	M-H	379.100954	3
HMDB0179525	C16H22O9	M+Na-2H	379.101048	3
HMDB ID	**Chemical formula**	**Adduct type**	**Adduct mass**	**Δppm**
HMDB0179528	C16H22O9	M+Na-2H	379.101048	3
HMDB0163183	C16H22O9	M+Na-2H	379.101048	3
HMDB0179515	C16H22O9	M+Na-2H	379.101048	3
HMDB0179513	C16H22O9	M+Na-2H	379.101048	3
HMDB0179516	C16H22O9	M+Na-2H	379.101048	3
HMDB0179519	C16H22O9	M+Na-2H	379.101048	3
HMDB0179523	C16H22O9	M+Na-2H	379.101048	3

HMDB0179521	C16H22O9	M+Na-2H	379.101048	3
HMDB0163179	C16H22O9	M+Na-2H	379.101048	3
HMDB0142127	C16H22O9	M+Na-2H	379.101048	3
HMDB0145928	C16H22O9	M+Na-2H	379.101048	3
HMDB0163170	C16H22O9	M+Na-2H	379.101048	3
HMDB0163171	C16H22O9	M+Na-2H	379.101048	3
HMDB0163173	C16H22O9	M+Na-2H	379.101048	3
HMDB0163176	C16H22O9	M+Na-2H	379.101048	3
HMDB0163182	C16H22O9	M+Na-2H	379.101048	3
HMDB0179530	C16H22O9	M+Na-2H	379.101048	3
HMDB0179533	C16H22O9	M+Na-2H	379.101048	3
HMDB0181723	C16H22O9	M+Na-2H	379.101048	3
HMDB0181722	C16H22O9	M+Na-2H	379.101048	3
HMDB0181725	C16H22O9	M+Na-2H	379.101048	3
HMDB0181728	C16H22O9	M+Na-2H	379.101048	3
HMDB0181726	C16H22O9	M+Na-2H	379.101048	3
HMDB0181729	C16H22O9	M+Na-2H	379.101048	3
HMDB0181731	C16H22O9	M+Na-2H	379.101048	3
HMDB0179547	C16H22O9	M+Na-2H	379.101048	3
HMDB0179546	C16H22O9	M+Na-2H	379.101048	3
HMDB0179542	C16H22O9	M+Na-2H	379.101048	3
HMDB0179535	C16H22O9	M+Na-2H	379.101048	3
HMDB0179534	C16H22O9	M+Na-2H	379.101048	3
HMDB0179532	C16H22O9	M+Na-2H	379.101048	3
HMDB0179536	C16H22O9	M+Na-2H	379.101048	3
HMDB0179539	C16H22O9	M+Na-2H	379.101048	3
HMDB0179538	C16H22O9	M+Na-2H	379.101048	3
HMDB0179543	C16H22O9	M+Na-2H	379.101048	3
HMDB0179540	C16H22O9	M+Na-2H	379.101048	3
HMDB0181732	C16H22O9	M+Na-2H	379.101048	3
HMDB0029651	C16H22O9	M+Na-2H	379.101048	3
HMDB0179544	C16H22O9	M+Na-2H	379.101048	3
HMDB0029911	C12H24O11	M+Cl	379.101264	3
HMDB0002928	C12H24O11	M+Cl	379.101264	3
HMDB0006791	C12H24O11	M+Cl	379.101264	3
HMDB0040937	C12H24O11	M+Cl	379.101264	3
HMDB0168558	C17H26O5S	M+K-2H	379.098701	3
HMDB0168557	C17H26O5S	M+K-2H	379.098701	3
HMDB ID	**Chemical formula**	**Adduct type**	**Adduct mass**	**Δppm**
HMDB0179425	C16H24O9	M+Na-2H	381.116698	3
HMDB0179421	C16H24O9	M+Na-2H	381.116698	3
HMDB0178809	C16H24O9	M+Na-2H	381.116698	3
HMDB0178810	C16H24O9	M+Na-2H	381.116698	3

HMDB0178806	C16H24O9	M+Na-2H	381.116698	3
HMDB0178803	C16H24O9	M+Na-2H	381.116698	3
HMDB0178800	C16H24O9	M+Na-2H	381.116698	3
HMDB0178801	C16H24O9	M+Na-2H	381.116698	3
HMDB0178795	C16H24O9	M+Na-2H	381.116698	3
HMDB0178798	C16H24O9	M+Na-2H	381.116698	3
HMDB0178797	C16H24O9	M+Na-2H	381.116698	3
HMDB0178794	C16H24O9	M+Na-2H	381.116698	3
HMDB0178791	C16H24O9	M+Na-2H	381.116698	3
HMDB0179422	C16H24O9	M+Na-2H	381.116698	3
HMDB0179424	C16H24O9	M+Na-2H	381.116698	3
HMDB0182678	C16H24O9	M+Na-2H	381.116698	3
HMDB0182674	C16H24O9	M+Na-2H	381.116698	3
HMDB0182677	C16H24O9	M+Na-2H	381.116698	3
HMDB0182672	C16H24O9	M+Na-2H	381.116698	3
HMDB0182671	C16H24O9	M+Na-2H	381.116698	3
HMDB0182668	C16H24O9	M+Na-2H	381.116698	3
HMDB0182669	C16H24O9	M+Na-2H	381.116698	3
HMDB0182666	C16H24O9	M+Na-2H	381.116698	3
HMDB0182665	C16H24O9	M+Na-2H	381.116698	3
HMDB0179434	C16H24O9	M+Na-2H	381.116698	3
HMDB0179433	C16H24O9	M+Na-2H	381.116698	3
HMDB0179430	C16H24O9	M+Na-2H	381.116698	3
HMDB0179427	C16H24O9	M+Na-2H	381.116698	3
HMDB0178792	C16H24O9	M+Na-2H	381.116698	3
HMDB0176305	C16H24O9	M+Na-2H	381.116698	3
HMDB0176306	C16H24O9	M+Na-2H	381.116698	3
HMDB0039473	C16H24O9	M+Na-2H	381.116698	3
HMDB0037028	C16H24O9	M+Na-2H	381.116698	3
HMDB0038381	C16H24O9	M+Na-2H	381.116698	3
HMDB0034626	C16H24O9	M+Na-2H	381.116698	3
HMDB0034627	C16H24O9	M+Na-2H	381.116698	3
HMDB0176301	C16H24O9	M+Na-2H	381.116698	3
HMDB0176302	C16H24O9	M+Na-2H	381.116698	3
HMDB0176297	C16H24O9	M+Na-2H	381.116698	3
HMDB0176298	C16H24O9	M+Na-2H	381.116698	3
HMDB0176294	C16H24O9	M+Na-2H	381.116698	3
HMDB0176293	C16H24O9	M+Na-2H	381.116698	3
HMDB0131112	C16H24O9	M+Na-2H	381.116698	3
HMDB0030224	C23H23NO2	M+K-2H	382.121485	1
HMDB0180562	C16H26O9	M+Na-2H	383.132348	3
HMDB ID	**Chemical formula**	**Adduct type**	**Adduct mass**	**Δppm**
HMDB0180155	C16H26O9	M+Na-2H	383.132348	3

HMDB0180156	C16H26O9	M+Na-2H	383.132348	3
HMDB0180095	C16H26O9	M+Na-2H	383.132348	3
HMDB0180094	C16H26O9	M+Na-2H	383.132348	3
HMDB0180091	C16H26O9	M+Na-2H	383.132348	3
HMDB0180092	C16H26O9	M+Na-2H	383.132348	3
HMDB0180085	C16H26O9	M+Na-2H	383.132348	3
HMDB0171120	C16H26O9	M+Na-2H	383.132348	3
HMDB0180086	C16H26O9	M+Na-2H	383.132348	3
HMDB0180083	C16H26O9	M+Na-2H	383.132348	3
HMDB0180084	C16H26O9	M+Na-2H	383.132348	3
HMDB0171122	C16H26O9	M+Na-2H	383.132348	3
HMDB0171123	C16H26O9	M+Na-2H	383.132348	3
HMDB0180088	C16H26O9	M+Na-2H	383.132348	3
HMDB0180563	C16H26O9	M+Na-2H	383.132348	3
HMDB0180566	C16H26O9	M+Na-2H	383.132348	3
HMDB0180568	C16H26O9	M+Na-2H	383.132348	3
HMDB0181027	C16H26O9	M+Na-2H	383.132348	3
HMDB0181028	C16H26O9	M+Na-2H	383.132348	3
HMDB0180583	C16H26O9	M+Na-2H	383.132348	3
HMDB0180582	C16H26O9	M+Na-2H	383.132348	3
HMDB0180578	C16H26O9	M+Na-2H	383.132348	3
HMDB0180577	C16H26O9	M+Na-2H	383.132348	3
HMDB0180580	C16H26O9	M+Na-2H	383.132348	3
HMDB0180574	C16H26O9	M+Na-2H	383.132348	3
HMDB0180575	C16H26O9	M+Na-2H	383.132348	3
HMDB0180571	C16H26O9	M+Na-2H	383.132348	3
HMDB0180572	C16H26O9	M+Na-2H	383.132348	3
HMDB0180569	C16H26O9	M+Na-2H	383.132348	3
HMDB0180565	C16H26O9	M+Na-2H	383.132348	3
HMDB0171119	C16H26O9	M+Na-2H	383.132348	3
HMDB0171118	C16H26O9	M+Na-2H	383.132348	3
HMDB0164903	C16H26O9	M+Na-2H	383.132348	3
HMDB0164970	C16H26O9	M+Na-2H	383.132348	3
HMDB0164902	C16H26O9	M+Na-2H	383.132348	3
HMDB0163832	C16H26O9	M+Na-2H	383.132348	3
HMDB0164972	C16H26O9	M+Na-2H	383.132348	3
HMDB0171113	C16H26O9	M+Na-2H	383.132348	3
HMDB0171117	C16H26O9	M+Na-2H	383.132348	3
HMDB0171116	C16H26O9	M+Na-2H	383.132348	3
HMDB0163831	C16H26O9	M+Na-2H	383.132348	3
HMDB0171114	C16H26O9	M+Na-2H	383.132348	3
HMDB0171115	C16H26O9	M+Na-2H	383.132348	3
HMDB0171121	C16H26O9	M+Na-2H	383.132348	3

HMDB0164971	C16H26O9	M+Na-2H	383.132348	3
HMDB ID	**Chemical formula**	**Adduct type**	**Adduct mass**	**Δppm**
HMDB0159382	C16H28O6S	M+Cl	383.130062	3
HMDB0159357	C16H28O6S	M+Cl	383.130062	3
HMDB0159354	C16H28O6S	M+Cl	383.130062	3
HMDB0159360	C16H28O6S	M+Cl	383.130062	3
HMDB0159369	C16H28O6S	M+Cl	383.130062	3
HMDB0159366	C16H28O6S	M+Cl	383.130062	3
HMDB0159378	C16H28O6S	M+Cl	383.130062	3
HMDB0159363	C16H28O6S	M+Cl	383.130062	3
HMDB0031033	C18H30NaO3S	M+Cl	383.143461	3
HMDB0039526	C20H17F2N3O3	M-H	384.116522	1
HMDB0038827	C23H25NO2	M+K-2H	384.137135	3
HMDB0040788	C23H25NO2	M+K-2H	384.137135	3
HMDB0038837	C23H25NO2	M+K-2H	384.137135	3
HMDB0038828	C23H25NO2	M+K-2H	384.137135	3
HMDB0133471	C21H22O7	M-H	385.129277	1
HMDB0133448	C21H22O7	M-H	385.129277	1
HMDB0133450	C21H22O7	M-H	385.129277	1
HMDB0133449	C21H22O7	M-H	385.129277	1
HMDB0133445	C21H22O7	M-H	385.129277	1
HMDB0133447	C21H22O7	M-H	385.129277	1
HMDB0133446	C21H22O7	M-H	385.129277	1
HMDB0137497	C21H22O7	M-H	385.129277	1
HMDB0137499	C21H22O7	M-H	385.129277	1
HMDB0137493	C21H22O7	M-H	385.129277	1
HMDB0137496	C21H22O7	M-H	385.129277	1
HMDB0137494	C21H22O7	M-H	385.129277	1
HMDB0133441	C21H22O7	M-H	385.129277	1
HMDB0133440	C21H22O7	M-H	385.129277	1
HMDB0132627	C21H22O7	M-H	385.129277	1
HMDB0131083	C21H22O7	M-H	385.129277	1
HMDB0133444	C21H22O7	M-H	385.129277	1
HMDB0132634	C21H22O7	M-H	385.129277	1
HMDB0131086	C21H22O7	M-H	385.129277	1
HMDB0131085	C21H22O7	M-H	385.129277	1
HMDB0131082	C21H22O7	M-H	385.129277	1
HMDB0153763	C21H22O7	M-H	385.129277	1
HMDB0148666	C21H22O7	M-H	385.129277	1
HMDB0141313	C21H22O7	M-H	385.129277	1
HMDB0141249	C21H22O7	M-H	385.129277	1
HMDB0141309	C21H22O7	M-H	385.129277	1
HMDB0141299	C21H22O7	M-H	385.129277	1

HMDB0039058	C21H22O7	M-H	385.129277	1
HMDB0034629	C21H22O7	M-H	385.129277	1
HMDB0150578	C21H22O7	M-H	385.129277	1
HMDB0149866	C21H22O7	M-H	385.129277	1
HMDB ID	**Chemical formula**	**Adduct type**	**Adduct mass**	**Δppm**
HMDB0030601	C21H22O7	M-H	385.129277	1
HMDB0040355	C21H22O7	M-H	385.129277	1
HMDB0149862	C21H22O7	M-H	385.129277	1
HMDB0149857	C21H22O7	M-H	385.129277	1
HMDB0149852	C21H22O7	M-H	385.129277	1
HMDB0149843	C21H22O7	M-H	385.129277	1
HMDB0149838	C21H22O7	M-H	385.129277	1
HMDB0141296	C21H22O7	M-H	385.129277	1
HMDB0137508	C21H22O7	M-H	385.129277	1
HMDB0137506	C21H22O7	M-H	385.129277	1
HMDB0137505	C21H22O7	M-H	385.129277	1
HMDB0137500	C21H22O7	M-H	385.129277	1
HMDB0137509	C21H22O7	M-H	385.129277	1
HMDB0141250	C21H22O7	M-H	385.129277	1
HMDB0141247	C21H22O7	M-H	385.129277	1
HMDB0141248	C21H22O7	M-H	385.129277	1
HMDB0141246	C21H22O7	M-H	385.129277	1
HMDB0141245	C21H22O7	M-H	385.129277	1
HMDB0141242	C21H22O7	M-H	385.129277	1
HMDB0139012	C21H22O7	M-H	385.129277	1
HMDB0176798	C21H24O8	M-H20-H	385.128728	3
HMDB0176795	C21H24O8	M-H20-H	385.128728	3
HMDB0176794	C21H24O8	M-H20-H	385.128728	3
HMDB0176791	C21H24O8	M-H20-H	385.128728	3
HMDB0176790	C21H24O8	M-H20-H	385.128728	3
HMDB0153898	C21H24O8	M-H20-H	385.128728	3
HMDB0153891	C21H24O8	M-H20-H	385.128728	3
HMDB0034117	C21H24O8	M-H20-H	385.128728	3
HMDB0037313	C21H24O8	M-H20-H	385.128728	3
HMDB0039273	C21H24O8	M-H20-H	385.128728	3
HMDB0180605	C16H28O9	M+Na-2H	385.147998	1
HMDB0180138	C16H28O9	M+Na-2H	385.147998	1
HMDB0180134	C16H28O9	M+Na-2H	385.147998	1
HMDB0180137	C16H28O9	M+Na-2H	385.147998	1
HMDB0180130	C16H28O9	M+Na-2H	385.147998	1
HMDB0180133	C16H28O9	M+Na-2H	385.147998	1
HMDB0180131	C16H28O9	M+Na-2H	385.147998	1
HMDB0180128	C16H28O9	M+Na-2H	385.147998	1

HMDB0180129	C16H28O9	M+Na-2H	385.147998	1
HMDB0180139	C16H28O9	M+Na-2H	385.147998	1
HMDB0180595	C16H28O9	M+Na-2H	385.147998	1
HMDB0180604	C16H28O9	M+Na-2H	385.147998	1
HMDB0180601	C16H28O9	M+Na-2H	385.147998	1
HMDB0180602	C16H28O9	M+Na-2H	385.147998	1
HMDB0180598	C16H28O9	M+Na-2H	385.147998	1
HMDB ID	**Chemical formula**	**Adduct type**	**Adduct mass**	**Δppm**
HMDB0180599	C16H28O9	M+Na-2H	385.147998	1
HMDB0180594	C16H28O9	M+Na-2H	385.147998	1
HMDB0180593	C16H28O9	M+Na-2H	385.147998	1
HMDB0180596	C16H28O9	M+Na-2H	385.147998	1
HMDB0179962	C16H28O9	M+Na-2H	385.147998	1
HMDB0179961	C16H28O9	M+Na-2H	385.147998	1
HMDB0179942	C16H28O9	M+Na-2H	385.147998	1
HMDB0179941	C16H28O9	M+Na-2H	385.147998	1
HMDB0164899	C16H28O9	M+Na-2H	385.147998	1
HMDB0164897	C16H28O9	M+Na-2H	385.147998	1
HMDB0164898	C16H28O9	M+Na-2H	385.147998	1
HMDB0163826	C16H28O9	M+Na-2H	385.147998	1
HMDB0163828	C16H28O9	M+Na-2H	385.147998	1
HMDB0163827	C16H28O9	M+Na-2H	385.147998	1
HMDB0179945	C16H28O9	M+Na-2H	385.147998	1
HMDB0179943	C16H28O9	M+Na-2H	385.147998	1
HMDB0179960	C16H28O9	M+Na-2H	385.147998	1
HMDB0179955	C16H28O9	M+Na-2H	385.147998	1
HMDB0179956	C16H28O9	M+Na-2H	385.147998	1
HMDB0179957	C16H28O9	M+Na-2H	385.147998	1
HMDB0179951	C16H28O9	M+Na-2H	385.147998	1
HMDB0179950	C16H28O9	M+Na-2H	385.147998	1
HMDB0179946	C16H28O9	M+Na-2H	385.147998	1
HMDB0179947	C16H28O9	M+Na-2H	385.147998	1
HMDB0163449	C15H28N2O8	M+Na-2H	385.159232	1
HMDB0185393	C21H29N2O4S	M-H20-H	385.158589	2
HMDB0015546	C21H23N3OS	M+Na-2H	386.130849	2
HMDB0167847	C14H10O9S	M+Cl	388.973955	1
HMDB0145491	C14H10O9S	M+Cl	388.973955	1
HMDB0132319	C14H10O9S	M+Cl	388.973955	1
HMDB0137572	C15H12O8S	M+K-2H	388.973895	2
HMDB0148864	C15H12O8S	M+K-2H	388.973895	2
HMDB0133387	C15H12O8S	M+K-2H	388.973895	2
HMDB0141959	C15H12O8S	M+K-2H	388.973895	2
HMDB0141341	C15H12O8S	M+K-2H	388.973895	2

HMDB0141192	C15H12O8S	M+K-2H	388.973895	2
HMDB0138613	C15H12O8S	M+K-2H	388.973895	2
HMDB0134578	C15H12O8S	M+K-2H	388.973895	2
HMDB0137597	C15H12O8S	M+K-2H	388.973895	2
HMDB0137588	C15H12O8S	M+K-2H	388.973895	2
HMDB0137580	C15H12O8S	M+K-2H	388.973895	2
HMDB0149624	C15H12O8S	M+K-2H	388.973895	2
HMDB0151702	C15H12O8S	M+K-2H	388.973895	2
HMDB0174519	C15H12O8S	M+K-2H	388.973895	2
HMDB0174515	C15H12O8S	M+K-2H	388.973895	2
HMDB ID	**Chemical formula**	**Adduct type**	**Adduct mass**	**Δppm**
HMDB0167922	C15H12O8S	M+K-2H	388.973895	2
HMDB0167921	C15H12O8S	M+K-2H	388.973895	2
HMDB0167917	C15H12O8S	M+K-2H	388.973895	2
HMDB0167918	C15H12O8S	M+K-2H	388.973895	2
HMDB0167800	C15H12O8S	M+K-2H	388.973895	2
HMDB0166460	C15H12O8S	M+K-2H	388.973895	2
HMDB0166456	C15H12O8S	M+K-2H	388.973895	2
HMDB0152661	C15H12O8S	M+K-2H	388.973895	2
HMDB0152567	C15H12O8S	M+K-2H	388.973895	2
HMDB0151703	C15H12O8S	M+K-2H	388.973895	2
HMDB0138617	C15H12O8S	M+K-2H	388.973895	2
HMDB0130791	C15H12O8S	M+K-2H	388.973895	2
HMDB0150622	C15H12O8S	M+K-2H	388.973895	2
HMDB0125406	C15H12O8S	M+K-2H	388.973895	2
HMDB0128084	C15H12O8S	M+K-2H	388.973895	2
HMDB0129980	C15H12O8S	M+K-2H	388.973895	2
HMDB0128106	C15H12O8S	M+K-2H	388.973895	2
HMDB0128088	C15H12O8S	M+K-2H	388.973895	2
HMDB0002685	C20H36O5	M+Cl	391.225676	2
HMDB0002689	C20H36O5	M+Cl	391.225676	2
HMDB0004239	C20H36O5	M+Cl	391.225676	2
HMDB0011568	C21H38O4	M+K-2H	391.225616	2
HMDB0011538	C21H38O4	M+K-2H	391.225616	2
HMDB0007003	C19H37O6P	M-H	391.225499	3
HMDB0041206	C24H34O3	M+Na-2H	391.225461	3
HMDB0000476	C24H34O3	M+Na-2H	391.225461	3
HMDB0015033	C24H34O3	M+Na-2H	391.225461	3
HMDB0031977	C26H32O3	M-H	391.227869	3
HMDB0184182	C19H39O7P	M-H20-H	391.224951	4
HMDB0007853	C19H39O7P	M-H20-H	391.22495	4
HMDB0007849	C19H39O7P	M-H20-H	391.22495	4
HMDB0155888	C19H37O7P	M-H20-H	391.22495	4

HMDB0184181	C19H37O7P	M-H20-H	391.22495	4
HMDB0039505	C14H25N3O9	M+Na-2H	400.133745	3
HMDB0164916	C16H28O10	M+Na-2H	401.142913	2
HMDB0164917	C16H28O10	M+Na-2H	401.142913	2
HMDB0164915	C16H28O10	M+Na-2H	401.142913	2
HMDB0164914	C16H28O10	M+Na-2H	401.142913	2
HMDB0031956	C16H28O10	M+Na-2H	401.142913	2
HMDB0041360	C16H28O10	M+Na-2H	401.142913	2
HMDB0031954	C16H28O10	M+Na-2H	401.142913	2
HMDB0182891	C20H29O5S	M+Na-2H	401.140412	4
HMDB0156491	C20H28O5S	M+Na-2H	401.140411	4
HMDB0156479	C20H28O5S	M+Na-2H	401.140411	4
HMDB0156477	C20H28O5S	M+Na-2H	401.140411	4
HMDB ID	**Chemical formula**	**Adduct type**	**Adduct mass**	**Δppm**
HMDB0156475	C20H28O5S	M+Na-2H	401.140411	4
HMDB0156473	C20H28O5S	M+Na-2H	401.140411	4
HMDB0156471	C20H28O5S	M+Na-2H	401.140411	4
HMDB0156469	C20H28O5S	M+Na-2H	401.140411	4
HMDB0015613	C20H28O5S	M+Na-2H	401.140411	4
HMDB0139160	C16H11ClO8	M+K-2H	402.962851	1
HMDB0181006	C19H23NO10	M-H20-H	406.113806	2
HMDB0181002	C19H23NO10	M-H20-H	406.113806	2
HMDB0181004	C19H23NO10	M-H20-H	406.113806	2
HMDB0180998	C19H23NO10	M-H20-H	406.113806	2
HMDB0181000	C19H23NO10	M-H20-H	406.113806	2
HMDB0180995	C19H23NO10	M-H20-H	406.113806	2
HMDB0180994	C19H23NO10	M-H20-H	406.113806	2
HMDB0181007	C19H23NO10	M-H20-H	406.113806	2
HMDB0152648	C15H14O9S	M+K-2H	406.984459	1
HMDB0146737	C15H14O9S	M+K-2H	406.984459	1
HMDB0146731	C15H14O9S	M+K-2H	406.984459	1
HMDB0146730	C15H14O9S	M+K-2H	406.984459	1
HMDB0141197	C15H14O9S	M+K-2H	406.984459	1
HMDB0140579	C15H14O9S	M+K-2H	406.984459	1
HMDB0140349	C15H14O9S	M+K-2H	406.984459	1
HMDB0137196	C15H14O9S	M+K-2H	406.984459	1
HMDB0152649	C15H14O9S	M+K-2H	406.984459	1
HMDB0152656	C15H14O9S	M+K-2H	406.984459	1
HMDB0152702	C15H14O9S	M+K-2H	406.984459	1
HMDB0152709	C15H14O9S	M+K-2H	406.984459	1
HMDB0152703	C15H14O9S	M+K-2H	406.984459	1
HMDB0136996	C15H14O9S	M+K-2H	406.984459	1
HMDB0136991	C15H14O9S	M+K-2H	406.984459	1

HMDB0136116	C15H14O9S	M+K-2H	406.984459	1
HMDB0131222	C15H14O9S	M+K-2H	406.984459	1
HMDB0127729	C15H14O9S	M+K-2H	406.984459	1
HMDB0130010	C15H14O9S	M+K-2H	406.984459	1
HMDB0130254	C15H14O9S	M+K-2H	406.984459	1
HMDB0131215	C15H14O9S	M+K-2H	406.984459	1
HMDB0133577	C15H14O9S	M+K-2H	406.984459	1
HMDB0136115	C15H14O9S	M+K-2H	406.984459	1
HMDB0136114	C15H14O9S	M+K-2H	406.984459	1
HMDB0135523	C15H14O9S	M+K-2H	406.984459	1
HMDB0135524	C15H14O9S	M+K-2H	406.984459	1
HMDB0135525	C15H14O9S	M+K-2H	406.984459	1
HMDB0134832	C15H14O9S	M+K-2H	406.984459	1
HMDB0134831	C15H14O9S	M+K-2H	406.984459	1
HMDB0133576	C15H14O9S	M+K-2H	406.984459	1
HMDB0164998	C14H12O10S	M+Cl	406.98452	1
HMDB ID	**Chemical formula**	**Adduct type**	**Adduct mass**	**Δppm**
HMDB0131441	C17H15O11S	M-H20-H	408.014569	3
HMDB0168540	C22H21NO8	M-H20-H	408.108327	3
HMDB0168541	C22H21NO8	M-H20-H	408.108327	3
HMDB0168835	C14H23N3O9S	M-H	408.108225	4
HMDB0172038	C14H23N3O9S	M-H	408.108225	4
HMDB0172039	C14H23N3O9S	M-H	408.108225	4
HMDB0015064	C22H38O5	M+Cl	417.241326	3
HMDB0011577	C23H40O4	M+K-2H	417.241266	3
HMDB0041103	C23H40O4	M+K-2H	417.241266	3
HMDB0032735	C23H40O4	M+K-2H	417.241266	3
HMDB0039403	C23H40O4	M+K-2H	417.241266	3
HMDB0011576	C23H40O4	M+K-2H	417.241266	3
HMDB0011575	C23H40O4	M+K-2H	417.241266	3
HMDB0011547	C23H40O4	M+K-2H	417.241266	3
HMDB0011545	C23H40O4	M+K-2H	417.241266	3
HMDB0011546	C23H40O4	M+K-2H	417.241266	3
HMDB0007006	C21H39O6P	M-H	417.241149	3
HMDB0007005	C21H39O6P	M-H	417.241149	3
HMDB0060944	C23H20N2O4S	M-H	419.107102	2
HMDB0167317	C15H24N4O6S2	M-H	419.106451	4
HMDB0041883	C15H24N4O6S2	M-H	419.10645	4
HMDB0011544	C23H42O4	M+K-2H	419.256916	3
HMDB0011574	C23H42O4	M+K-2H	419.256916	3
HMDB0035959	C23H42O4	M+K-2H	419.256916	3
HMDB0036865	C23H42O4	M+K-2H	419.256916	3
HMDB0007004	C21H41O6P	M-H	419.2568	3

HMDB0173215	C26H38O3	M+Na-2H	419.256761	3
HMDB0181364	C15H25N3O7S2	M-H	422.106117	4
HMDB0062636	C12H18N4O7P2S	M-H	423.029867	0
HMDB0001372	C12H19N4O7P2S	M-H	423.030416	2
HMDB0178400	C20H18O6S	M+K-2H	423.031015	3
HMDB0178399	C20H18O6S	M+K-2H	423.031015	3
HMDB0142811	C22H22N2O8	M-H20-H	423.119226	2
HMDB0015066	C22H22N2O8	M-H20-H	423.119226	2
HMDB0142652	C22H22N2O8	M-H20-H	423.119226	2
HMDB0142688	C22H22N2O8	M-H20-H	423.119226	2
HMDB0142700	C22H22N2O8	M-H20-H	423.119226	2
HMDB0035405	C22H26O6	M+K-2H	423.121545	4
HMDB0030810	C22H26O6	M+K-2H	423.121545	4
HMDB0035404	C22H26O6	M+K-2H	423.121545	4
HMDB0138810	C22H26O6	M+K-2H	423.121545	4
HMDB0138812	C22H26O6	M+K-2H	423.121545	4
HMDB0138806	C22H26O6	M+K-2H	423.121545	4
HMDB0152803	C22H26O6	M+K-2H	423.121545	4
HMDB0138805	C22H26O6	M+K-2H	423.121545	4
HMDB ID	**Chemical formula**	**Adduct type**	**Adduct mass**	**Δppm**
HMDB0138807	C22H26O6	M+K-2H	423.121545	4
HMDB0150585	C21H24O7	M+Cl	423.121605	4
HMDB0176777	C21H24O7	M+Cl	423.121605	4
HMDB0149867	C21H24O7	M+Cl	423.121605	4
HMDB0133525	C21H24O7	M+Cl	423.121605	4
HMDB0133711	C21H24O7	M+Cl	423.121605	4
HMDB0133710	C21H24O7	M+Cl	423.121605	4
HMDB0133709	C21H24O7	M+Cl	423.121605	4
HMDB0135229	C21H24O7	M+Cl	423.121605	4
HMDB0135552	C21H24O7	M+Cl	423.121605	4
HMDB0135582	C21H24O7	M+Cl	423.121605	4
HMDB0135581	C21H24O7	M+Cl	423.121605	4
HMDB0149853	C21H24O7	M+Cl	423.121605	4
HMDB0149845	C21H24O7	M+Cl	423.121605	4
HMDB0149844	C21H24O7	M+Cl	423.121605	4
HMDB0148672	C21H24O7	M+Cl	423.121605	4
HMDB0149839	C21H24O7	M+Cl	423.121605	4
HMDB0133518	C21H24O7	M+Cl	423.121605	4
HMDB0133454	C21H24O7	M+Cl	423.121605	4
HMDB0149863	C21H24O7	M+Cl	423.121605	4
HMDB0149864	C21H24O7	M+Cl	423.121605	4
HMDB0135584	C21H24O7	M+Cl	423.121605	4
HMDB0149854	C21H24O7	M+Cl	423.121605	4

HMDB0125487	C21H24O7	M+Cl	423.121605	4
HMDB0132645	C21H24O7	M+Cl	423.121605	4
HMDB0133451	C21H24O7	M+Cl	423.121605	4
HMDB0133455	C21H24O7	M+Cl	423.121605	4
HMDB0133453	C21H24O7	M+Cl	423.121605	4
HMDB0149859	C21H24O7	M+Cl	423.121605	4
HMDB0149858	C21H24O7	M+Cl	423.121605	4
HMDB0149840	C21H24O7	M+Cl	423.121605	4
HMDB0033284	C21H24O7	M+Cl	423.121605	4
HMDB0035110	C21H24O7	M+Cl	423.121605	4
HMDB0039059	C21H24O7	M+Cl	423.121605	4
HMDB0041197	C21H24O7	M+Cl	423.121605	4
HMDB0036557	C21H24O7	M+Cl	423.121605	4
HMDB0015014	C23H24N2O4S	M-H	423.138402	0
HMDB0148115	C18H13NO9	M+K-2H	424.007637	1
HMDB0152296	C18H13NO9	M+K-2H	424.007637	1
HMDB0161156	C19H24N2O11	M-H20-H	437.11962	1
HMDB0029887	C22H42O6	M+Cl	437.267541	1
HMDB0093022	C23H44O5	M+K-2H	437.267481	1
HMDB0092904	C23H44O5	M+K-2H	437.267481	1
HMDB0093021	C23H44O5	M+K-2H	437.267481	1
HMDB0093019	C23H44O5	M+K-2H	437.267481	1
HMDB ID	**Chemical formula**	**Adduct type**	**Adduct mass**	**Δppm**
HMDB0092905	C23H44O5	M+K-2H	437.267481	1
HMDB0092903	C23H44O5	M+K-2H	437.267481	1
HMDB0093020	C23H44O5	M+K-2H	437.267481	1
HMDB0092906	C23H44O5	M+K-2H	437.267481	1
HMDB0059929	C23H44O5	M+K-2H	437.267481	1
HMDB0092961	C23H44O5	M+K-2H	437.267481	1
HMDB0092962	C23H44O5	M+K-2H	437.267481	1
HMDB0007854	C21H43O7P	M-H	437.267365	1
HMDB0007850	C21H43O7P	M-H	437.267364	1
HMDB0165756	C28H40O5	M-H20-H	437.269184	3
HMDB0173217	C28H40O5	M-H20-H	437.269184	3
HMDB0173220	C28H40O5	M-H20-H	437.269184	3
HMDB0173216	C28H40O5	M-H20-H	437.269184	3
HMDB0173218	C28H40O5	M-H20-H	437.269184	3
HMDB0173222	C28H40O5	M-H20-H	437.269184	3
HMDB0173219	C28H40O5	M-H20-H	437.269184	3
HMDB0173221	C28H40O5	M-H20-H	437.269184	3
HMDB0146022	C17H24O12	M+Na-2H	441.101442	1
HMDB0177560	C19H24O13	M-H20-H	441.103301	3
HMDB0177558	C19H24O13	M-H20-H	441.103301	3

HMDB0142039	C19H24O13	M-H20-H	441.103301	3
HMDB0142038	C19H24O13	M-H20-H	441.103301	3
HMDB0142040	C19H24O13	M-H20-H	441.103301	3
HMDB0177559	C19H24O13	M-H20-H	441.103301	3
HMDB0181387	C11H12Cl3NO9	M+Cl	441.927166	2
HMDB0059648	C10H15N5O11P2	M-H	442.017053	1
HMDB0001201	C10H15N5O11P2	M-H	442.017053	1
HMDB0176764	C15H16ClNO11	M+Na-2H	442.015854	3
HMDB0149468	C19H21NO7S	M+Cl	442.073275	1
HMDB0149465	C19H21NO7S	M+Cl	442.073275	1
HMDB0149467	C19H21NO7S	M+Cl	442.073275	1
HMDB0149471	C19H21NO7S	M+Cl	442.073275	1
HMDB0149470	C19H21NO7S	M+Cl	442.073275	1
HMDB0149475	C19H21NO7S	M+Cl	442.073275	1
HMDB0149473	C19H21NO7S	M+Cl	442.073275	1
HMDB0173733	C19H21NO7S	M+Cl	442.073275	1
HMDB0149462	C19H21NO7S	M+Cl	442.073275	1
HMDB0149461	C19H21NO7S	M+Cl	442.073275	1
HMDB0149464	C19H21NO7S	M+Cl	442.073275	1
HMDB0149459	C19H21NO7S	M+Cl	442.073275	1
HMDB0149456	C19H21NO7S	M+Cl	442.073275	1
HMDB0030257	C19H21NO7S	M+Cl	442.073275	1
HMDB0061128	C19H21NO7S	M+Cl	442.073275	1
HMDB0015390	C16H15F6N5O	M+Cl	442.087481	2
HMDB0037737	C16H10N2O8S2	M+Na-2H	442.962523	2
HMDB ID	**Chemical formula**	**Adduct type**	**Adduct mass**	**Δppm**
HMDB0059912	C16H10N2O8S2	M+Na-2H	442.962523	2
HMDB0169064	C16H10N2O8S2	M+Na-2H	442.962524	2
HMDB0131010	C18H18O9S	M+Cl	445.036555	1
HMDB0138469	C18H18O9S	M+Cl	445.036555	1
HMDB0151173	C18H18O9S	M+Cl	445.036555	1
HMDB0151677	C18H18O9S	M+Cl	445.036555	1
HMDB0151695	C18H18O9S	M+Cl	445.036555	1
HMDB0151698	C18H18O9S	M+Cl	445.036555	1
HMDB0129050	C19H20O8S	M+K-2H	445.036495	2
HMDB0140239	C19H20O8S	M+K-2H	445.036495	2
HMDB0140131	C19H20O8S	M+K-2H	445.036495	2
HMDB0140123	C19H20O8S	M+K-2H	445.036495	2
HMDB0140121	C19H20O8S	M+K-2H	445.036495	2
HMDB0129071	C19H20O8S	M+K-2H	445.036495	2
HMDB0125570	C19H20O8S	M+K-2H	445.036495	2
HMDB0129084	C19H20O8S	M+K-2H	445.036495	2
HMDB0129083	C19H20O8S	M+K-2H	445.036495	2

HMDB0129078	C19H20O8S	M+K-2H	445.036495	2
HMDB0129043	C19H20O8S	M+K-2H	445.036495	2
HMDB0129065	C19H20O8S	M+K-2H	445.036495	2
HMDB0129060	C19H20O8S	M+K-2H	445.036495	2
HMDB0033694	C20H26O13	M-H20-H	455.118951	0
HMDB0169176	C20H24O12	M-H	455.1195	2
HMDB0147111	C20H24O12	M-H	455.1195	2
HMDB0147112	C20H24O12	M-H	455.1195	2
HMDB0147113	C20H24O12	M-H	455.1195	2
HMDB0169166	C20H24O12	M-H	455.1195	2
HMDB0169164	C20H24O12	M-H	455.1195	2
HMDB0169179	C20H24O12	M-H	455.1195	2
HMDB0169178	C20H24O12	M-H	455.1195	2
HMDB0169167	C20H24O12	M-H	455.1195	2
HMDB0169174	C20H24O12	M-H	455.1195	2
HMDB0169172	C20H24O12	M-H	455.1195	2
HMDB0169175	C20H24O12	M-H	455.1195	2
HMDB0169177	C20H24O12	M-H	455.1195	2
HMDB0169163	C20H24O12	M-H	455.1195	2
HMDB0169173	C20H24O12	M-H	455.1195	2
HMDB0059974	C18H26O12	M+Na-2H	455.117092	4
HMDB0059972	C18H26O12	M+Na-2H	455.117092	4
HMDB0154967	C10H14N5O11PS	M+Na-2H	463.98948	2
HMDB0154968	C10H14N5O11PS	M+Na-2H	463.98948	2
HMDB0140638	C25H28O8S	M-H20-H	469.132099	2
HMDB0140641	C25H28O8S	M-H20-H	469.132099	2
HMDB0140644	C25H28O8S	M-H20-H	469.132099	2
HMDB0140647	C25H28O8S	M-H20-H	469.132099	2
HMDB ID	**Chemical formula**	**Adduct type**	**Adduct mass**	**Δppm**
HMDB0147701	C25H28O8S	M-H20-H	469.132099	2
HMDB0147704	C25H28O8S	M-H20-H	469.132099	2
HMDB0147707	C25H28O8S	M-H20-H	469.132099	2
HMDB0178254	C21H28O13	M-H20-H	469.134601	3
HMDB0180876	C21H28O13	M-H20-H	469.134601	3
HMDB0140861	C21H28O13	M-H20-H	469.134601	3
HMDB0167482	C22H31NO9	M+Na-2H	474.174548	1
HMDB0167483	C22H31NO9	M+Na-2H	474.174548	1
HMDB0145295	C25H28N2O9	M-H	499.172204	3
HMDB0145310	C25H28N2O9	M-H	499.172204	3
HMDB0145381	C25H28N2O9	M-H	499.172204	3
HMDB0145380	C25H28N2O9	M-H	499.172204	3
HMDB0160203	C27H47O8S	M-H20-H	512.280775	2
HMDB0160202	C27H47O8S	M-H20-H	512.280775	2

HMDB0159420	C27H47O8S	M-H20-H	512.280775	2
HMDB0159421	C27H47O8S	M-H20-H	512.280775	2
HMDB0010697	C34H69NO4	M-H	554.515384	0
HMDB0037105	C34H69NO4	M-H	554.515384	0
HMDB0139450	C26H28N2O12	M-H	559.156948	1
HMDB0139451	C26H28N2O12	M-H	559.156948	1
HMDB0139458	C26H28N2O12	M-H	559.156948	1
HMDB0139459	C26H28N2O12	M-H	559.156948	1
HMDB0139457	C26H28N2O12	M-H	559.156948	1
HMDB0139462	C26H28N2O12	M-H	559.156948	1
HMDB0139463	C26H28N2O12	M-H	559.156948	1
HMDB0034749	C26H34O11	M+K-2H	559.158718	2
HMDB0177211	C26H34O11	M+K-2H	559.158718	2
HMDB0038927	C26H34O11	M+K-2H	559.158718	2
HMDB0032907	C26H34O11	M+K-2H	559.158718	2
HMDB0038711	C26H34O11	M+K-2H	559.158718	2
HMDB0040471	C26H34O11	M+K-2H	559.158718	2
HMDB0182817	C25H32O12	M+Cl	559.158778	2
HMDB0182816	C25H32O12	M+Cl	559.158778	2
HMDB0182815	C25H32O12	M+Cl	559.158778	2
HMDB0034751	C25H32O12	M+Cl	559.158778	2
HMDB0034706	C32H48O8	M+Na-2H	581.309585	3
HMDB0164983	C34H50O10	M-H20-H	599.322008	3
HMDB ID	**Chemical formula**	**Adduct type**	**Adduct mass**	**Δppm**
HMDB0170491	C28H31ClO13S	M+Na-2H	663.092056	1
HMDB0142396	C30H28O13S	M+Cl	663.094464	3
HMDB0142397	C30H28O13S	M+Cl	663.094464	3
HMDB0142395	C30H28O13S	M+Cl	663.094464	3
HMDB0135127	C30H28O13S	M+Cl	663.094464	3
HMDB0135125	C30H28O13S	M+Cl	663.094464	3
HMDB0135126	C30H28O13S	M+Cl	663.094464	3
HMDB0135117	C30H28O13S	M+Cl	663.094464	3
HMDB0135115	C30H28O13S	M+Cl	663.094464	3
HMDB0135116	C30H28O13S	M+Cl	663.094464	3
HMDB0182948	C29H35ClO13	M+K-2H	663.125225	1
HMDB0182939	C29H35ClO13	M+K-2H	663.125225	1
HMDB0182943	C29H35ClO13	M+K-2H	663.125225	1
HMDB0182942	C29H35ClO13	M+K-2H	663.125225	1
HMDB0182940	C29H35ClO13	M+K-2H	663.125225	1
HMDB0182945	C29H35ClO13	M+K-2H	663.125225	1
HMDB0182947	C29H35ClO13	M+K-2H	663.125225	1
HMDB0182946	C29H35ClO13	M+K-2H	663.125225	1
HMDB0182950	C29H35ClO13	M+K-2H	663.125225	1

HMDB0182949	C29H35ClO13	M+K-2H	663.125225	1
HMDB0182936	C29H35ClO13	M+K-2H	663.125225	1
HMDB0182937	C29H35ClO13	M+K-2H	663.125225	1
HMDB0182927	C29H35ClO13	M+K-2H	663.125225	1
HMDB0182930	C29H35ClO13	M+K-2H	663.125225	1
HMDB0182931	C29H35ClO13	M+K-2H	663.125225	1
HMDB0182928	C29H35ClO13	M+K-2H	663.125225	1
HMDB0182935	C29H35ClO13	M+K-2H	663.125225	1
HMDB0182933	C29H35ClO13	M+K-2H	663.125225	1

HMDB0182934	C29H35ClO13	M+K-2H	663.125225	1
HMDB0030121	C35H30O11	M+K-2H	663.127418	2
HMDB0036400	C33H44O14	M-H	663.26583	0
HMDB0036529	C33H46O15	M-H20-H	663.265281	1
HMDB0036528	C33H46O15	M-H20-H	663.265281	1
HMDB0173804	C36H58O11S	M-H	697.362708	0
HMDB0173802	C36H58O11S	M-H	697.362708	0
HMDB0173803	C36H58O11S	M-H	697.362708	0

Table S2. List of metabolite annotations according to HMDB.

The table shows HMDB identification, chemical formula, adduct type, adduct mass and delta ppm. Metabolites were annotated by accurate mass matching with databases (mass accuracy ≤ 4 ppm defines molecular weight tolerance for Human Metabolome Database [http://www.hmdb.ca/] and METASPACE [http://annotate.metaspace2020.eu/] searches). An adduct ion is formed by the adduction of an ionic species to a molecule. The following adduct types were considered: ion mode negative, adduct type: [M-H], [M-H-H2O], [M+Na-2H], [M+Cl] and [M+K-2H]. HMDB ID, human metabolome database identification; mass accuracy represented in ppm, parts per million.

Mass peaks	Correlation scores with GDP
442.017	1
362.051	0.803467
120.685	0.791905
435.974	0.777913
463.999	0.774531
363.054	0.768627
384.033	0.763013
419.997	0.744551
437.972	0.709454
441.992	0.686314
421.994	0.68091
479.964	0.680169
211.001	0.655386
509.898	0.588395
420.01	0.572187
424.007	0.556816

Table S3. Mass peaks co-localized with distribution pattern 2.

The mass peaks following the GDP (guanosine diphosphate) distribution pattern 2 are shown with relative GDP correlation scores. The correlation scores were elucidated using SCiLS Lab v. 2019

using Pearson's correlation analysis. Mass spectrometry images of the GDP distribution pattern are shown in **Figure 2** of the main manuscript.

Discriminative pathways in Region 1		
	P-value	**Pathway impact**
Amino sugar and nucleotide sugar metabolism	0.00059766	0.54996
Pentose phosphate pathway	0.0014556	0.51867
Fructose and mannose metabolism	0.021297	0.59558
Purine metabolism	0.040132	0.20949
Phosphatidylinositol signaling system	0.07878	0.15378
Glycerophospholipid metabolism	0.17831	0.32357
Discriminative pathways in Region 2		
	P-value	**Pathway impact**
Purine metabolism	0.0023472	0.20949
Pentose phosphate pathway	0.03	0.36474
Pentose and glucuronate interconversions	0.26352	0.07812
Pantothenate and CoA biosynthesis	0.28464	0.05357
Discriminative pathways in Region 3		
	P-value	**Pathway impact**
Amino sugar and nucleotide sugar metabolism	0.00236	0.48361
Fructose and mannose metabolism	0.017668	0.48792
Glycolysis / Gluconeogenesis	0.042987	0.10571
Galactose metabolism	0.048515	0.04821
Phosphatidylinositol signaling system	0.054419	0.05631
Alanine, aspartate and glutamate metabolism	0.054419	0.3101

Table S4. Discriminative pathways in CYP11B2-positive Regions 1, 2 and 3.
P-value indicates the statistical significance of the overall metabolic changes within the indicated pathway; pathway impact represents the relative impact of enriched metabolites within the pathway and is calculated as the sum of importance measures of enriched metabolites within a pathway normalized by the sum of importance measures of all metabolites within that pathway. Regions 1, 2 and 3 corresponding to CYP11B2-positive regions are shown in **Figure 2**, pathway impact analysis using MetaboAnalyst 4.0 (http://www.metaboanalyst.ca) is shown in **Figure 3** of the main manuscript.

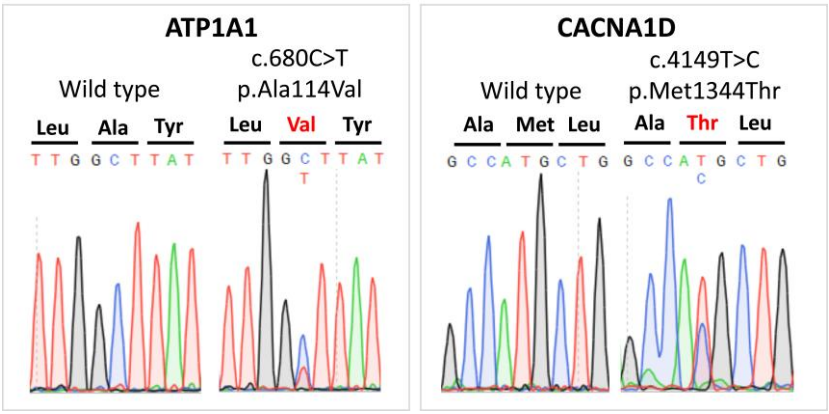

Figure S1. Sequencing chromatograms showing an *ATP1A1* and *CACNA1D* double mutation in APCC ROI01 in adrenal 1-2